To: N.C.L. Library.
With Best Compliments.

Goswami
26/9/73

210

6-7-95

COMPUTERISED

Donated by Dr. A. Goswami
Scientist-E Physical Chemistry
Division N.C.L. PUNE-411 008.

DIELECTRIC AND OTHER PROPERTIES OF THIN FILMS

COMPUTERISED

A Thesis submitted to the
UNIVERSITY OF POONA
for the degree of
DOCTOR OF PHILOSOPHY
IN PHYSICS

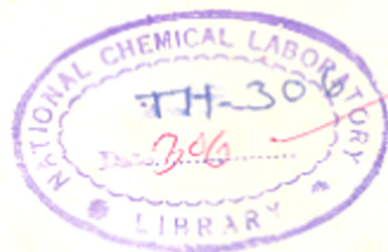

By

AMIT PRASUN GOSWAMI, M. Sc.

539.234:537.226(043)
GOS

Electron Diffraction and Thin Film Laboratory
NATIONAL CHEMICAL LABORATORY
POONA-8 (India)

September 1 9 7 3

CONTENTS

Page

CHAPTER I GENERAL INTRODUCTION

(A) Thin films, their nature, structures and properties 1

(B) Dielectric Properties

(i) General theory of dielectrics 6
(ii) Relative permittivity 7
(iii) Dielectric Loss 8
(iv) Polarisation 9
(v) Temperature coefficient of capacitance 17
(vi) Frequency behaviour of tan δ in thin films 18
(vii) Breakdown voltage and dielectric field strength 20

(C) Optical Properties

(i) Electromagnetic wave 22
(ii) Dispersion of the electromagnetic wave by a dielectric 26
(iii) Dispersion in metals and semiconductors 30
(iv) Interband transitions 32
(v) Optical constants of thin files 33
(vi) Normal transmittance and reflectance through a thin film 36

Present work 39

CHAPTER II EXPERIMENTAL TECHNIQUES

(A) Dielectric Properties

(i) preparation of films 40
(ii) Fabrication of capacitors 41
(iii) Ageing 42
(vi) Measurement of file thickness 43
(v) Cryostst 45
(vi) Measurement of capacitance and tan δ 46
(vii) Dielectric constant 48
(iii) Breakdown voltage (VB) and dielectric field strength (F_B) 48

CHAPTER II Page

(B) Optical Preparation

(i) Film preparation 50
(ii) Optical measurements 50
(iii) Equipment 51
(iv) Measurement of optical constants 54

(C) Structure

Electron diffraction studies 61

CHAPTER III STUDIES ON ZINC SULPHIDS FILMS 62

(A) INTRODUCTION 62

(B) EXPERIMENTAL

(i) Preparation of films 67
(ii) Measurement of capacitance(C) and tan 69
(iii) Measurements for optical studies 70

(C) RESULTS

(a) Structure 71
(b) Dielectric properties

(i) Ageing effect 71
(ii) Effect of film thickness 72
(iii) Temperature coefficient of capacitance (ICC) 73
(iv) Effect of frequency and temperature on capacitance 73
(v) Effect of frequency on the 74
(vi) Percentage variation of capacitance with frequency 75
(vii) Breakdown voltage and dielectric field strength 75

(c) Optical Properties

(i) Measurement of transmittance 76
(ii) Optical constants 77

(D) DISCUSSION 77

CHAPTER IV STUDIES ON PRASEODXMIUM OXIDE FILMS

(A) INTRODUCTION 94

CHAPTER IV Page

(B) EXPERIMENTAL 96

(C) RESULTS

(a) Structure 97
(b) Dielectric Properties 98
(c) Optical Properties 102

(D) DISCUSSION 104

CHAPTER V STUDIES ON ANTIMONY TRIOXIDE FILMS

(A) INTRODUCTION 111

(B) EXPERIMENTAL 114

(C) RESULTS

(a) Structure 115
(b) Dielectric Properties 116
(c) Optical Properties 119

(D) DISCUSSION 121

CHAPTER VI STUDIES ON THERMALYY EVAPOHATEL NIOBIUM OXIDE FILMS

(A) INTRODUCTION 125

(B) EXPERIMENTAL 129

(C) RESULTS

(a) Structure 130
(b) Dielectric Properties 131
(c) Optical Properties 136

(D) DISCUSSION 137

CHAPTER VII STUDIES ON VACUUM DEPOGITED INDIUM OXIIDE FILMS

(A) INTRODUCTION 149

PART A

(B) EXPERIMENTAL 153

CHAPTER VII Page

(C) RESULTS

(a) Structure 154
(b) Dielectric Properties 154
(c) Optical Properties 158

(D) DISCUSSION 160

PART B

(B) EXPERIMENTAL 165

(C) RESULTS

(a) Structure 167
(b) Dielectric Properties 167
(c) Optical Properties 171

(D) DISCUSSION 173

SUMMARY AND CONCLUSIONS 176

ACKNOWLEDGEMENTS

REFERENCES i - xiii

CHAPTER I

GENERAL INTRODUCTION

(A) Thin films, their nature, structures and properties

It is over a century, that Grove (1852) studied the glow discharge at reduced gas pressures and observed sputtering of the cathode by positive ion bombardment and the deposition of a metal film on the glass enclosure. Since then, the study of thin films has come a long way. Today the study of thin films has ceased to be of mere casual academic interest. The phenomenal rise in the investigations of the properties of these two dimensional solids is due to their extensively wide applications in electronic, optical, plastic, textile, aircraft and defence industries. Intensive researches in this field have been rewarded in the form of useful inventions such as a variety of active and passive microminiaturised components and devices, solar cells, radiation sources and detectors, magnetic memory devices, piezo electric transducers, cryotrons, bolometers, interference filters, reflection and antireflection coatings and many others.

An ideal film is generally regarded as bound by two parallel planes extended infinitely in two directions

but is restricted along the third direction (i.e. thickness) which is perpendicular to the other two. The thickness of such films may vary from one atomic layer to a few times the wavelength of light or more, but always remaining less than the other two dimensions. In reality, however, solid films deviate very much from the idealised case since the two surfaces (planes) are unlikely to be exactly parallel due to the growth conditions of the deposits, and also because the material contained between the two may not be the same and/or uniformly distributed. Numerous defects such as voids, discontinuities, impurities, grain boundaries, dislocations, surface asperities, etc. are often predominant in the growing film unless the deposition is made in an idealised condition, which is generally not feasible in reality; even then, these cannot altogether be eliminated.

Films can be prepared by various methods, namely, chemical depositions, electrodeposition, cathodic sputtering (reactive or otherwise), anodic oxidation, electron beam or laser bombardment, pyrolysis, vacuum evaporation, etc. Of these the last method is commonly used because of its simplicity. It is now well known that various film properties such as mechanical, optical,

electrical, dielectric, structural, etc. are influenced by the purity of the material, but more so by the preparative conditions of these films. Some of the latter factors which affect the physical properties of solid films are the rate of deposition, substrate temperature, cleanliness of the substrate, film thickness, ambient gas pressure, annealing, phase transition, morphological features of the deposits, grain size, etc. Thus it was shown by Mayer (1959, 1961), Neugebauer and Webb (1962) that alkali metals like potassium, sodium, rubidium, cesium, etc. and noble metals such as gold, platinum, etc. with positive temperature coefficient of resistance, behaved like semiconductors showing negative temperature coefficient of resistance in the thin film form. Similarly thin bismuth films unlike the bulk exhibit superconductivity at low temperatures (Buckel and Hilsch, 1954).

The growth mechanism of these films from the vapour phase involves several processes, namely, the impingement of vapour molecules on the substrate, adsorption and sticking of them to it, recrystallisations, surface migration, cluster formation, reevaporation in a finite time and sometimes the complete bouncing off of the vapours from the surface, etc. Depending upon the deposition conditions, such as the rate of deposition,

substrate temperature, etc., some of the above processes become more predominant over the others. According to Pashley et al (1964), the growth of films from their initial nucleations to the continuous film state may be visualised by the following stages: (i) nucleation and island structure, (ii) coalescence stage of the islands, (iii) elongated growth of the islands to form a continuous network structure in which the deposited material is separated by long, irregular and narrow channels (channel stage) and (iv) the continuous film formed by the bridging of these channels. It may be mentioned here that films even in the last stage may also have some voids. Many of the physical properties of thin films are structure sensitive. Pashley (1959), Mathews (1959), Phillips (1960) and several other workers have already shown the presence of many defects viz. dislocations, stacking faults, voids, impurities, etc. in the deposited films. These defects play a predominant role in the electrical (Mayer, 1959), dielectric (Weaver, 1965; Harrop and Wanklyn, 1965; Argall and Jonscher, 1968) mechanical (Campbell, 1970), optical (Heavens, 1955) and other properties of these films.

Although extensive work has been carried out on

these properties for the bulk material (Shockley, 1950; Smyth, 1955; Frohlich, 1958; Moss, 1959; Kittel, 1966), it is only recently that special interests have been taken for the study of thin film properties (Heavens, 1955; Holland, 1958; Axelrod, 1968; Chopra, 1969; Vratny, 1969; Maissel and Glang, 1970). Our interest in the present investigations would be mostly on dielectric and optical behaviour of vacuum deposited films. In the following sections the general theories for these have briefly been summarised.

(B) Dielectric Properties

The study of dielectric materials sprang from the practical need of insulators, and with the advent of microelectronics in the recent years, the properties of these materials have been studied more closely for their increasing practical demands in both active and passive circuits. Dielectric properties such as the storage of electrical and magnetic energy are observed for solids, as well as for liquids and gases. In the present investigations, however, we shall restrict our work mainly to solids particularly in the form of thin films. These materials have resistivities ranging between 10^4 to 10^{13} ohm cm or greater, thus embracing materials having large forbidden band gap which could

include both semiconductors and insulators.

(i) General theory of dielectrics

Coulomb's law introduces the concept of permittivity as

$$\bar{F} = \frac{1}{4\pi} \cdot \frac{q_1 q_2}{\epsilon r^2} \cdot \bar{n} \text{ newtons (in MKS units)} \quad .. (1.1)$$

where $\bar{F}$ is defined as the force between the charges q_1 and q_2 and $\bar{n}$ is a unit vector pointing from one charge directly away from the other. r is the distance between the charges and ϵ is a constant defining the inherent property of the medium called its permittivity and has the dimensions of farads/metre. Another way in which the permittivity (ϵ) of a medium enters into the physical laws is through one of the well known Maxwell's material equations (to be mentioned later),

$$\bar{D} = \epsilon \bar{E} \quad .. \quad .. \quad (1.2)$$

where $\bar{D}$ is the displacement vector or the electrical flux density of the dielectric when kept in an electrical field $\bar{E}$.

Now if a capacitor made of parallel plates of area 'a' (metres)^2 and separated by a distance d (metres)

apart in vacuum, carries a charge Q due to a potential V applied between the plates, then from a scalar equation of the form (1.2) (Anderson, 1964) we have,

$$\epsilon = \frac{D}{E} = \frac{Q/a}{V/d}$$

But Q/V = C (capacitance in farads)

$$\therefore \quad \epsilon = \frac{C \times d}{a} \text{ farads/metre} \quad .. \quad (1.3)$$

which in the case of vacuum would have a value,

$\epsilon_o = 8.85 \times 10^{-12}$ farads/metre or $\frac{10^{-9}}{36}$ m.k.s. units.

(ii) Relative permittivity

The term relative permittivity ϵ_r is defined as

$$\epsilon_r = \epsilon/\epsilon_0 \quad .. \quad .. \quad (1.4)$$

where ϵ_r is a pure number. This is also referred to as the apparent dielectric constant. If now the parallel plate condenser has a capacitance C_o in air, and the space between the plates is filled by a medium of permittivity ϵ_r, then neglecting fringing effects the capacitance becomes $C = \epsilon_r C_o$.

(iii) Dielectric loss

When a dielectric is subjected to an alternating field $E = E_o \cos \omega t$, then the displacement or electric flux density D will also vary in the same fashion but lags behind in phase relative to E so that the scalar equation becomes,

$$D = D_o \cos(\omega t - \delta) = D_1 \cos \omega t + D_2 \sin \omega t$$

where δ is the phase angle. Then

$$D_1 = D_o \cos \delta \quad \text{and} \quad D_2 = D_o \sin \delta \qquad .. \qquad (1.5)$$

For most dielectrics though D_o is proportional to E_o, the ratio D_o/E_o is generally frequency dependent. Hence the above equations are modified to introduce two frequency dependent dielectric constants viz.

$$\epsilon'(\omega) = D_1/E_o = D_o/E_o \cos \delta \qquad .. \qquad (1.6a)$$

$$\epsilon''(\omega) = D_2/E_o = D_o/E_o \sin \delta \qquad .. \qquad (1.6b)$$

These can now be expressed by a single complex dielectric constant (ϵ_r^*) where

$$\epsilon_r^* = \epsilon' - j\epsilon'' \qquad .. \qquad (1.7)$$

The loss factor of such a capacitor is then given as

$$\tan \delta = \frac{\epsilon''}{\epsilon'} \qquad .. \qquad (1.8)$$

and is sometimes referred to as the ratio of the loss current due to the resistance of the medium between the plates to the charging current of the capacitor. In case of a loss free medium ϵ'' is zero.

Another important parameter which gives a measure of the performance of the dielectric as an insulator is the dielectric conductivity (σ_D), where,

$$\sigma_D = \omega \epsilon_0 \epsilon'' \qquad .. \qquad (1.9)$$

represents the sum of all the loss mechanisms in the material. This conductivity may be caused by the actual migration of charge carriers, or by some other sources such as the orientation of dipoles etc. (See Polarisation).

(iv) Polarisation

It is well known that a dielectric material increases the storage capacity of a capacitor by neutralising some of the free charges at the electrodes which would otherwise contribute to the potential difference opposing the charging voltage. This can be

visulised as arising from the alignment of the electrostatic dipoles (with positive charge at one end and negative at the other) in the medium under the influence of the applied field and the binding of the counter charges with their free ends on the metal surfaces (Von Hippel, 1967). In doing so more charge can flow into the condenser which now has an increased storage capacity given by

$$C = \epsilon_r C_o$$

where C_o is the original capacity in air. This phenomenon is known as dielectric polarisation and was first discovered by Faraday (1837-1838). Polarisation can be written in a vector form $\overline{P}$ and is related to $\overline{D}$ and $\overline{E}$ as

$$\overline{D} = \epsilon_o \overline{E} + \overline{P} \quad \text{(for vacuum)}$$

However, for a dielectric material of permittivity ϵ' this reduces to

$$\overline{P} = \epsilon_o (\epsilon' - 1) \overline{E} \qquad .. \quad (1.10)$$

$\overline{P}$ is also known as the dipole moment per unit volume of the material and is expressed as

$$\overline{P} = N \hat{\overline{p}} \quad .. \quad (1.11)$$

where $\hat{\overline{p}}$ is the average dipole moment due to the charged particles, and N is the number of dipoles. Since $\overline{p}$ is assumed to be proportional to the electric field <u>inside</u> the dielectric, then $\overline{E}_{int}$ ($\neq$ applied field $\overline{E}$) is the value of field acting on the dipoles, we can define $\overline{p}$ as

$$\overline{p} = \alpha \overline{E}_{int} \quad .. \quad (1.12)$$

where α is the polarisability of the dipole. Thus the relation

$$\overline{P} = (\epsilon' - 1) \epsilon_o \overline{E} = N \alpha \overline{E}_{int} \quad .. \quad (1.13)$$

known as the Clausius equation, links the macroscopically measured permittivity to three molecular parameters viz. N, α and E_{int}. A study of these parameters helps in the understanding of the phenomenon of polarisation and its dependence on the frequency, temperature and applied field strength.

From equation (1.12) it can be seen that permittivity (ϵ') is determined by the polarizability (α) of the constituent charges or ions and is little affected by the structure of the material. Hence

permittivity of thin films should also exhibit values similar to those of bulk materials from which the film is made.

There are in general four mechanisms that contribute to the value of α.

(a) Electronic polarisation (α_e)

This arises from the displacement of the electron cloud in an atom relative to the nucleus viz. from the deformation of the electronic shell about the nucleus. In such cases the polarisability per unit volume (mole) is given by the Lorentz equation at optical frequencies as,

$$\Pi = \frac{N_0 \alpha}{3 \epsilon_0} = \frac{n^2 - 1}{n^2 + 2} \cdot \frac{M}{\rho} \qquad \ldots \quad (1.13)$$

where N_0 is the Avogadro's number, M is the molecular weight of the material, ρ is its density and n is the refractive index. These materials show little absorption in the infrared region and hence α obtained at optical and radio frequencies should yield the same value. In other words one would obtain the square of the refractive index (n^2) of the material at optical frequencies to be equal to the dielectric constant of the material at low

frequencies. Dielectrics having single type of atoms whether solids, liquids or gases, and group IV elements such as C, Si and Ge exhibit electronic polarisability (Harrop and Campbell, 1970).

(b) Ionic polarisation (α_a)

This arises from the displacement of ions of opposite signs when an electric field is applied and also from the deformation of the electron shells of the ions as a result of the motion of the ions. In general, solids containing more than one type of atom, but no permanent dipoles, exhibit ionic polarisation e.g. alkali halides.

In such materials absorption takes place in the infrared and the square of the refractive index is not equal to the low frequency or static dielectric constant. The difference $\Delta\epsilon$ between the static and optical dielectric constants is ascribed to the ionic polarisability, and has been shown by Born that

$$\Delta\epsilon = \frac{2\pi e^2}{\omega_o^2 a^3}\left(\frac{1}{m} + \frac{1}{M}\right) \quad .. \quad (1.14)$$

where 'e' is the electronic charge, 'ω_o' is the infrared

frequency absorption, 'a' is the lattice constant and m M are the masses of the respective ions (Kittel, 1966). In the case of ionic crystals polarisation P is given as

$$P = \frac{e^2 E_o}{2 \omega_o^2 a^3} \left(\frac{1}{m} + \frac{1}{M}\right) \quad .. \quad (1.15)$$

where E_o is the field.

(c) <u>Orientational polarisation</u>

The orientational or dipolar polarisation, giving rise to high dielectric constants, arises when the substance is built up of molecules possessing a permanent electronic dipole moments which may be more or less free to change orientation in an applied electric field (Debye, 1912). The variation of ϵ' and ϵ'' with frequency is then given by the Debye equations,

$$\epsilon'(\omega) = \epsilon_\infty + \frac{\epsilon_s - \epsilon_\infty}{1 + \omega^2 \tau^2} \quad .. \quad (1.16a)$$

$$\epsilon''(\omega) = \frac{(\epsilon_s - \epsilon_\infty)\omega\tau}{1 + \omega^2 \tau^2} \quad .. \quad (1.16b)$$

$$\text{and } \tan\delta = \frac{(\epsilon_s - \epsilon_\infty)\omega\tau}{\epsilon_s + \omega^2 \tau^2} \quad .. \quad (1.16c)$$

where ϵ_s and ϵ_∞ are the static and high frequency dielectric constants, ω is the angular frequency and τ is the relaxation time or the time interval characterising the restoration of a disturbed system to its equilibrium configuration. The maximum value of $\tan\delta$ is obtained when $\omega\tau = 1$, i.e. when $\omega = 1/\tau$ is the relaxation frequency. For frequencies $\ll \frac{1}{\tau}$, ϵ' is equal to the static dielectric constant. At this frequency, the loss vanishes and the dipoles contribute their full share to polarisation. On the other hand, for frequencies larger than $1/\tau$ the dipoles are no longer able to follow the field variations and ϵ' approaches ϵ_∞.

(d) Interfacial polarisation (α_i)

In real crystals and more so in case of thin films there exists a large number of defects such as lattice vacancies, impurity centres, dislocations, etc. Under the influence of an applied field free charge carriers migrating through the crystal may be trapped or pile up against such defects. This may cause the creation of a localised accumulation of charge which will induce its image charge on an electrode and thus giving rise to a dipole moment. This mechanism is known as interfacial polarisation. Vacuum deposited thin film

dielectrics are more likely to show this type of polarisation on account of the large concentration of defects that are generally present in the film (Sutton, 1964; Argall and Jonscher, 1968). The Maxwell-Wagner theory gave a classical treatment for this type of polarisation. Anderson (1964) treats this as a parallel plate condenser with two dielectric slabs of thicknesses d_1 and d_2, permittivity ϵ_1 and ϵ_2, resistances R_1 and R_2 and relaxation times τ_1 and τ_2. The real and imaginary parts of the dielectric constant therefore become,

$$\epsilon' = \epsilon_\infty + (\epsilon_s - \epsilon_\infty)/(1 + \omega^2\tau^2) \quad .. \quad (1.17a)$$

and

$$\epsilon'' = \left[\omega C_o (R_1+R_2)\right]^{-1} + (\epsilon_s - \epsilon_\infty)\,\omega\tau/(1+\omega^2\tau^2) \quad .. \quad (1.17b)$$

where τ is the relaxation time of the total system and C_o is the capacity without the dielectric.

Although ϵ' varies in the same manner as in the case of Debye equations, ϵ'' however tends to infinity as $\omega \to 0$. Thus below the relaxation frequency $\omega\tau = 1$, loss continuously increases.

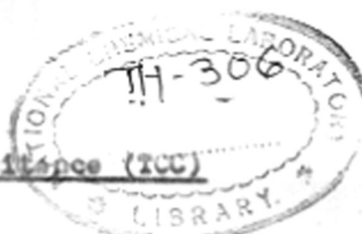

(v) Temperature coefficient of capacitance (TCC)

The temperature coefficient of capacitance γ_c is an important parameter for assessing the application of bulk materials as well as films in different circuits. TCC (γ_c) is defined as

$$\mathrm{TCC}\ (\gamma_c) = \frac{1}{C}\ \frac{dC}{dt} = \gamma_p + \beta \quad .. (1.18)$$

where $\gamma_p = \frac{1}{\epsilon}\ \frac{d\epsilon}{dt}$ and β is the linear expansion coefficient of the dielectric. According to Gevers (1946) loss factor ($\tan\delta$), permittivity (ϵ), polarisability (α_m), γ_c and β are related as

$$\gamma_c = \frac{(\epsilon - 1)(\epsilon + 2)}{3\epsilon\alpha_m}\left(\frac{\partial\alpha_m}{\partial T}\right) - \beta\frac{(\epsilon - 1)(\epsilon + 2)}{\epsilon} + A\tan\delta + \beta \quad .. (1.19)$$

for intrinsic contribution to permittivity i.e. when permittivity due to the structural defects of the material are absent. It may be mentioned here that permittivity due to interfacial polarisation and dipolar orientations is not intrinsic.

539.234:537.226(043)
GOS

For extrinsic contributions to permittivity

$$\gamma_c = A \tan\delta + \beta \qquad .. \qquad (1.20)$$

where A is a constant. These relations have been experimentally verified for bulk ceramics (Cockbain and Harrop, 1968) as well as for thin films (Harrop and Campbell, 1968).

(vi) <u>Frequency dependent behaviour of tan δ in thin films</u>

The dependence of tan δ on frequency in case of orientational and interfacial polarisation has already been briefly mentioned. Peaks in loss factor have been found for films of SiO (Argall and Jonscher, 1968) and many alkali halides (Weaver, 1965; Macfarlane and Weaver, 1966) at low frequencies, say near 0.01 Hz, and these have been attributed to the interfacial polarisation. Peaks in dielectric loss are rare between 100 Hz and 1 MHz and when found especially at low temperatures have often been ascribed to the relaxation of pairs of point defects, examples being fluorine in ZrO_2 films (Harrop and Wanklyn, 1964) and Si in SiO_2 films (Burkhardt, 1966). At higher frequencies peaks are caused by the structural vibrations as observed in polymer films (Mikhailov and Borisova, 1964). In all cases these peaks shift to higher

frequencies as the temperature is raised.

Dielectric losses invariant with frequency have also been observed in many dielectric films. Several models have been put forward to explain this cause. Initially it was thought that such a loss in a dielectric arises due to pinholes in the deposited films, but this speculation has been rejected by Harrop and Campbell (1968) on the ground that tan δ shows some correlation with the forbidden energy gap of the dielectric. Young (1961) suggested that the loss was due to an exponential variation of conductivity through the thickness of the film. However the slightest deviation from the exponential law caused the model to breakdown.

The model proposed by Simmons and coworkers (1970) has been able to explain both qualitatively and quantitatively the a.c. behaviour of vacuum deposited highly doped M_gO_3 films, by assuming the presence of an added series capacitance due to Schottky barriers at the electrode-dielectric interface. However, very recently we (Goswami and Goswami, 1973) have proposed a capacitor model comprising of an inherent capacitance in parallel with the dielectric resistance and in series with a very small lead resistance. This has proved to be effective in explaining the a.c. behaviour of ZnS films.

(vii) Breakdown voltage and dielectric field strength

Breakdown voltage (V_B) and dielectric field strength (F_B) are two important parameters of a dielectric material. This represents the voltage or the electrical field the dielectric can withstand before succumbing to a large conduction in the material. This problem in case of thin films is complicated because of the presence of asperities, weak spots and flaws (Klein, 1966; 1967) and stresses (Campbell, 1970) present in the deposited film. However some of the mechanisms which may cause such a breakdown are (i) electron avalanching by impact ionisation of the lattice, (ii) collective breakdown by electron-electron interaction, (iii) breakdown from ionic transport, (iv) Joule heating breakaway, etc.

Mechanism (ii) suggested by Frohlich and Paranjape (1956) seems to be unlikely in good amorphous insulators as the number of electrons necessary ($> 10^{14}/cm^3$) for this process is too large compared to the number actually available. Mechanism (iii) is also not possible as it requires the destruction of the electrodes by the build up of ions and this occurs only after long periods (Cooper, 1966). Breakdown observed is therefore most likely to be due to mechanisms (i) and (iv).

Zener (1934) suggested tunnelling between the valence and conduction bands, but this was found to be restricted to very thin films only, say less than 20 Å. Forlani and Minnaja (1964) considered the growth of the electron current by collision ionization when the initiating electrons are injected by field emissions at the cathode. They observed that the field strength followed the relation

$$F_B = Ad^{-\beta} \quad .. \quad (1.21)$$

for a given solid or film, where $1/2 \leq \beta \leq 1/4$, d is the film thickness and A is a constant. Klein et al (1966, 1967), on the other hand, have dealt with breakdowns caused by Joule heating.

(C) Optical Properties

The growth of interest in the optical properties of thin solid films has arisen because of their extensive applications in various optical and electro-optical devices. These studies also offer a relatively simpler technique to probe into the electronic and band structures of a material, their degeneracy, energy band gap, lattice bonding and a host of other informations. In the subsequent paragraphs we shall discuss some of the important

optical properties of materials that arise chiefly because of the interaction of the electromagnetic radiation with the charged particles in the material.

(i) Electromagnetic wave

Maxwell's mathematical treatment of the electromagnetic field theory has for the first time showed a connection between electromagnetism and optics. The space and time derivatives of the different vectors are related by Maxwell's material equations which hold at every point in whose neighbourhood the physical properties of the medium are continuous. The equations are,

$$\text{Curl } \bar{H} = \frac{1}{c} \cdot \frac{\partial \bar{D}}{\partial t} + \frac{4\pi \bar{J}}{c} \qquad .. \quad (1.22a)$$

$$\text{Curl } \bar{E} = -\frac{1}{c} \cdot \frac{\partial \bar{B}}{\partial t} \qquad .. \quad (1.22b)$$

$$\text{Div } \bar{E} = 4\pi\rho \qquad .. \quad (1.22c)$$

$$\text{Div } \bar{B} = 0 \qquad .. \quad (1.22d)$$

where $\bar{E}$ is the electrical field, $\bar{H}$ is the magnetic field, $\bar{D}$ is the displacement caused by $\bar{E}$, $\bar{B}$ is the magnetic induction and $\bar{J}$ is the electric current density; the

scalar ρ is the electric charge density and c is the velocity of light. The above vectors are further related by

$$\bar{J} = \sigma \bar{E}, \bar{D} = \epsilon \bar{E} \text{ and } \bar{B} = \mu \bar{H}$$

where σ is the specific conductivity, ϵ is the permittivity (or dielectric constant) and μ is the magnetic permeability of the medium.

With the help of these equations, Maxwell arrived at the wave equations of the electromagnetic field, viz.

$$\frac{\partial^2 \bar{E}}{\partial x^2} = \epsilon \mu \frac{\partial^2 \bar{E}}{\partial t^2} \quad .. \quad (1.23a)$$

$$\frac{\partial^2 \bar{H}}{\partial x^2} = \epsilon \mu \frac{\partial^2 \bar{H}}{\partial t^2} \quad .. \quad (1.23b)$$

The solution of the differential equations (1.23a and b) is a plane wave,

$$\bar{E} = \bar{E}_o \exp (j\omega t - \gamma x) \quad .. \quad (1.24a)$$

$$\bar{H} = \bar{H}_o \exp (j\omega t - \gamma x) \quad .. \quad (1.24b)$$

varying periodically in time with a frequency $\nu = \omega/2\pi$ and moves in the +x direction with a complex propogation factor,

$$\gamma = j\omega(\epsilon\mu)^{1/2} = \alpha + j\beta \quad .. \quad (1.25)$$

where α is the attenuation factor and β is the phase factor. The phase velocity of the wave is then given as

$$\vartheta = 1/(\epsilon\mu)^{1/2} \quad .. \quad (1.26)$$

In vacuo this wave travels with a phase velocity equal to that of light (c), but slows down in any other medium so that the ratio of the two phase velocities gives the refractive index 'n' of the medium as (equation 1.26),

$$n = (\epsilon\mu)^{1/2} \quad .. \quad (1.27)$$

It may be mentioned here that since the dielectric constant is a complex quantity as explained earlier, ϵ in the above equations should actually be replaced by ϵ^*. By a similar analogy it can be shown that permeability (μ) too is a complex quantity and hence should be replaced as μ^*. For a loss free non magnetic material, $\mu = 1$ so that the equation (1.27) reduces to

$$n^2 = \frac{\epsilon'}{\epsilon_o} = \epsilon' \qquad .. \quad (1.28)$$

Similarly one defines the absorption index (k) as the attenuation per unit radian, viz.

$$k = \frac{\alpha \lambda}{4 \pi} \qquad .. \quad (1.29)$$

where λ is the space period defining the distance the wave moves in a periodic time, and α which was previously called the attenuation of the wave is now known as the absorption coefficient. The latter is given by Lambert's law

$$I = I_o \exp(-\alpha x)$$

where x is the distance through which the electromagnetic wave travels to change its intensity from I_o to I.

The above relations clearly show that both the dielectric constants (ϵ' and ϵ'') and the optical constants (n and k) are interrelated. As a consequence of equations (1.25) and (1.28) the refractive index is very often expressed as a complex quantity n^* where

$$n^* = (n - jk) \quad .. \quad (1.30)$$

This is analogous to the complex dielectric constant ϵ^*. Since both n^* and ϵ^* are related by equations similar to (1.28), we then have

$$\epsilon' = n^2 - k^2 \quad .. \quad (1.31a)$$

and

$$\epsilon'' = 2nk \quad .. \quad (1.31b)$$

ϵ' and ϵ'' are then known as the optical dielectric constants of the material. In case of a nonmagnetic material n and k are related to ϵ' and $\tan\delta$ as (von Hippel, 1967)

$$n = \left[1/2 \, \epsilon' \left\{ \sqrt{1+\tan^2\delta} + 1 \right\} \right]^{1/2} \quad ..(1.32a)$$

and

$$k = \left[\frac{\sqrt{1+\tan^2\delta} - 1}{\sqrt{1+\tan^2\delta} + 1} \right]^{1/2} \quad ..(1.32b)$$

(ii) <u>Dispersion of the electromagnetic wave by a dielectric</u>

Maxwell's equations show that refractive index (n) which is equal to the square root of the dielectric constant (ϵ) is invariant at all frequencies (1.28) as

the latter is a constant quantity. This is in contrast to actual observed experimental results. Hence ϵ^* must be a function of the applied frequencies. This can be explained from the atomic structures of the materials.

In the case of dielectric materials, one generally considers the interaction of the electromagnetic wave with the bound charges in the dielectric. Under the influence of the applied field (electromagnetic radiation) the bound electrons are displaced from its equilibrium position. Assuming a restoring force proportional to the displacement x, and a damping force (due to the scattering of the electromagnetic wave by electrons, or collisions with the lattice) proportional to the velocity $\frac{dx}{dt}$; then if the restoring force is given by $m\omega_o^2 x$ and the damping be $mg\frac{dx}{dt}$, the equation of motion of the electron becomes,

$$m\frac{d^2x}{dt^2} + mg\frac{dx}{dt} + m\omega_o^2 x = eEe^{j\omega t} \quad .. \quad (1.33)$$

where $Ee^{j\omega t}$ is the applied electromagnetic field and ω_o is the natural frequency of the electrons. The solution of this equation shows that 'x' varies sinusoidally with the applied frequency with an amplitude given by

$$x = \frac{eE/m}{\omega_o^2 - \omega^2 + j\omega g} \quad .. \quad (1.34)$$

Now if there are N electrons per unit volume, the polarisability will be $P = Nex/E$ so that the dielectric constant (ϵ^*) given by $1+P/\epsilon_o$ (MKS units) becomes (Moss, 1959),

$$\epsilon^* = (n-jk)^2 = \frac{Ne^2/m\epsilon_o}{\omega_o^2 - \omega^2 + j\omega g} + 1$$

$$\text{or } n^2-k^2 = \left(\frac{Ne^2}{m\epsilon_o}\right)\left\{\frac{\omega_o^2 - \omega^2}{(\omega_o^2-\omega^2)^2 + \omega^2 g^2}\right\} \quad .. \quad (1.35)$$

$$\text{and } 2nk = \left(\frac{Ne^2}{m\epsilon_o}\right)\left\{\frac{\omega g}{(\omega_o^2-\omega^2)^2 + \omega^2 g^2}\right\} \quad .. \quad (1.36)$$

The above formulae show that in the neighbourhood of $\omega = \omega_o$ there is an absorption maximum and that n increases rapidly with decreasing ω through this region. With continuing decrease in ω, n passes through a maximum and then falls asymptotically as the frequency gets further away from ω_o.

A more detailed quantum mechanical treatment of dispersion (Rosenfeld, 1951; Mott and Jones, 1936; Nozieyes and Pines, 1958), where the interaction of the field and absorbing atom are also taken into account, leads to the following equations

$$n^2 - k^2 - 1 = \sum_p \frac{(Ne^2 f_p / m \epsilon_o)(\omega_p^2 - \omega^2)}{(\omega_p^2 - \omega^2)^2 + (\omega^2 g_p)} \quad .. \quad (1.37)$$

$$\text{and } 2nk = \sum_p \frac{(Ne^2 f_p / m \epsilon_o)\, \omega\, g_p}{(\omega_p^2 - \omega^2)^2 + \omega^2 g_p^2} \quad .. \quad (1.38)$$

having close similarity with those obtained by the semiclassical treatment. It is now possible to obtain the static dielectric constant of materials from the optical data alone (Moss, 1959), because at very long wavelengths viz. when $\omega \rightarrow 0$, k in (1.35) becomes insignificant and the equation reduces to,

$$n_o^2 - 1 = Ne^2 f / m \epsilon_o \omega_o^2 \quad .. \quad (1.39)$$

Using Bode's (1945) formulae, it can be shown that at any

frequency 's', the real $(n^2 - k^2)$ and imaginary (2nk) parts of the dielectric constant are given as,

$$(n^2 - k^2)_s - 1 = \frac{2}{\pi} \int_0^\infty \frac{2nk\,\omega - s(2nk)_s}{\omega^2 - s^2}\, d\omega$$

$$\text{and } (2nk)_s = \frac{-2s}{\pi} \int_0^\infty \frac{n^2 - k^2 - (n^2 - k^2)_s}{\omega^2 - s^2}\, d\omega \qquad \text{.. (1.40)}$$

At zero frequency (s = 0) for a nonconducting medium ($k_o = 0$) the above formula reduces to (Moss, 1959)

$$n_o^2 - 1 = \frac{2}{\pi} \int_0^\infty 2nk \frac{d\lambda}{\lambda} \qquad \text{.. (1.41)}$$

Moss (1953) integrated graphically $\frac{2nk}{\lambda}$ over a wide range of λ and computed n_o for PbTe, Si and Ge. These values agreed well with the experimental values of n_o obtained from the audio frequency measurements of dielectric constant.

(iii) <u>Dispersions in metals and semiconductors</u>

In the case of metals the electrons are no longer

bound but are free to move thus giving rise to a large conductivity. If the classical treatment (equations 1.35 and 1.36) is applied, then in the absence of a restoring force we shall have,

$$n^2 - k^2 - 1 = \frac{Ne^2/m\epsilon_o}{\omega^2 + g^2}$$

$$\text{and } 2nk = g\,\frac{Ne^2/m\epsilon_o}{\omega^2 + g^2} \quad .. \quad (1.42)$$

In a steady field the latter equation can be rewritten as (Moss, 1959),

$$2nk = \left(\frac{\sigma_o}{\epsilon_o}\right) \Big/ \left[1 + (\omega\mu m/e)^2\right] \quad .. \quad (1.43)$$

where σ_o is the static conductivity and μ is the mobility at the frequencies involved.

In the case of a semiconductor, however, both the bound as well as free electrons interact with the electromagnetic wave and hence the complete expression for 2nk will be given by a series of terms like equation (1.38) along with a term like equation (1.43) for each

type of free carrier present. At long wavelengths, however, only the latter term is important.

(iv) Intraband transitions

We have already seen that in insulators and semiconductors the interaction of the incident electromagnetic radiation with the bound and free charges can explain the absorption and dispersion in the spectral region. In case of semiconductors and insulators the valence band electrons are of considerable importance. In the absence of any assistance from thermal energy, i.e. at zero temperature, the only possible absorption that can take place is when the quanta of incident radiation have sufficient energy to excite the valence electrons across the forbidden zone into the empty conduction band. In practice the resulting absorption spectrum is a continum of intense absorption at short wavelengths, bounded by a more or less steep absorption edge beyond which the material is relatively transparent.

If the material or crystal is free from imperfections, then from quantum mechanical treatments and selection rules it can be shown that direct and allowed transitions from the valence band to the conduction band can take place (Brooks, 1955; Bardeen et al, 1956;

Dexter, 1956) only when

α (absorption coefficient) is proportional to

$$(h\nu - E_g)^{1/2} \qquad .. \quad (1.44)$$

where $h\nu$ is the incident energy and E_g is the forbidden energy band gap. If, however, the power index is 3/2 instead of 1/2 then direct but forbidden transition takes place. When the crystal contains defects such as impurities, dislocations, etc., then one has to consider the perturbation in the system due to these defects and also the interaction with the phonons as quanta of the vibrational modes of the crystal lattice. All these perturbations give rise to an additional transition mechanism, called indirect transition which is allowed (Bardeen et al, 1956, 1956) only when

$$\alpha \propto (h\nu - E_g)^2 \qquad .. \quad (1.45a)$$

and forbidden if

$$\alpha \propto (h\nu - E_g)^3 \qquad .. \quad (1.45b)$$

(v) <u>Optical constants of thin films</u>

Since the optical behaviour of a material is

determined principally from its optical constants, viz. refractive index (n) and absorption index (k), it is therefore of utmost importance to determine these accurately. In the case of thin films, however, the film thickness 'd' plays a very important role. Some of the commonly used techniques to determine the optical constants of films are outlined below:

(a) Abbe's refractometer

This instrument which employs the principle of the critical angle theory has been successfully used to compute the refractive indices of many films of thickness 1-2 μ and over. Schulz (1949) showed the remarkable potentialities of this method, from which considerable information about film structure could be obtained. Since we are interested in films $\lesssim$ 5000 Å thick, the above method is not very suitable and some other experimental techniques have to be adopted.

(b) Abele's Method (1950)

Abelè's method makes use of the fact that for light polarised with the electric vector in the plane of incidence, the reflectance of a film of index n, on a substrate of index n_2 at the angle defined by tan ϕ_B = n_1/n_0 (n_0 = refractive index of air) is the same as that

of the uncovered substrate. This method which is independent of the film thickness has been successfully used by many workers (Kelly and Heavens, 1959; Hacskaylo, 1964). Hacskaylo claims an accuracy of ± 0.0002 in the measurement of n using improved light detection techniques.

(c) Polarimetric Method

The refractive index and absorption index can also be calculated from the reflectance data of the parallel (R_p) and perpendicular (R_s) components of a polarised light (Heavens, 1955).

(d) Ellipsometric Method

This is perhaps one of the most widely employed techniques for measuring n and k. Ellipsometry is based on evaluating the change in the state of polarisation of light reflected from a film (Vasicek, 1960; Heavens, 1955; Mayer, 1950). The state of polarisation is determined by the relative amplitudes of the parallel and perpendicular components of the radiation and the phase difference between the two components.

(e) Spectrophotometric Method

This involves the measurement of reflectance and transmittance of films at a near normal angle of incidence

using an unpolarised light. This method, however, requires additional information about the film thickness, refractive index of substrate and the wavelength of the incident light. Although the measurements involves are very simple, this technique requires laborious computations for obtaining the optical constants.

Hadley (1947) has greatly simplified this process by preparing a comprehensive set of curves calculating R and T as a function of d/λ (thickness/wavelength) for a range of values of n producing one set of curves for each of a range of values of k and a given substrate index.

(vi) Normal transmittance and reflectance through a thin film

In the present study, as we shall be utilizing the spectrophotometric method dealing with the normal transmittance and reflectance of films deposited on glass substrates, it would be therefore worthwhile for practical purposes to give an outline of the theoretical treatment for this mechanism.

It has already been shown that the solutions to Maxwells' equations are described by two perpendicular plane waves $\bar{E}$ and $\bar{H}$, the forms of which are given in equations 1.24a and 1.24b. When the electromagnetic wave passes from a medium 'm' to a medium 'm+1', then for the

continuity of the equations to be valid the boundary conditions must be satisfied. Stratton (1941) showed that the magnitude of the electrical and magnetic vectors E_m, H_m in the medium 'm', and E_{m+1} and H_{m+1} in the medium 'm+1' would be determined by the refractive indices and the thicknesses of the media, as well as the wavelength of the incident electromagnetic radiation. However, for a more practical case such as the transmission and reflection through a thin film on a semiinfinite non absorbing substrate (e.g. glass), one generally considers three interfaces namely

(a) air-substrate interface
(b) Substrate-film interface
and (c) film-air interface

Further, reflections and transmissions at all the three interfaces must be taken into account along with the boundary conditions. Harris et al (1951) have dealt with this problem in details. Their analysis shows that the normal transmittance (T_o) and reflectance (R_o) can be written as

$$T_0 = \frac{4 n_b}{\left[(n_b+1)\cos\frac{2\pi d}{\lambda}(n_f+ik_f) - i\left\{\frac{n_b}{n_f+ik_f} + (n_f+ik_f)\right\}\sin\frac{2\pi d}{\lambda}(n_f+ik_f)\right]^2} \quad \text{— (I.46)}$$

and

$$R_0 = \frac{\left[(n_b-1)\cos\frac{2\pi d}{\lambda}(n_f+ik_f) + i\left\{\frac{n_b}{n_f+ik_f} + (n_f+ik_f)\right\}\sin\frac{2\pi d}{\lambda}(n_f+ik_f)\right]^2}{\left[(n_b+1)\cos\frac{2\pi d}{\lambda}(n_f+ik_f) - i\left\{\frac{n_b}{n_f+ik_f} + (n_f+ik_f)\right\}\sin\frac{2\pi d}{\lambda}(n_f+ik_f)\right]^2} \quad \text{— (I.47)}$$

where

- n_f - refractive index of film
- n_b - refractive index of substrate
- k_f - absorption index of film
- d - film thickness
- λ - wavelength of incident light

The above formulae have been utilized by several workers (Hass and Salzberg, 1954; Hass, Ramsey and Thun, 1959) to compute the optical constants of thin films in the infrared, visible and ultraviolet regions. In order to compute the values of n_f and k_f the above equations

have been solved by us by adopting the iterative procedure and the solutions have been shown in Chapter II (Experimental) without including the different steps.

Present work

From the above survey it can be seen that the studies of dielectric and optical properties give an insight into the structure of matter viz. the nature of charges and species constituting the matter, the state of polarisation, band structure, bond strength between atoms, band gap, etc. Even though extensive investigations have been made for the dielectric properties of bulk material, very few studies have so far been carried out on the dielectric properties and much less on the simultaneous studies of dielectric and optical behaviour of thin films. Further, since many of the electrical parameters of thin films have been found to be structure sensitive and also dependent on the evaporation conditions as well as film thickness, it has been felt worthwhile to investigate the influence of these parameters on the dielectric and optical properties and obtain a coherent picture of the electronic and band structure of the vacuum deposited films. With these ideas in view, the following investigations have been undertaken for the dielectric, optical and structural studies of ZnS and also various oxidic films deposited by thermal evaporation techniques.

CHAPTER II

EXPERIMENTAL TECHNIQUES

In order to study the dielectric and the optical properties of thin films, several experimental techniques were adopted and these are described in details in the subsequent paragraphs. Special care was taken in their preparations so that these films were homogeneous, uniform in thickness, structure, etc. The reproducibility of the measurements for different physical parameters was found to be very much facilitated by maintaining the above conditions. As these films were flimsy in nature and very much prone to scratches and pinhole formation due to dust particles, etc., every possible precaution was taken to avoid or minimise them.

(A) Dielectric Properties

(i) Preparation of films

The deposits were generally prepared by the thermal evaporation of the bulk material in vacuo ($\simeq 10^{-6}$ mm of Hg) or by other methods as described in the appropriate chapters. In the thermal evaporation method, a small amount of the bulk material was evaporated directly from molybdenum boats or tungsten filaments

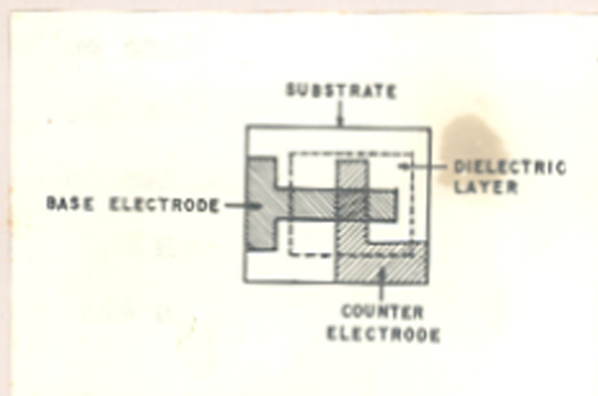

Fig II.1

which were initially flashed to remove the surface contamination if any. Some times special methods had to be adopted to ensure uniform depositions, etc.

(ii) Fabrication of capacitors

'Gold seal' glass slides 2.5x3.0 cm^2 were used as substrates for the preparation of thin film capacitors. These substrates were cleaned with chromic acid solution and then washed with running distilled water for about half an hour. They were then 'fire polished' over a flame and kept in an oven at about 100°C. Occasionally, prior to the actual deposition, the substrates thus cleaned were degassed in vacuo ($\approx 10^{-5}$ mm Hg) at about 200°C for two hours and then cooled down to the room temperature.

Aluminium wire (99.9% purity) was flash deposited in vacuo ($\approx 10^{-5}$ mm Hg) from a multistrand tungsten spiral filament on glass substrates through 'T' shaped masks at room temperature. These films formed the base electrodes of the capacitors. The substrates with aluminium electrodes were then placed in contact with another set of masks through which the dielectric layer was deposited on the base electrodes. In order to have uniform deposition and also to avoid spitting, the dielectric material was initially degassed by slow heating of the powder in vacuo at a low heat which was below the actual

temperature of deposition. The thicknesses of the dielectric films were controlled by adjusting the time and the rate of deposition. The latter was however adjusted by varying the distance between the substrate and the source. The counter electrodes also of thick aluminium films were vacuum deposited cross wise (Fig. II.1) over the dielectric layers so that the effective geometrical area of the capacitors determined by the electrodes was about 0.30 cm^2. These film electrodes were about 100 Å thick and had a resistance less than a few ohms. It may be mentioned here that during the capacitor preparation the vacuum had to be broken at successive stages of deposition.

A special substrate holder with appropriate masks were designed so that the deposition could be made on three glass substrates simultaneously, thus avoiding uncertainties in the deposition conditions. When the dielectric films were deposited at higher temperatures a flat ceramic heater was used for heating the substrates. The temperature was measured by a chromel-p-alumel thermocouple kept in contact with the substrates.

(iii) Ageing

All film capacitors were aged in air for a period of ten to twenty days and the changes in capacitance and

loss factor were also measured. The samples were further stabilised by cyclic heating and cooling in vacuo. These samples were generally stored in an air-tight dessicator.

(iv) Measurement of film thickness

Unlike bulk materials film thickness plays a very important role in the semiconducting, dielectric and optical properties of thin films. The dielectric constant of a deposited layer was evaluated from the knowledge of the capacitance of the sandwiched layer, the effective electrode area and the dielectric film thickness. Similarly the different optical parameters viz. refractive index and absorption index, etc. were computed using appropriate relations wherein the knowledge of the film thickness was essential. Thus the accuracy of the results depended on the precision with which the thickness measurements were carried out.

One of the simplest way of measuring the film thickness is by the weighing method. From the knowledge of the mass of the film deposited and its surface area, the film thickness can be determined assuming the density of the deposited film to be constant and same as that of bulk (Sennett and Scott, 1950; Phillip and Tromptee, 1955; Ramazanov, 1962). Since in the present case the density of most of the materials especially in the film

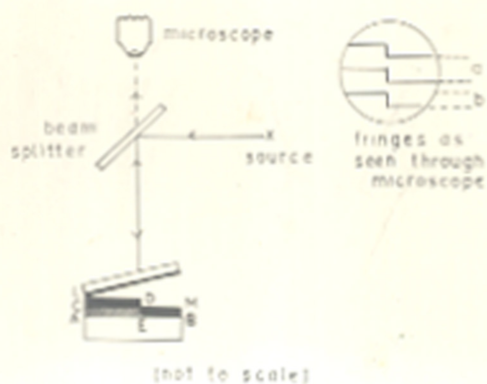

Fig II.2

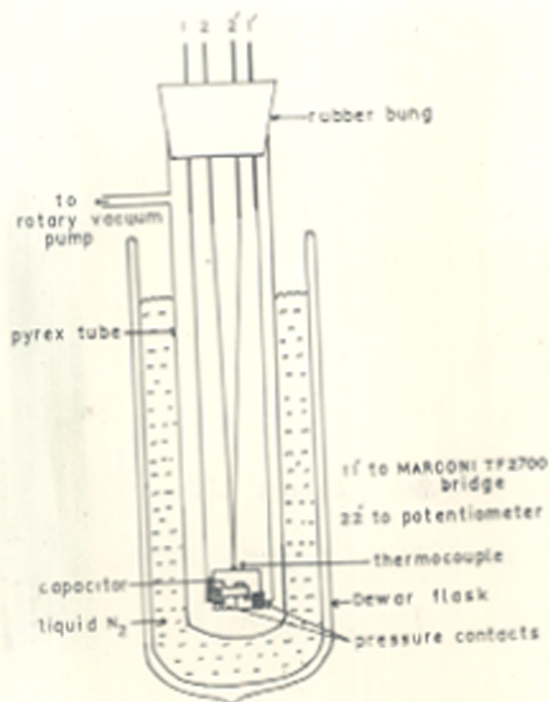

Fig II.3

state is unknown, the error in estimating film thickness by the difference in weight method is often largely magnified. Therefore the multiple beam interferometry method (Tolansky, 1948), was adopted by us for the measurement of film thickness. A simple instrument employing the above technique has been designed and built by us in this laboratory (Fig. II.2).

The substrate AB supports a film ACDE whose thickness is to be measured. Over this an opaque layer CIDMBE of aluminium or silver is evaporated thus forming a step DE. An optically flat glass slice coated with a partially transmitting layer of aluminium or silver is placed in contact with this so that the two plates form a wedge whose angle is very small. A monochromatic light of wavelength 'λ' is reflected by a beam splitter on to the plates and then reflected back normally into a low power microscope (Fig. II.2). Dark fringes can be observed which trace out the points of equal air gap thickness, the fringe distance being $\frac{\lambda}{2}$. By adjusting the relative positions of the plates the fringes could be made to run in straight lines perpendicular to the steps on the opaque film, thus giving rise to a fringe displacement as they pass over this step edge (Fig. II.2). The film thickness (d) is then expressed as

$$d = b\lambda/2a$$

where 'b' is the fringe displacement at the step edge, 'a' is the fringe width and λ is the wavelength of the light used. An instrument designed by us could measure film thickness down to about 70-80 Å. The only assumption made in this method is that the films were uniform in thickness which is in general true if they are carefully prepared.

(v) Cryostat

All dielectric measurements were carried out in a cryostat where the temperature could be varied between 77 to 400°K. The capacitor leads were put inside a glass tube one end of which was closed. A rubber bung through which the leads for the capacitor, thermocouple, etc. were taken out was used to close the other end of the tube and the set-up was continuously evacuated by a rotary oil pump. Short lengths of r.f. cables were used as leads for the capacitance bridge. The cryostat which was kept inside a Dewar flask was cooled by liquid nitrogen. By adjusting the level of the liquid nitrogen in the flask, the temperature of the cryostat could be varied to any desired value (Fig. II.3). An external heater was however used for all measurements to be made above the room temperature.

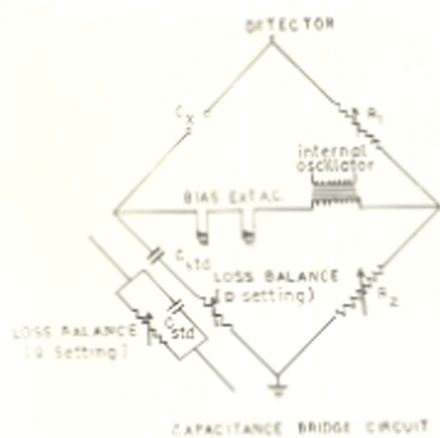

CAPACITANCE BRIDGE CIRCUIT

Fig II.4

(vi) Measurements of capacitance and tan δ

Capacitance (C) and loss factor (tan δ), the two most important parameters in the dielectric study were directly measured by using a Marconi TF2700 universal bridge. The basic capacitance bridge network is shown in Fig. II.4. This is actually a slightly modified form of the Wheatstone bridge circuit where the two resistive arms of the bridge are replaced by the unknown capacitance C_x and a standard capacitance C_{std} having a value of 0.1 µF; R_1 and R_2 are two standard resistances. The bridge is excited by an internal oscillator of 170 mV and 1 kHz and the balance point (null point in this case) is read on a sensitive microammeter. To increase the sensitivity of the null point, the output of the signal is amplified by a three stage transistorised amplifier and this is then rectified and fed to the meter, so that the needle of the meter always deflects to one side of zero for all a.c. measurements. When both the arms of the bridge are balanced then,

$$\frac{C_x}{C_{std}} = \frac{R_2}{R_1} \quad \text{or} \quad C_x = C_{std} \frac{R_2}{R_1}$$

Thus the unknown capacitance (C_x) is evaluated from the ratio of the two resistances and C_{std}. In this instrument

when R_1 and R_2 are properly adjusted the unknown capacitance can be directly read from the dial readings.

The instrument has also a small variable resistance ($0 \rightarrow 175\ \Omega$) connected in series with C_{std} (see Fig. II.4) known as the loss balance resistor which helps to measure the loss factor or $\tan\delta$ directly. The instrument also has two positions i.e. D and Q for measurements of loss factor. In the D position of the bridge the measured quantities are known as C_s and $\tan\delta$. For higher values of $\tan\delta$ the 'Q' range is selected, where the standard capacitance becomes parallel to a larger variable resistance and the measured capacitance (C_p), in 'Q' range, is related to C_s of 'D' range by the relation

$$C_s/C_p = 1 + Q^2 \text{ where } Q = 1/\tan\delta$$

In all our experimental results capacitance has been expressed in terms of C_s only.

The above bridge has also the provision for measuring C and $\tan\delta$ at variable frequencies (100 Hz to 100 kHz) by using an external oscillator (Philips PM 5100). The loss factor is then given as

$$\tan\delta = \tan\delta_f \times \frac{f}{1000}$$

where tan δ_f is the loss measured at any frequency f. This bridge has a sensitivity of about 0.5 pF at 10 pF range and can measure tan δ down to about 0.001.

(vii) Dielectric constant

The capacitance C of a sandwiched layer of thickness d (metres) with the effective geometrical area of the parallel electrodes being 'A' (metre^2) can be expressed as

$$C = 8.85 \times 10^{-12} \epsilon \frac{A}{d} \text{ farads} \qquad .. \qquad (II.1)$$

where ϵ is the permittivity of the sandwiched layer. Permittivity has therefore the dimensions of farad/metre. For practical purposes a dimensionless quantity, namely relative permittivity or dielectric constant, which is the ratio of permittivity of the medium to that in vacuo is used. In the present work this dimensionless dielectric constant term has constantly been used.

(viii) Breakdown voltage (V_B) and dielectric field strength (F_B)

Although there are numerous sophisticated methods available for measuring the breakdown voltage accurately (Budenstein et al, 1967; Klein et al, 1966; 1967) here, however, a simple circuit consisting of a variable d.c.

source (0 → 50 volts), a microammeter in series with the test capacitor and a voltmeter parallel to it has been used. The voltage was slowly increased and the current passing through the condenser is noted. As the voltage approaches the breakdown voltage, a large amount of conduction will take place through the condenser giving a sudden increase in current for a very small change in the applied voltage. The J-V curve is then plotted and through the steepest portion of the curve a straight line is drawn which intersects the voltage axis at V_B. V_B is then taken to be the breakdown voltage. The dielectric field strength F_B is then given as

$$F_B = \frac{V_B}{d} \text{ volts/cm} \qquad .. \qquad (II.2)$$

where d is the thickness of the dielectric layer (in cm).

It may be pointed out here that since both the electrodes of the capacitors were of the same material (aluminium), no appreciable change in the J-V characteristics and hence in V_B was observed when the polarity of the electrodes was reversed.

(B) Optical Properties

(i) Film preparation

For studying the optical properties of thin films, cleaned glass substrates of dimensions about 1.4x3.0 cm^2 and refractive index (n_b) 1.52, were placed on a substrate holder at about 10 to 15 cm above the source. In order to have films of different thicknesses from the same set of evaporation the substrates were spaced apart such that the distance between the source and the substrate varied. After the optical studies were made, the film thickness was estimated by interferometric methods as described before.

(ii) Optical measurements

Optical properties of these films were chiefly studied by transmission and reflection in the visible region (λ 7000 Å to λ 4000 Å). The film thickness studied was in the range of 300 Å to 2000 Å for semi transparent films, and often greater than 3000 Å for transparent films. From the knowledge of transmittance and reflectance at near normal angle of incidence the optical constants n_f (refractive index), k_f (absorption index) and α (absorption coefficient) were estimated.

(iii) Equipment

(a) A double beam Beckman DK2 with an automatic recording arrangement was used for measuring transmittance through the films. This instrument had a maximum error of ± 5 Å in its wavelength calibration, and an error ± 1% for the recorded transmittance value. A Unicam SP500 was also used for measuring transmittance in the visible region. This was however a single beam instrument and had to be operated manually. The range of errors in the Unicam SP500 was of the same order as the Beckman DK2.

(b) Unfortunately these instruments had no arrangement to measure reflectance at near normal angle of incidence which offers a very convenient and precise method for evaluating the optical constants. With this in view, a special spectrophotometer was designed and constructed in this laboratory by Goswami (A.G.). The general features of this instrument which measures reflectance between 20° and 80° angles of incidences have been briefly described by Goswami and Rao (1973). It has been further modified to enable the angle of incidence to vary between 5° and 80° (Fig. II.5a and b).

The spectrophotometer consists of a light source 1, a condensing lens, 2, a polaroid 3, a collimator 4, a

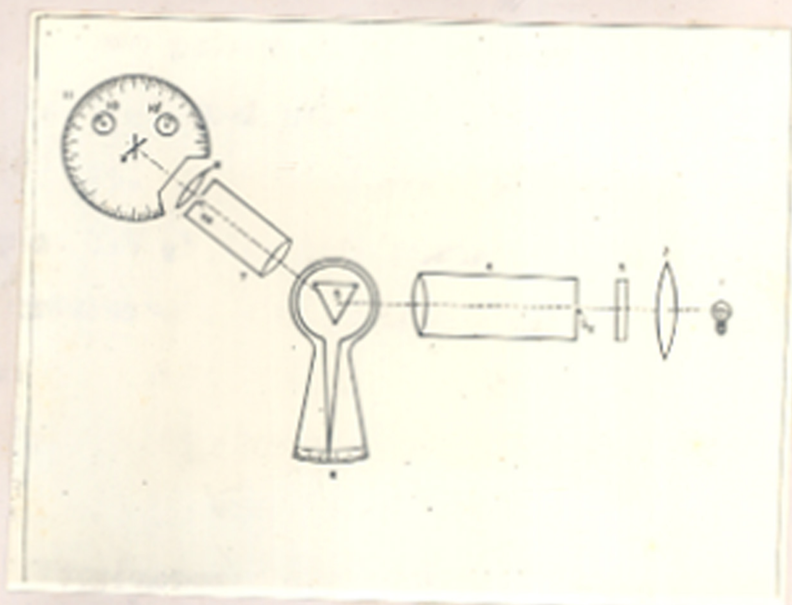

Fig II.5a

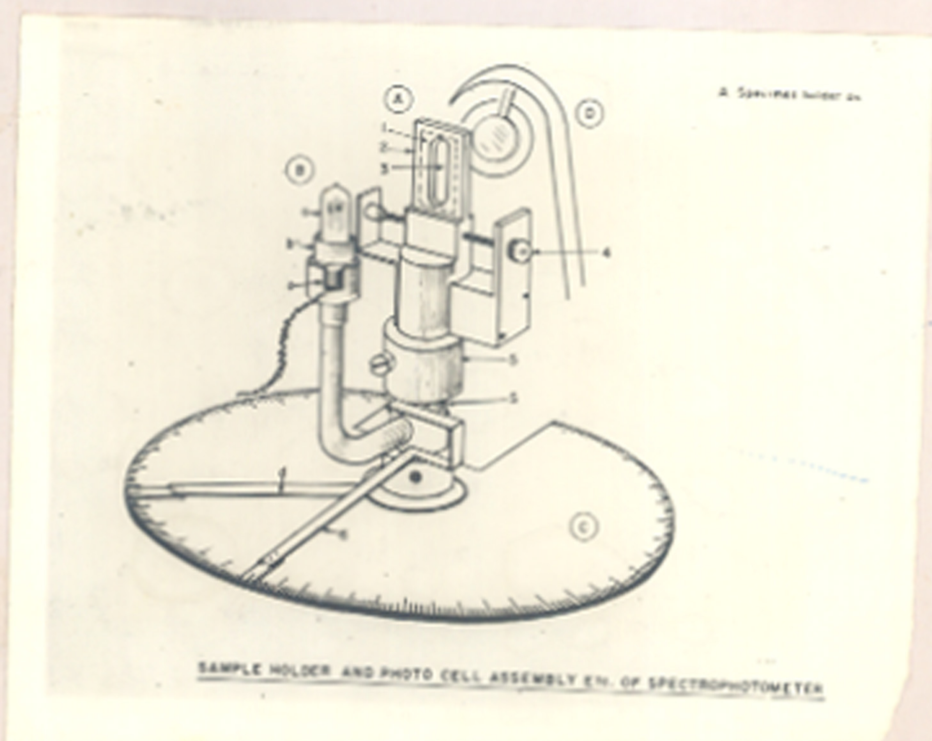

SAMPLE HOLDER AND PHOTO CELL ASSEMBLY ETC. OF SPECTROPHOTOMETER

Fig II.5b

prism 5, on a rotating table moving over a graduated scale 6, a telescope 7, a focussing lens 8, a sample holder 9, a photocell 10 and a graduated disc 11. The light source consisted of a tungsten lamp (10 V, 7.5 amp) which was excited by a high capacity 12 V accumulator or a stabilised power source (0.1% regulation). Both the collimator and the telescope were provided with adjustable slits (S_1 and S_2). The prism 5 can be rotated on the graduated base 6 so as to select the suitable monochromatic light. The sample holder 9 placed nearly at the focus of the second lens 8 can be rotated freely around its vertical axis coinciding with the central shaft of the disc 11 and its portion over the disc (not shown) can be read by a pointer. The photocell placed very close to the sample holder can similarly be rotated around the sample axis say to position 10' and its position similarly recorded (not shown). The intensity of light incident on the photocell (Philips 90 CV or 92 AV) or the photocell current was measured by measuring the potential drop across a 470 K Ohm resistance with the help of a micro voltmeter. The prism scale 6 was calibrated with respect to the wavelength by inserting suitable narrow band width filters in place of polaroid 3, and measuring the maximum intensity of light emerging through the telescope by adjusting the position of the scale 6. The accuracy of the calibration was ± 50 Å.

Necessary precautions were taken to eliminate extreneous light falling on the sample and photocell. The whole instrument was kept in a light proof case. Necessary care was also taken to see that the same position of the photocell was exposed at all angles of incidence.

Since in the normal reflectance method unpolarised light is used, the polaroid 3 was removed from the system. Deposits formed on glass substrates (n_b = 1.52) were placed vertically on the sample holder in such a way that the monochromatic beam was transmitted normally to the film surface, and caught on the photocell behind it at position 10. This was, however, achieved by a suitable adjustment of the positions of the sample holder and also of the photocell so as to obtain a maximum deflection on the microvoltmeter. This then corresponded to the normal incidence of the beam and the zero position of the photocell. The position of the photocell could be read from the graduated disc 11.

To measure reflectance at near normal angles of incidence, say about 10°, the sample and photocell assembly (Fig. II.5a) was shifted about 8 cm away from the collimeter slit S_2, but was kept in line with the optical axis of the system. If the sample holder with the film was shifted by an angle θ around its axis in an

anticlockwise direction, then the reflected light could be obtained at 2 θ by rotating clockwsise the photocell to a position 10'. The minimum angle of incidence so obtained by this instrument was about 3°.

(iv) Measurement of optical constants

The optical constants viz. refractive index (n_f), absorption index (k_f) and absorption coefficient (α) can be computed from reflectance and transmittance data at normal angle of incidence. Since the measurement of reflectance at an exact normal angle of incidence is not possible, a recourse has been adopted to measure reflectance at very small angles of incidence ($\lesssim 12^{\circ}$), and the evaluated n_f and k_f from such measurements do not significantly differ from those of the ideal normal incidence method.

Although there are various methods available for calculating n_f and k_f, in the present study only the spectrophotometric methods which are outlined below have been adopted.

(a) As explained earlier in Chapter I, Harris et al. (1951) applied the Maxwell boundary conditions for a film on glass substrate and obtained the expressions of T_o and R_o (Harris et al, 1951; Hass and Salzberg, 1954) as

$$T_0 = \frac{4n_b}{\left[(n_b+1)\cos\frac{2\pi d}{\lambda}(n_f+iK_f) - i\left\{\frac{n_b}{n_f+iK_f} + (n_f+iK_f)\right\}\sin\frac{2\pi d}{\lambda}(n_f+iK_f)\right]^2} \quad \text{—(II.3)}$$

and

$$R_0 = \frac{\left[(n_b-1)\cos\frac{2\pi d}{\lambda}(n_f+iK_f) + i\left\{\frac{n_b}{n_f+iK_f} - (n_f+iK_f)\right\}\sin\frac{2\pi d}{\lambda}(n_f+iK_f)\right]^2}{\left[(n_b+1)\cos\frac{2\pi d}{\lambda}(n_f+iK_f) - i\left\{\frac{n_b}{n_f+iK_f} + (n_f+iK_f)\right\}\sin\frac{2\pi d}{\lambda}(n_f+iK_f)\right]^2} \quad \text{—(II.4)}$$

These two complex equations have been solved by removing the imaginary terms in the expression with the help of modulus quantities. The complete solution for T_o and R_o involves many steps and hence not given. The final expressions for T_o and R_o then assume the form,

$$\left|\frac{T_o}{4\ n_b}\right|^2 = \frac{1}{\left\{\left[J^2 - k^2\right]^2 + 4J^2 k^2\right\}} \quad .. \quad (II.5)$$

and

$$\left|\frac{R_o\ 4n_b}{T_o}\right|^2 = \left[J'^2 - K'^2\right]^2 + 4J'^2 K'^2 \quad .. \quad (II.6)$$

where

$$J = \left[\left\{ (n_b+1)\,(\cos an_f \cosh ak_f) \right\} + \left\{ \left(n_f + \frac{n_b n_f}{(n_f^2+k_f^2)}\right) \cos an_f \sinh ak_f \right\} - \left\{ \left(\frac{n_b\,k_f}{n_f^2+k_f^2} - k_f \right) \sin an_f \cosh ak_f \right\} \right]$$

$$K = \left[\left\{ (n_b+1) \sin an_f \sinh ak_f \right\} + \left\{ \left(n_f + \frac{n_b\,n_f}{n_f^2 + k_f^2}\right) \sin an_f \cosh ak_f \right\} + \left\{ \left(\frac{n_b\,k_f}{n_f^2+k_f^2} - k_f \right) \cos an_f \sinh ak_f \right\} \right]$$

$$J' = \left[\left\{ (n_b-1) \cos an_f \cosh ak_f \right\} + \left\{ \left(\frac{n_b\,k_f}{n_f^2+k_f^2} + k_f \right) \sin an_f \cosh ak_f \right\} - \left\{ \left(\frac{n_b\,n_f}{n_f^2+k_f^2} - n_f \right) \cos an_f \sinh ak_f \right\} \right]$$

$$K' = \left[\left\{ -(n_b - 1) \sin an_f \sinh ak_f \right\} + \left\{ \left(\frac{n_b k_f}{n_f^2 + k_f^2} + k_f \right) \cos an_f \sinh ak_f \right\} + \left\{ \left(\frac{n_b n_f}{n_f^2 + k_f^2} - n_f \right) \sin an_f \cosh ak_f \right\} \right]$$

and $a = \dfrac{2\pi d}{\lambda}$

The simplified expression can now be solved for n_f and k_f by an iterative procedure as given below.

A rough value of k_f is selected and different values of n_f are fitted into the equation so that the LHS and RHS of the transmittance equation have the same value, the other parameters being experimentally determined. Once the proper value of n_f is selected (say n_1), another value of k_f (say k_2) near to k_1 is chosen and the computation is continued to obtain the best fit value say n_2. The same method is adopted for computing n_f and k_f from the reflectance data, say (n_3, k_3)

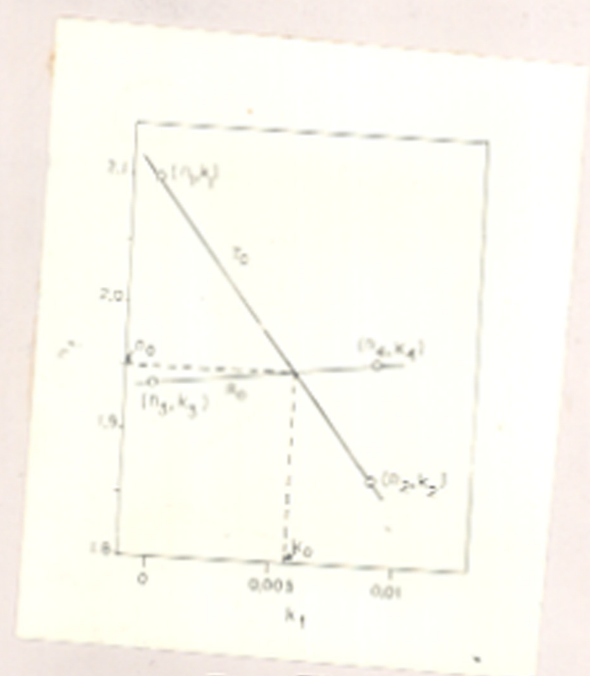

Fig II.6

and (n_4, k_4). Now to get a unique solution for n_f and k_f that satisfies both the transmittance and reflectance equations, graphical plots of n and k from the two data are made (Fig. II.6). The point of intersection (n_o, k_o) of the two curves will then satisfy both the equations. To obtain a better accuracy numerous values of n's and k's are computed.

This method involves heavy computations and is very laborious. However, if one of the parameters n_f, or k_f is known then the computation is very much simplified.

(b) Graphical method for computing k_f

Absorption index (k_f) can be calculated graphically from the slope of log T_o (transmittance) versus thickness (d) curves for various wavelengths (λ), k_f is then given by

$$k_f = \frac{2.303\,(\mathrm{Log}_{10} T_1 - \mathrm{Log}_{10} T_2)}{4\,\pi \times (d_2 - d_1)} . \lambda \quad .. \quad (II.7)$$

However this method is not very suitable if k_f is dependent on film thickness.

(c) Estimating k_f from T_o and R_o data

k_f can also be estimated from the knowledge of T_o and R_o as

$$T_o = (1-R_o)\exp(-4\pi k_f d/\lambda) \quad .. \quad (II.8)$$

The values of k_f so obtained are in good agreement with those computed from equations (II.3) and II.4).

(d) Non-absorbing films

For those films where absorption is very small, viz. $k_f \simeq 0$, then from equations (II.3) and (II.4) we have

$$T_o = \frac{4\, n_b}{\left[(n_b+1)\cos\frac{2\pi n_f d}{\lambda} - (\frac{n_b}{n_f} + n_f)\sin\frac{2\pi n_f d}{\lambda}\right]^2} \quad .. \quad (II.9)$$

and

$$R_o = \frac{\left[(n_b-1)\cos\frac{2\pi n_f d}{\lambda} + i\,(\frac{n_b}{n_f} - n_f)\sin\frac{2\pi n_f d}{\lambda}\right]^2}{\left[(n_b+1)\cos\frac{2\pi n_f d}{\lambda} - i\,(\frac{n_b}{n_f} + n_f)\sin\frac{2\pi n_f d}{\lambda}\right]^2} \quad .. \quad (II.10)$$

When $n_f d = (2m + 1)\frac{\lambda}{4}$ the above equations reduce to

$$n_f = \left[n_b \, (1+R_o^{\frac{1}{2}})/(1-R_o^{\frac{1}{2}}) \right]^{\frac{1}{2}} \text{ for } n_f^2 > n_b \quad .. \text{(II.11)}$$

and

$$n_f = \left[n_b \, (1-R_o^{\frac{1}{2}})/(1+R_o^{\frac{1}{2}}) \right]^{\frac{1}{2}} \text{ for } n_f^2 < n_b \quad .. \text{(II.12)}$$

The transmission curves in the visible region would then have interference fringes associated with maxima and minima. Refractive index n_f can also be computed from these using the relations

$$\text{(i)} \quad n_f d = \frac{m\lambda}{2} \quad .. \text{(II.13)}$$

for maxima, where m is the order of the fringe maxima and λ is the wavelength for the mth order.

$$\text{(ii)} \quad n_f d = (m+\tfrac{1}{2})\frac{\lambda}{2} \quad .. \text{(II.14)}$$

for minima, where m is the order of the fringe minima, and λ is the wavelength associated with the mth order.

The order of the fringe may be calculated from the relation $m = \frac{\bar{\nu}_1}{\bar{\nu}_2 \sim \bar{\nu}_1}$ where $\bar{\nu}_1$ and $\bar{\nu}_2$ are the wave

numbers of the mth and $(m+1)^{th}$ fringes.

(d) Absorption coefficient (α)

α can very easily be calculated from the absorption index k_f as

$$= \frac{4\pi k_f}{\lambda} \quad cm^{-1} \qquad .. \qquad (II.15)$$

(C) Structure

Electron diffraction studies

In order to identify the nature of the films and also their phase composition these were examined in an electron diffraction camera both by reflection and transmittance techniques. These studies were made on separate samples prepared simultaneously with the dielectric film of the capacitor. The substrates used for transmission methods were polycrystalline NaCl tablets and (100) faces of NaCl crystals. Films deposited on these both at room and high substrate temperatures were stripped off in distilled water and picked up on a grid having a thin collodion film on it as a support. Films deposited on glass substrates, however, were examined in the electron diffraction camera by the reflection method.

CHAPTER III

STUDIES ON ZINC SULPHIDE FILMS

(A) INTRODUCTION

Zinc sulphide occurs in nature in two forms namely, sphalerite (or zinc blende, β -ZnS) and würtzite (α -ZnS), the former having a cubic structure (B_3 type) whereas the latter h.c.p. type (B_4 type). Hochshild (1908) made a crystallographic study of the sphalerite mineral. Wurzburg (1908), on the other hand, investigated the heat effect for the phase transition from the zinc blende to würtzite forms. X-ray investigations by Bragg (1920) showed that whilst the former had a cubic structure, the latter was h.c.p. type. Various other workers (Aminoff, 1923; Ulrich and Zachariasen, 1926) later also investigated the structures of these forms and the lattice constants for the cubic and h.c.p. respectively were found to be, a = 5.406 Å and a = 3.820 Å, c = 6.260 Å. The phase transitions of the two forms were also investigated by several workers. Ramdhor (1931) observed that the β -form changed to the α -phase between 880°C and 1020°C. Bridgman (1939) found that the latter irreversibly changed to the former by shearing even at room temperature. This phase transition was however found to occur more easily in thin film state. Aggarwal and Goswami (1963) observed

that evaporated ZnS films growing epitaxially on different faces of NaCl, could develop either β or α structure or both depending on substrate temperatures even though the bulk might have either of these structures. Similar phase changes were also observed for other chalcogenides of Zn and Cd (Dhere and Goswami, 1969). Preparative techniques of epitaxial films or wafers have recently been reported by several workers (Tamura et al, 1965; Vohl et al, 1971; Behrndt and Moreno, 1971).

Although zinc sulphide has been subjected to intensive investigations for its photoconducting, insulating and other properties during the last thirty years, very little work has however been carried out on the bulk ZnS crystals for their optical properties. Gudden and Pohl (1921, 1922) reported a sharp rise of the photoconductivity at a wavelength of about 3350 Å in natural zinc blende crystals. This was later confirmed by Piper (1953) and several other workers (Reynolds and Czyzak, 1950; 1954) who found that the wavelength in question was the region of the fundamental absorption edge of ZnS crystals. Similar results were also obtained for the activated ZnS powders (Gisolf, 1939). Refractive indices of these materials were found to vary between 2.4 to 2.9 between the wavelength region 5000 Å to 3300 Å respectively.

Investigations on thin films have, however, been

fairly exhaustive. Hammer (1943), Rood (1951) and Kuwabara and Ishiguru (1952) calculated the refractive indices of ZnS films and found them to be non absorbing in the visible region. Hall and Fergusson (1955) studied the ageing effect of these films. They observed that the optical constants were independent of the film thickness and the values of refractive index were similar to bulk. Since the presence of voids in the evaporated ZnS films was found to alter its refractive index (Polster and Woodruff, 1953), Heavens and Smith (1957) investigated the effects of pressure, rate of deposition, film thickness, voids, etc. on the optical properties of ZnS films. Coogan (1957) observed that the absorption edge shifted with the temperature and this shift was about -4×10^{-4} eV/^{o}C between -186°C and 20°C. The optical properties of ZnS films were also studied in the u.v. region by Cox et al (1959). They found that the refractive index decreased rapidly from 3.13 at λ 2200 Å to 0.64 at λ 735 Å, and that the absorption index which had a minimum value of 1.75 at λ 1800 Å decreased to 0.23 at λ 584 Å. These parameters were found to be independent of the deposition conditions and ageing. Huldt and Staflin (1959) reported that the refractive indices of thick (1 to 5 μ) ZnS films were higher than the bulk values. Recently Miloslavskii et al (1967)

showed that the long wavelength absorption edge became steeper when the substrate or annealing temperature of ZnS films was increased, and this was adduced to the increase in the grain dimensions as well as the reduction of the lattice defects in these films.

Electroluminescence in ZnS films doped with Mn, Cu and Cl have been studied in great details. (Koller et al, 1960; Soeya and Kimura, 1966; Saski et al, 1968; Uchida, 1968; Malkin et al, 1971). Cathodoluminescence of ZnS films as a function of substrate temperatures has been studied by Shalimova et al (1971). Large photo voltages upto several hundred volts were observed for these films (Merz, 1958; Gagaliano et al, 1967). This property was utilised by Kazan and Nicoll (1957) to prepare effective solid state light amplifiers. In a similar way other optical properties of ZnS films have been extensively exploited for the preparation of reflectors, interference filters and frustrated total internal reflectors (Holland, 1956; Heavens, 1955).

Transport properties of bulk ZnS have been studied by a few workers. Piper (1953) measured the temperature dependence of the conductivity of high resistance ZnS crystals between 500°K and 700°K. His data obeyed the relation σ (conductivity) = A exp (E/2 kT) with

E = 3.77 ± 0.1 eV and found the band gap energy to be 3.67 ± 0.1 eV and 3.58 ± 0.1 eV at near 0° and $300^{o}K$ respectively. Kroger (1956) measured the Hall mobility of several n-type wurtzite crystals under illumination and found that mobility (μ_H) was between 110 to 140 $cm^2/V.sec$ at $300^{o}K$. Aven and coworkers (1962, 1965) measured the temperature dependence of the Hall mobility of doped ZnS crystals. Narita and Nagasaka (1965) measured the Hall mobility and free electron concentration as a function of the light intensity. The conduction mechanism in these crystals was found to be generally governed by the scattering due to the ionized impurity levels lying in the forbidden gap. Several such impurity levels have been observed by a number of workers using Hall effect (Aven and Mead, 1965), thermoluminescence (Hoogenstratten, 1958) and thermally stimulated current (Kroger, 1956) measurements.

Al/ZnS/Al thin film capacitors have been successfully prepared by Fuchshuber et al (1960) who found the dielectric constant (ϵ) of ZnS films to be about 10.3. Hacskaylo and Feldman (1962) reported an anomalous rise in ϵ (34.7) for a film thickness of 900 Å, and also its decrease to a shallow minimum value (5.3) at 1 μ thickness. Maddocks and Thun (1962) and later Chopra (1965) on reinvestigation did not observe any such anomaly in the dielectric constant which was about 8.5 and more or less invariant with the

frequency. Chopra, however, found that ϵ was dependent on film thickness in the case of very thin films only (< 500 Å). Weaver (1963) made a detailed study on the ageing effect of ZnS film capacitors. Laksmanan and Mitchell (1965) prepared ZnS film capacitors by reactive sputtering and reported them to have a low loss factor, moderate breakdown voltages and good stability.

From the above survey it is seen that although a good amount of work has been carried out on the optical properties of ZnS films, very little investigations have so far been made on the a.c. behaviour of these films. Recent investigations by a number of workers and especially by Goswami and his collaborators (1964, 1966, 1968) have shown that the semiconducting properties of thin films are considerably influenced by film thickness, deposition conditions, annealing and substrate temperature. It is therefore likely that some of the above factors may also influence the dielectric and optical properties of thin films. Unfortunately no such work has yet been reported on ZnS films. With this end in view, a systematic study has been made on the dielectric and optical properties of ZnS films.

(B) EXPERIMENTAL

(1) Preparation of films

Thin film capacitors with ZnS films as sandwiched

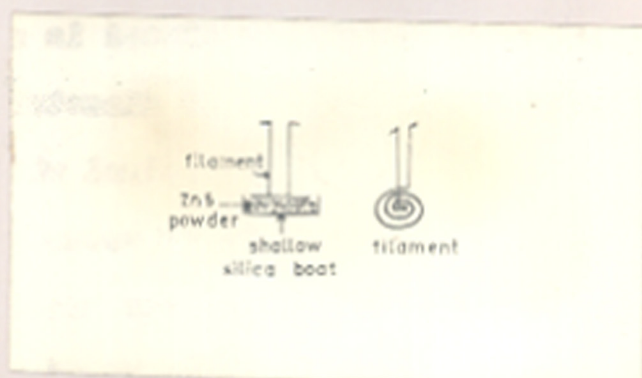

Fig III.1

layers (Al/ZnS/Al) were prepared by the vacuum deposition method. Aluminium film electrodes deposited from a tungsten spiral were in general about 1000 Å thick and had a resistance of about a few ohms. The uniform deposition of ZnS films presented quite a problem as ZnS powder invariably spitted off during evaporation from a molybdenum boat. A radiation type of heating (Fig. III.1) was, therefore, adopted for this purpose. Pure ZnS powder (M/s Riedel de Haen AG) was placed in a clean shallow silica boat of about 1.5 cm in diameter. A tungsten wire shaped in the form of a flat spiral which was at first cleaned by repeated flashing in vacuo was then placed just above the ZnS powder kept in the boat. The powder was at first slowly heated in vacuo so as to degass it. When this was over the temperature of the spiral was further raised so that the evaporation of the ZnS powder could commence. These deposits were in general transparent and showed interference colours. ZnS films were also deposited at higher substrate temperatures (130°C).

For studying the optical properties, ZnS films having thickness varying from 3000 to 7000 Å were also deposited on glass substrates (refractive index n_b = 1.52) having dimensions 3x1.4 cm^2 and then annealed in vacuo.

Film thickness was estimated by the interferometric

method as described earlier.

In order to investigate the nature and the phase structure of ZnS films used for the dielectric and optical properties, the electron diffraction technique was employed. For these studies depositions were also made simultaneously on polycrystalline NaCl tablets or on (100) faces of NaCl. The films were then stripped off from the surface in the usual way and examined in the electron diffraction camera by transmission methods.

(ii) Measurements of capacitance (C) and tan δ

Measurements of C and tan δ were generally made in vacuo at different temperatures. The actual measurements were carried out in a special cryostat described in Chapter II. Both C and tan δ were measured by a Marconi TF 2700 bridge at variable frequencies (10^2 to 10^5 Hz). The dielectric constant (ϵ) was then calculated from the value of the capacitance (C), dielectric thickness (d), and from the electrode area A of the capacitors as explained earlier.

In order to measure C and tan δ at various frequencies (10^2 to 10^5 Hz) an external oscillator (Philips PM 5100) was used to excite the above bridge. Measurements were also made at various temperatures (77^0K to 380^0K) for

different dielectric film thicknesses.

It was observed that Al/ZnS/Al capacitors did not attain stability even if the dielectric films were annealed at 180°C. In order to have reproducible results, these capacitors were allowed to age for a few days and then subjected to cyclic heating ($\simeq$ 380°K) and cooling (300°K) processes in vacuo. Further measurements on these capacitors were then carried out.

Temperature coefficient of capacitance (TCC) which is defined as $\frac{1}{C} \cdot \frac{dC}{dT}$ was calculated from the variation of C with temperature at 1 kHz.

When all the dielectric measurements were completed, the breakdown voltage V_B was estimated because this involves the destruction of the film capacitor.

(iii) Measurements for optical studies

The transmittance of ZnS films (film thickness ranging between 3000 Å to 7000 Å) was scanned in a Beckman DK-2 double beam spectrophotometer in the visible region viz. λ 7000 Å to λ 4000 Å. These curves showed interference fringes consisting of maxima and minima at different wavelengths and from these extrema the order of the fringes (m) could be calculated. Refractive index

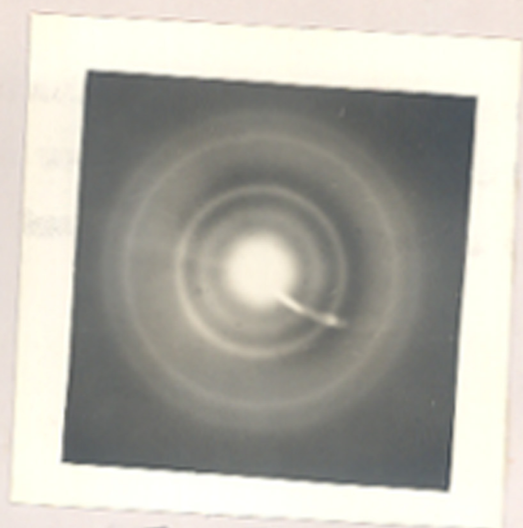

Fig III.2

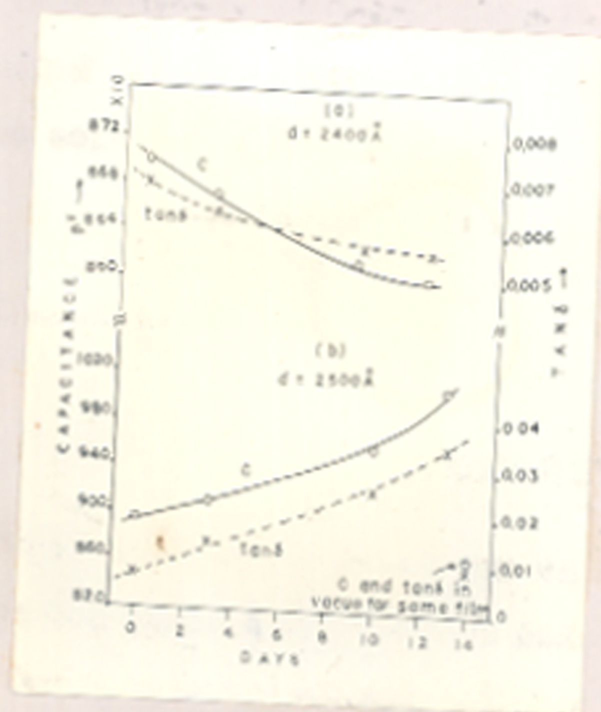

Fig III.3

(n_f) of these films were then evaluated from the knowledge of film thickness (d) and the order of the fringe (m), taking help of equations (II.14) and (II.15).

(C) RESULTS

(a) Structure

The bulk ZnS powder when subjected to X-ray analysis showed to have a h.c.p. structure (α-form). The deposits formed on polycrystalline NaCl tablets at room temperature or at 130°C, on the other hand, yielded polycrystalline ring patterns corresponding to an f.c.c. structure when studied by transmission in the electron diffraction camera (Fig. III.2). Reflection patterns of thick ZnS films formed on glass also conformed to the zinc blende type of structure.

(b) Dielectric Properties

(i) Ageing effect

As mentioned earlier all capacitor films had to be annealed in vacuo by heating and cooling cycles for stabilization. Samples that were not annealed by this process showed considerable ageing effects when kept at room temperature in air for several days. Fig. (III.3a)

shows the typical ageing effect on capacitance and tan δ for a film capacitor about 2400 Å thick. In some cases it was found that due to the absorption of atmospheric moisture, both capacitance and tan δ increased with time, but reduced to lower values when measured in vacuo (Fig. III.3b). Heating and cooling cycles (annealing) in vacuo reduced both C and tan δ, and eventually they became constant showing a final stabilization of the capacitors. All measurements after the stabilization became reproducible even when measured after long periods. In fact such annealed samples showed a variation less than 2% in C and tan δ when measurements were made on them after an interval of about a year or so.

(ii) <u>Effect of film thickness</u>

It was found that whilst the capacity decreased with the rise of film thickness as expected, dielectric constant, on the other hand, showed initially a gradual rise and later on it became constant. This trend was found to be true for all ZnS film capacitors, irrespective of whether the dielectric films were deposited at room or higher substrate temperatures. These features are clearly shown when both C and ϵ are plotted against d (Fig. III.4). Films deposited at room temperature attained a constant value of ϵ at a

⊙ } Deposited at
● } Room Temperature

X } Deposited at
Δ } 130°C

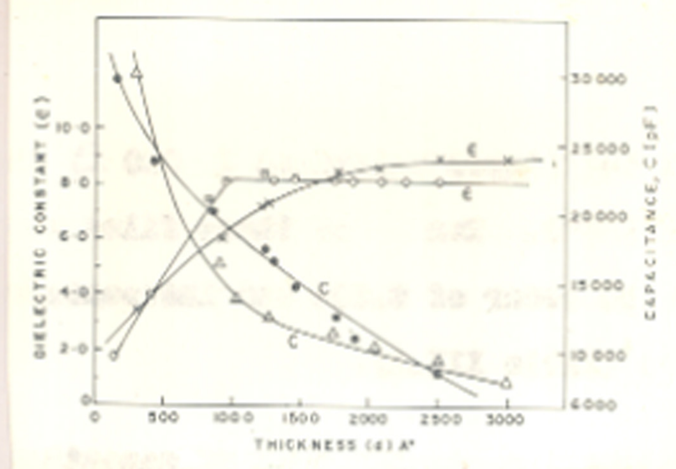

Fig III. 4

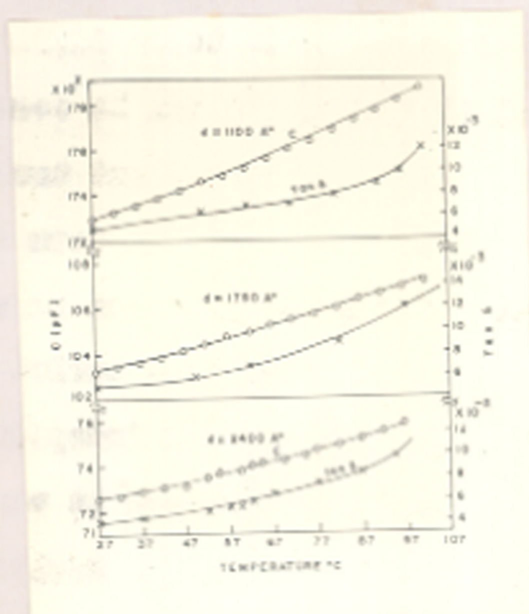

Fig III. 5

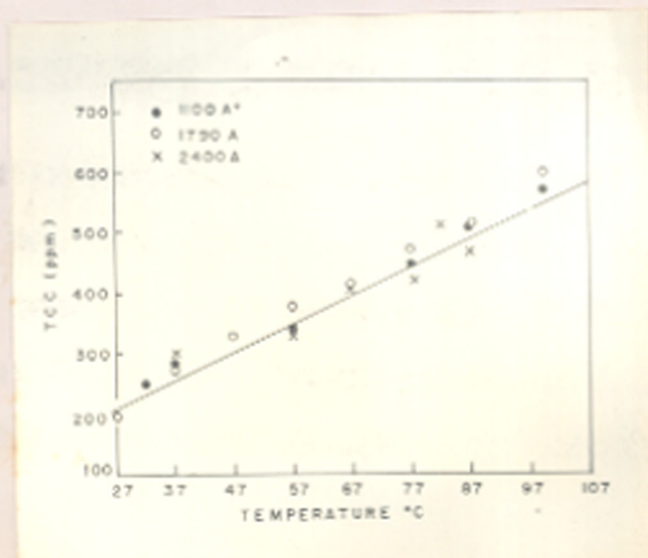

Fig III. 6

comparatively lower thickness ($\approx$ 900 Å) than those formed at about 120°C. Tan δ of these films was found to be low, of the order of 0.005 and independent of the film thickness (Table III.1).

(iii) Temperature coefficient of capacitance (TCC)

Fig. (III.5) shows the effect of temperature on capacitance and tan δ for three different film thicknesses when measured at 1 kHz. It can be seen that with the increase of temperature both C and tan δ increased. This rise was, however, small between room temperature and 50°C, but beyond this range the increase in tan δ was rapid. Tan δ of these samples varied from 0.005 to 0.012 between 27°C and 100°C and was independent of the film thickness. TCC was positive and it varied between 200 ppm/°C to 600 ppm/°C in the temperature region studied and was also found to be more or less independent of the film thickness (Fig. III.6).

(iv) Effect of frequency and temperature on capacitance

The variation of capacitance with frequency in the frequency spectrum of 0.1 to 100 kHz and temperatures (77° to 390°K) was studied for different film thicknesses. Fig. III.7 shows the typical graphs of capacitance with the frequency at different temperatures for a ZnS capacitor

TABLE III.1

Thickness (d) Å	Capacity pF	ϵ	tan δ
	Deposited at Room Temperature		
150	29,800	1.76	0.015
421	23,800	3.36	0.01
840	21,000	6.9	0.008
950	29,800	8.19	0.01
1230	17,200	8.35	0.006
1300	16,400	8.36	0.007
1455	14,400	8.28	0.013
1760	11,900	8.28	0.007
1880	10,800	8.2	0.007
2400	8,600	8.2	0.007
2500	8,300	8.2	0.010
	Deposited at 130°C		
290	30,000	3.88	0.012
910	16,700	6.0	0.005
1200	13,800	6.55	0.005
1760	11,600	8.06	0.008
2050	10,640	8.7	0.01
2500	9,070	8.95	0.005
3000	7,700	9.0	0.005

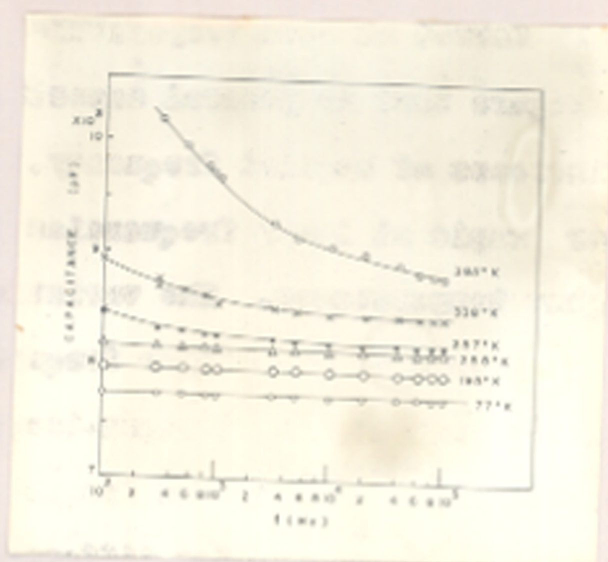

Fig III.7

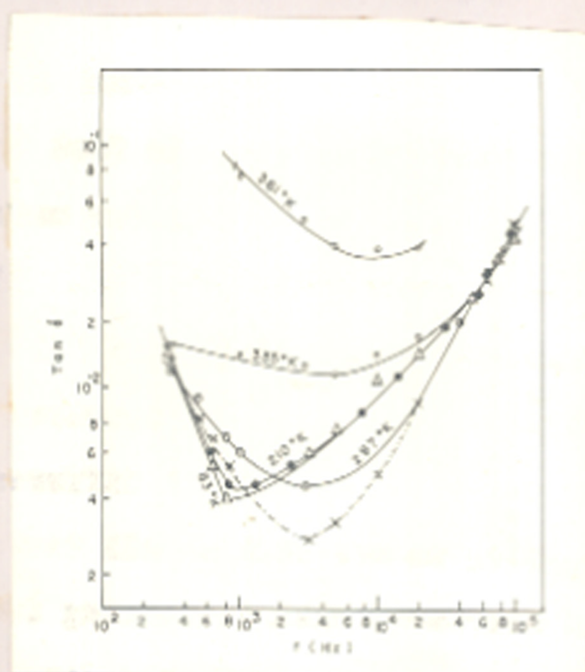

Fig III.8

(d = 2500 Å) formed at room temperature. It is seen from the above figure that in general capacitance decreased with the increase of applied frequency. This decrease was however rapid at lower frequencies (0.1 to 5 kHz) and at higher temperatures. The variation in C became less at lower temperatures and higher frequencies (say $\geq$ 60 kHz) and eventually near liquid nitrogen-temperature capacitance became almost invariant with the frequency. Similar results were also obtained for different films deposited at room as well as at higher substrate temperatures.(130°C).

(v) Effect of frequency on tan δ

Frequency had a pronounced influence on the loss factor of a film capacitor. In fact this is one of the most widely studied parameters for understanding the behaviour of a dielectric material. Fig. III.8 shows the behaviour of tan δ for a ZnS film capacitor (d = 2500 Å) in the frequency spectrum of 0.1 to 100 kHz when measurements were made at different temperatures. It is interesting to see that at all temperatures tan δ gradually decreased with increasing frequencies, attained a minimum value (tan δ_{min}) at a frequency f_{min} and then again increased at higher frequencies. From the above figure it is seen that the value of tan δ at a fixed frequency also increased with the rise of temperature.

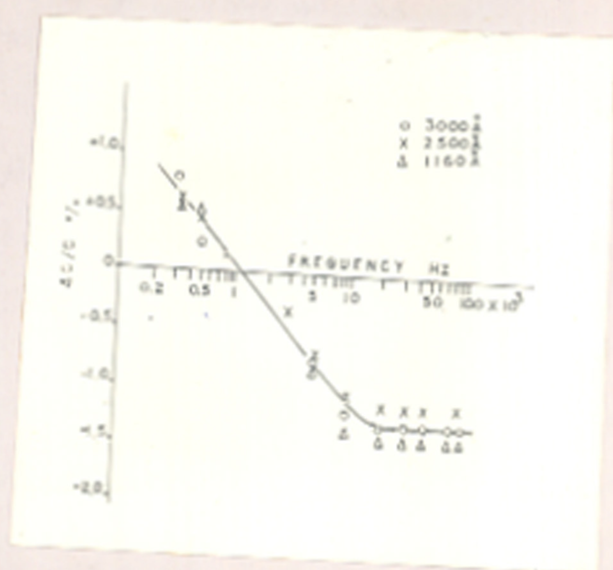

Fig III.9

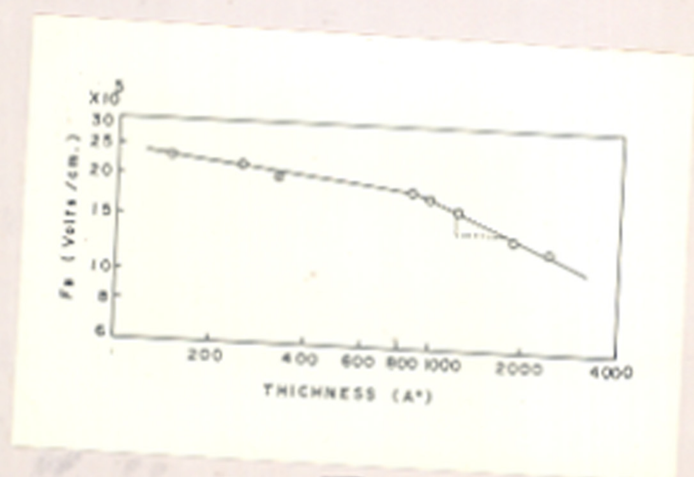

Fig. III.10

A peculiar feature of these curves was the shifting of the position of tan δ_{min} to higher frequencies with the rise of temperature. Its magnitude also increased (cf. Fig. III.8). At higher frequencies, the values of tan δ were large and independent of temperature. Similar results were also obtained for ZnS capacitors of different film thickness.

(vi) Percentage variation of capacitance with frequency

It is also useful to know the variation of capacitance with the frequency. This is defined as the percentage change of the capacitance at any frequency (C_f), from the value of capacitance at any arbitrary frequency (C_a) which is taken in the present case as 1 kHz. Mathematically it can be expressed as

$$\frac{\Delta C}{C}\% = (C_f - C_a) \times 100/C_a$$

Fig. III.9 shows the percentage change of capacitance with the frequency for three different capacitors when measured at room temperature. This variation was between +1% and -1.5% in the frequency spectrum of 0.3 and 100 kHz and was more or less independent of the film thickness.

(vii) Breakdown voltage and dielectric field strength

Breakdown voltage (V_B) and dielectric field

strength (F_B) for ZnS film capacitors were measured by the method described in Chapter II. These measurements were however carried out in air. Table III.2 shows the values of V_B and F_B for different film thickness. It is interesting to see that although V_B increased with the film thickness, F_B, on the other hand, decreased. The average value of F_B for ZnS capacitors was about 1.5 meV/cm. A plot of F_B and film thickness (log-log scale) is shown in Fig. III.10. It can be seen that for thinner films F_B was nearly independent of the film thickness, but for thicker films, say > 800 Å, it reduced and had a slope of -0.5.

(C) Optical Properties

(i) Measurement of transmittance

Transmittance of ZnS films in the visible region (λ 7000 Å – λ 4000 Å) was measured by a Beckman DK 2 spectrophotometer. A typical transmission curve for a ZnS film (d = 4200 Å) is shown in Fig. III.11. It is seen that the transmission curve showed many extrema in the visible region and the transmittance was about 85% at the maxima, but reduced to about 73% at the minima. For another film say 6500 Å thick, similar results were obtained except that the number of extrema increased.

TABLE III.2

Thickness (d) Å	Breakdown voltage V_B (volts)	Field strength F_B meV/cm
150	3.45	2.3
250	5.5	2.2
320	6.0	1.9
890	13.5	1.85
1000	18.0	1.8
1230	20.5	1.65
1830	25.0	1.35
2440	30.5	1.24

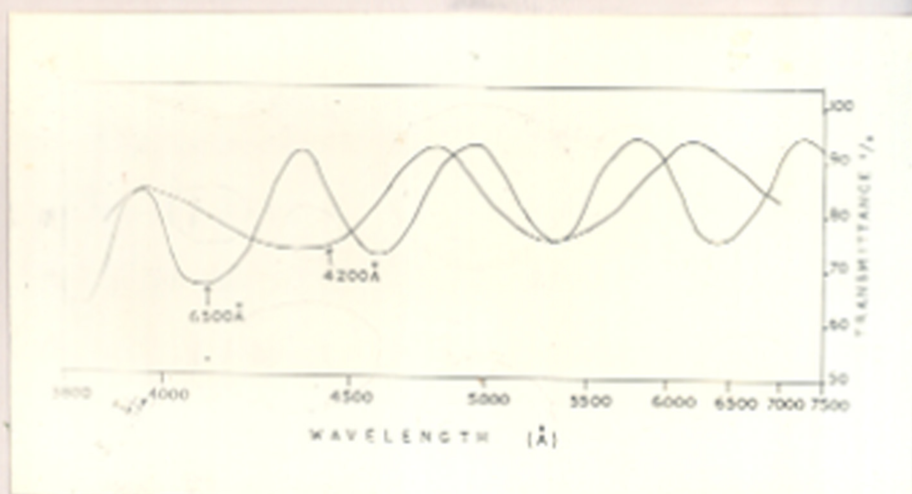

Fig III.11

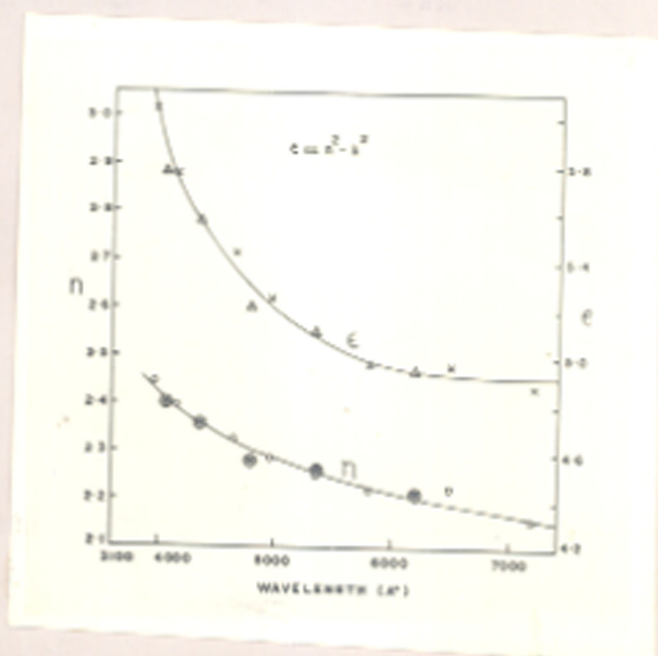

Fig III.12

Δ, ⊙ } $d = 4200$ Å

x, o } $d = 6500$ Å

(ii) Optical constants

Refractive index for these films were computed with the help of equations (II.13) and (II.14), given in Chapter II. Table III.3 shows the order of the extreme and the refractive indices of two ZnS films at different wavelengths. It can be seen that although n_f varied from 2.21 at 7000 Å to 2.4 at 4150 Å it was independent of film thickness (Fig. III.12). Since the absolute value of transmittance at the maxima and minima were almost the same for a wide range of film thickness, absorption index (k_f) could therefore be assumed to be practically zero in the visible region. This was confirmed by calculating k_f from the complex relation given by equation (II.3).

It is also possible to calculate the dielectric constant at optical frequencies from n_f and k_f data using the Maxwell's relations viz.

$$\epsilon = n_f^2 - k_f^2$$

Optical dielectric constant so obtained varied between 4.9 and 6.0 in the visible region (Fig. III.12).

(D) DISCUSSION

ZnS bulk powder when examined by the X-ray method

TABLE III.3

	For maxima $n_f = m\lambda/2d$				For minima $n_f = (m+\frac{1}{2})\lambda/2d$			
Film thickness d (Å)	λ(Å)	m	k_f	n_f	λ(Å)	m	k_f	n_f
	6200	3	negligible	2.22	5350	3	negligible	2.26
4200	4800	4	"	2.28	4350	4	"	2.36
	4050	5	"	2.40				
	7200	4	"	2.21	6500	4	"	2.23
	5800	5	"	2.23	5350	5	"	2.26
6600	4950	6	"	2.29	4650	6	"	2.33
	4350	7	"	2.36	4150	7	"	2.40
	3960	8	"	2.45				

was found to consist primarily of the h.c.p. form (wurtzite type). ZnS deposits, on the other hand, developed a cubic structure (zinc blende type) whether formed at room or at higher substrate temperatures. It thus appears that during the deposition these films assumed the cubic structure even though the starting material was of the h.c.p. form. Such types of structural changes are not uncommon for vacuum deposited films, and in fact Aggarwal and Goswami (1963) observed such a cubic structure for ZnS films not only from the cubic bulk but also from the bulk having a hexagonal structure (wurtzite). Similar results were also obtained for other chalcogenide films (Badachhape and Goswami, 1964; Dhere and Goswami, 1969). The present observation of the cubic structure of ZnS films from the bulk hexagonal structure is thus in agreement with the results of the previous workers.

An unusual observation of ZnS film capacitors is that the dielectric constant (ϵ) was dependent on film thickness for thinner film but became independent as the thickness became larger than 1000 Å. This appears to be related to the defects, particularly voids and discontinuities present in the deposited ZnS films. Capacitors made from such films may then be considered, in the idealised case, to comprise of many parallel capacity elements consisting of two types of dielectric media namely (1) ZnS film and

(ii) air or vacuo (where $\epsilon = 1$) in the void and discontinuity regions. As the film thickness decreases the void content in the films will increase. In the limiting case, a capacitor element will then be formed whose dielectric constant is nearly unity. The effective capacity (C_{eff}) of the total capacity elements will hence depend on the amount of voids, etc. present in the dielectric films. C_{eff} can then be written as $C_{eff} = C_{voids} + C_{ZnS}$. The value of ϵ so calculated from C_{eff} will be less than the true value of ϵ for ZnS films. Thus with the increase in the film thickness, voids will continuously be reduced and hence ϵ will increase eventually attaining the constant value for ZnS films.

The characteristic features of ZnS film capacitors, i.e. the variation of capacitance and tan δ with frequency, temperature and especially the observation of loss factor minimum (tan δ_{min}) and the corresponding shift of the frequency minimum (or ω_{min}) position cannot be easily explained on the basis of the existent theories. Mention can be made in particular of tan δ_{min} also observed by Maddocks and Thun (1962) for ZnS films. These features cannot possibly be due to the natural relaxation effect of a capacitor or due to interfacial polarisation, since the frequency region for such effects to be observable is

too large ($> 10^9$ Hz) for the former and far too small (10^{-3} to 1.0 Hz) for the latter. Further, the presence of such processes would give a tan δ_{max} and not tan δ_{min} as observed here. Recently Simmons et al (1970) have given a very elegant theory to explain both qualitatively and quantitatively the a.c. behaviour of highly doped MoO_3 films. In the frequency region (0.1 to 100 kHz) studied, they however predict that tan δ would show a maximum which would also shift with temperature, a feature that is not in agreement with our experimental observations. Thus there seems to be no suitable theory available to explain the a.c. behaviour of ZnS films. In the subsequent paragraphs a model has been proposed by us (Goswami and Goswami, 1973) to explain both qualitatively and quantitatively the a.c. behaviour of ZnS film capacitors.

Theory

Any capacitor comprises of the following elements, namely,

> (i) a capacitor, (ii) a dielectric resistance between the electrodes, and (iii) a negligible resistance due to leads, etc.

In the case of thin films, the capacitor system is proposed to comprise of (i) an inherent capacity element C,

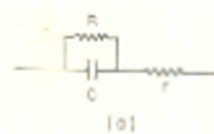

(a)

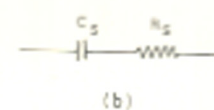

(b)

Fig III.13

unaffected by frequency and temperature, (ii) a discrete resistance element R due to the dielectric film in parallel with C and (iii) a small series resistance r due to electrodes, leads, etc. It is further assumed that whilst R will be affected by temperature due to the exponential factor in the relation $R = R_0 \exp(\Delta E/kT)$, the electrode and lead resistances r will be more or less constant in value. In general $R \gg r$. Figs. III.13a and 13b show the different elements and the equivalent series circuit (C_s and R_s) respectively. A mathematical analysis of the above equivalent circuit leads to several significant conclusions as will be shown below.

The impedance Z of the circuit in Fig. III.13a in terms of C, R, r and angular frequency ω ($= 2\pi f$) is given as

$$Z = \frac{R}{(1 + j\omega CR)} + r$$

$$= \frac{R + r(1 + \omega^2 C^2 R^2)}{(1 + \omega^2 R^2 C^2)} - j \frac{\omega C R^2}{(1 + \omega^2 C^2 R^2)} \quad \ldots \quad \text{(III.1)}$$

If the capacity elements are replaced in a simpler series

circuit comprising of R_s and C_s (Fig. III.13b), then the above impedance can also be represented as

$$Z = R_s + \frac{1}{j\omega C_s} \quad \text{or } R_s - j \frac{1}{\omega C_s} \qquad .. \quad (III.2)$$

Since the two impedances are equal, the values of R_s and C_s are obtained by separating the real and imaginary parts of equation (III.1) and (III.2). Then

$$C_s = \frac{1 + \omega^2 R^2 C^2}{\omega^2 R^2 C} \qquad .. \quad (III.3a)$$

and

$$R_s = \frac{R + r(1 + \omega^2 R^2 C^2)}{(1 + \omega^2 R^2 C^2)} \qquad .. \quad (III.3b)$$

By defining D as $D = \frac{1}{\omega RC}$, C_s and R_s can be written as

$$C_s = (1 + D^2)C \text{ and } R_s = r + \frac{D^2}{1+D^2} . R \qquad .. \quad (II.4)$$

Now loss factor, $\tan\delta$, is defined as $\tan\delta = \omega C_{series} \times R_{series} = \omega C_s R_s$

∴ we have from equation (III.3a) and (III.3b)

$$\tan \delta = \frac{\omega(1+\omega^2R^2C^2)\left[R + r(1+\omega^2R^2C^2)\right]}{(\omega^2R^2C^2)(1+\omega^2R^2C^2)}$$

$$= \frac{1}{\omega RC} + \frac{r}{\omega R^2C} + \omega rC \qquad .. \qquad (III.5)$$

$$= D\left(1 + \frac{r}{R}\right) + \omega rC \qquad .. \qquad (III.6)$$

Thus loss can be expressed in terms of C, R, r and ω .

(i) Frequency effect and loss minimum

Differentiating $\tan \delta$ with respect to ω , the equation (III.5) reduces to

$$\tan \delta'_\omega = -\frac{1}{\omega^2RC} - \frac{r}{\omega^2R^2C} + rC \qquad .. \qquad (III.7)$$

and the second differentiatial becomes

$$\tan \delta''_\omega = \frac{2}{\omega^3RC} + \frac{2r}{\omega^3R^2C} \qquad .. \qquad (III.8)$$

which is a positive quantity for all values of ω , R, C and r. Hence $\tan\delta$ must pass through a minimum value and this will occur only when equation (III.7) is zero, viz. when

$$rC = \frac{r}{\omega^2 R^2 C} + \frac{1}{\omega^2 RC} = \frac{1}{\omega^2 RC}\left(1 + \frac{r}{R}\right) \quad .. \text{(III.9)}$$

Since $\frac{r}{R} \ll 1$ in all cases, we then have $rC = \frac{1}{\omega^2 RC}$

Hence the loss minimum will be observed at a frequency given by

$$\omega_{min} = \sqrt{\frac{1}{rRC^2}} \quad .. \text{(III.10)}$$

Again as $r/R \ll 1$, equation (III.6) and hence (III.5) reduces to

$$\tan\delta = D + \omega rC \text{ or } \tan\delta = \frac{1}{\omega RC} + \omega rC \quad .. \text{(III.11)}$$

Now when ω is small, $\frac{1}{\omega RC} \gg \omega rC$, then

$$\tan\delta = \frac{1}{\omega RC} \quad .. \text{(III.11a)}$$

This shows that $\tan\delta$ is inversely proportional to frequency.

If, on the other hand, ω is large then in general $\frac{1}{\omega RC} \ll \omega rC$ and hence

$$\tan \delta = \omega rC \qquad .. \quad \text{(III.11b)}$$

Thus with large values of ω , tan δ will increase with the applied frequency.

(ii) Temperature effects

It is seen from equation (III.10) that ω_{min} is determined by $\sqrt{\frac{1}{rRC^2}}$. Now, as R is related to temperature by the expression $R = R_o \exp(\Delta E/kT)$, it will reduce in value with increasing temperatures, whereas r remains practically unchanged as mentioned before. The effect would then be to reduce the value of the denominator in equation (III.10) and ω_{min} would increase with temperature. Thus a shift of ω_{min} to higher frequencies should be observed with the rise in temperature and vice versa. Similarly the value of tan δ_{min} at ω_{min} should also increase with the temperature because of equation (III.11). If the frequency is kept constant, say at 1 kHz, then in most practical cases $\frac{1}{\omega RC} \gg \omega rC$ and therefore tan δ would also increase with the temperature, the value being given by

$$\tan \delta = \frac{1}{\omega RC} \qquad .. \quad \text{(III.12)}$$

The effect of temperature on capacitance can be considered from equation (III.4) where

$$C_s = (1+D^2)\,C \text{ or } C_s = C + \frac{1}{\omega^2 R^2 C} \quad .. \quad (III.13)$$

If however $\frac{1}{\omega^2 R^2 C} \ll C$ or $D^2 \ll 1$ then

$$C_s = C \quad .. \quad (III.13a)$$

This condition can be realised in a capacitor system either by increasing R, or by lowering the temperature, or by raising the value of ω . A suitable combination of these features along with an appropriate value of C will lead to the frequency independent capacitance behaviour.

(iii) Electrode and lead resistance

From the relation given in (III.11b) the electrode and lead resistance r can also be calculated by measuring the value of tan δ and capacitance at two different but higher frequencies viz.,

$$\tan\delta_1 = \omega_1 C_1 r \text{ and } \tan\delta_2 = \omega_2 C_2 r$$

$$\text{or} \quad r = \frac{\tan\delta_1 \sim \tan\delta_2}{(\omega_1 C_1 \sim \omega_2 C_2)} \quad .. \quad (III.14)$$

It is thus seen that by treating the basic discrete elements of the film capacitor system of ZnS to their equivalent series circuit, deductions as given by various equations, especially (III.5), (III.10), (III.11a), (III.11b), (III.13) and (III.14), on loss factor and also its minimum, frequency and temperature effects on them, capacitance at low temperatures, etc. have been made and fully verified by the experiments.

It may be mentioned here that, for all capacity measurements, the D position of the bridge which measures the series equivalent capacitance was adopted and hence the measured capacitance was really C_s.

In order to prove that the basic assumptions on the circuitry elements are justifiable, tan δ was also calculated from C, R and r which were independently measured. For a typical case, C was about 8330 pF, R and r were 5×10^6 and 10 ohms respectively. The dotted (-.-.-) curve in Fig. (III.8) shows its variation with frequency at the room temperature using equation (III.11). It has also a pronounced loss minimum and the general feature of the curve is similar to the experimental ones. Calculated tan δ_{min} ($\simeq$ 0.003) was also close to the measured value ($\simeq$ 0.004). This agreement suggests that the assumptions made in the above theory were valid. Further from equation

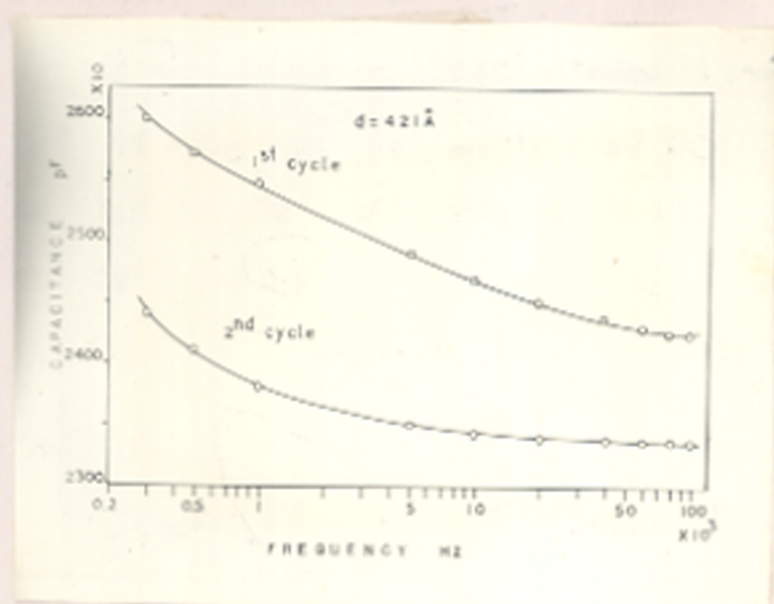

Fig III.14

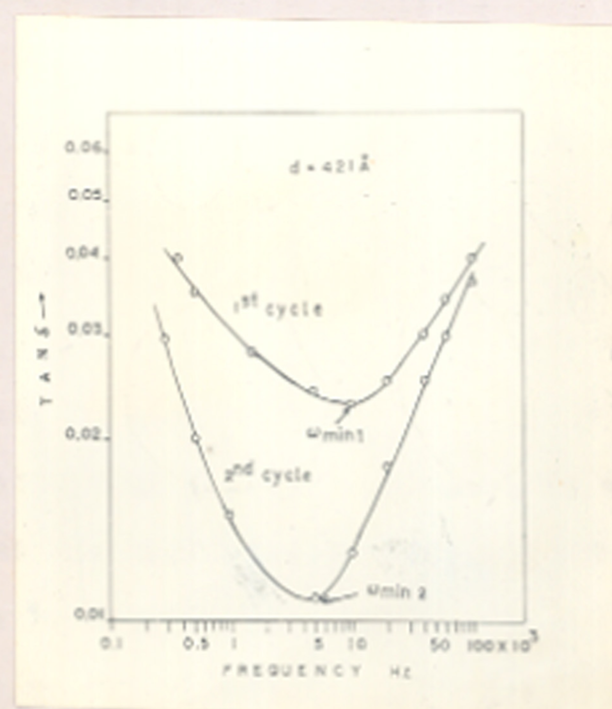

Fig III.15

(III.11), McLean's (1961) relation for the loss factor also follows automatically. The term $1/\omega CR$ of equation (III.11) then corresponds to ωCR_1 of McLeans equation, since R_1 was assumed to be in series with the capacity element.

In the light of the above theory the experimental results will now be discussed in details.

Annealing

Ageing in air and annealing of capacitors in vacuo invariably showed that C and tan δ reduced with time and with the number of heating and cooling cycles. Figs. III.14 and 15 show the effect of two cycles of heating and cooling on capacitance and tan δ when studied in the frequency range of 0.1 to 100 kHz for a capacitor of 421 Å thickness. ω_{min1} after the first cycle of annealing shifts to a lower frequency ω_{min2} (Fig. III.15). Such a shift in ω_{min} is possible if the value of the denominator in equation (III.10) increases. Among the parameters that might possibly increase was the dielectric resistance R only, since r was always of a constant value and the value of C reduced with each cycle of annealing (Fig. III.16). This can be explained in the following manner. Freshly deposited films contained many

defects such as voids, grain boundaries, dislocation, etc. But with time, a self-annealing process took place whereby many of the above defects were reduced or removed from the film. Annealing the films in vacuo also resulted in the same process. Such a reduction or removal of defects in the film would lower the concentration of charge carriers and thereby increase the resistivity of the film as observed above.

The increase in the value of C and tan δ with time, for a few cases (Fig. III.3b) could be attributed to the absorption of moisture in the dielectric film whereby a low shunting resistance was created between the electrodes. The effective resistance of the sandwiched dielectric R would therefore reduce considerably and thereby increasing the value of tan δ and C_s through equations (II.11a) and (III.13). This was more obvious when the capacitor was placed in vacuo. As the moisture evaporated the resistance between the electrodes would eventually increase to the true value of the sandwiched dielectric and thereby reducing the values of tan δ and C_s.

Effect of frequency on tan δ

The relations (III.8), (III.9), (III.10), (III.11a) and (III.11b) explain the general behaviour of the variation of tan δ with frequency when measured at

different temperatures. The resistance (R) of the sandwiched dielectric layer can also be estimated from ω_{min} at different temperatures. The measured room temperature value of 'R' and the value evaluated from the $\tan\delta$ curve agree very well as can be seen from the experimental and the theoretical curves (Fig. III.8). Table III.4 shows the values of ω_{min} at different temperatures.

It may not be out of place to mention here that since at higher frequencies $\tan\delta$ is governed by the relation $\tan\delta = \omega rC$, the increase of $\tan\delta$ with the frequency can be considerably reduced in this region by lowering the electrode and lead resistances (r). This can be achieved by depositing thick aluminium film electrodes with good ohmic contacts.

Effects of frequency on capacitance

Capacitance in general decreased with the increase of frequency but at higher frequencies C was more or less constant. This can be explained from equation (III.13) of the theory. At higher frequencies $\frac{1}{\omega^2 R^2 C} << 1$, as a result the measured capacitance C_s will be constant since C is invariant with frequency. As the temperature is reduced the dielectric resistance R will increase

TABLE III.4

Temperature ^{o}K	ω_{min} rad/sec	$\tan \delta_{min}$
83	5.0×10^3	0.004
210	5.95×10^3	0.0043
297	18.8×10^3	0.0045
335	31.5×10^3	0.012
361	50.0×10^3	0.37

considerably, thus increasing the value of the denominator in equation (III.13) and resulting once again in C_s being equal to C even at low frequencies. At higher frequencies also the above mentioned effects will take place and thus making capacitance invariant with frequency throughout the frequency spectrum at low temperatures.

The positive nature of TCC of these capacitors (Fig. III.6) also results from equation (III.13). Its magnitude (300 to 650 ppm/^{o}C) is comparable to any other dielectric film successively used as capacitor elements.

Breakdown voltage

Although breakdown voltage (V_B) increased with the film thickness, the field strength (F_B) however decreased. Fig. III.10 shows a definite power law between F_B and film thickness (d). In general $F_B \propto d^{-\beta}$, where β is the value of the slope of the graphs. It is interesting to see that the graph has a very small slope in the thinner region ($\lesssim$ 800 Å) and a value of -0.5 for thicker films. Thus for thicker film $F_B \propto d^{-\frac{1}{2}}$. Forlani and Minnaja (1964, 1969) showed theoretically that if an avalanche mechanism is initiated by the injection of electrons from the electrode by a tunnelling process, then F_B follows a power law. If the film thickness is much lower than the recombination length of the electrons, then $F_B \propto d^{-\frac{1}{2}}$. If,

on the other hand, the potential barrier at the cathode electrode interface is very low, then $F_B \propto d^{-\frac{1}{4}}$. Lomer (1950), Merril and West (1963), and Nicol (1968) showed that for Al_2O_3 films F_B followed a definite power law, where β = -0.25 for thinner films and β = -0.50 for thicker films. In the case of ZnS films, β = -0.5 for films thicker than 800 Å. Moreover in this region the dielectric constant (ϵ) was also found to be a constant quantity (8.2). For thinner films where ϵ increases with the film thickness, β was very small and much less than -0.5. In fact a sort of saturation in the value of F_B was observed. Korzo and Korobov (1966) reported such a saturation in very thin films of pyrolitically prepared Al_2O_3. The power law with β ranging from -0.45 to -0.85 was obeyed for all such films. Korzo and Lyaschenko (1968) suggested that the power law relations observed for both thinner and thicker films of SiO_2 was essentially due to the presence of charge defects in the dielectric films near the cathode.

As mentioned before, transmittance curves of ZnS film in the visible region showed many extrema, and n_f calculated with the help of equations (II.13 and 14) showed that it increased with decreasing wavelength. This can be explained in the following manner. It is well known that

the optical energy band gap for ZnS films is as high as 3.6 eV, and hence its fundamental absorption edge must lie in the ultra violet region. Both from classical and quantum mechanical treatments (Ditchburn, 1955; Moss, 1959; Born and Wolf, 1965), it can be shown that at frequencies in the neighbourhood of the absorption edge n_f and k_f will rise rapidly, because the frequency of the incident radiation approaches the frequency of the oscillating bound electrons of the dielectric. Although our study could not be extended to the u.v. region, the above measurements clearly indicate the increasing trend in n_f as this region is approached. Absorption index was too small to be measured in the visible region and hence it was assumed to be zero or negligible. In fact Hall (1956) and Coogan (1957) reported that ZnS films had negligible absorption for wavelengths down to 0.37 μ.

It may be mentioned here that the dielectric constant at optical frequencies (ϵ_{op}) was smaller than the ϵ measured in the audio frequency range. This was because at low frequencies both ionic and electronic polarisation contributed towards the dielectric constant, whereas at optical frequencies only the latter was significant.

CHAPTER IV

STUDIES ON PRASEODYMIUM OXIDE FILMS

(A) INTRODUCTION

The wide use of thin films in electrical and optical devices has necessitated a search for newer materials that would improve their performance and quality of these devices. In the field of dielectrics, except for some well known insulators such as SiO and some anodic oxides, no other material has been studied thoroughly for this purpose. The performance of reflectors and interference filters in optical devices depend greatly on the quality of these materials. Unfortunately the availability of transparent materials with a high refractive index is severely restricted to a few materials only. In recent years, attention has been focussed on the rare earth compounds as potential materials for these devices. Rare earth compounds particularly their oxides are known to have high melting points and are chemically very stable. Studies on some of these compounds such as CeO_2, CeF_3, La_2O_3 for their dielectric and optical properties have shown very encouraging results (Hass et al, 1959; Maddocks and Thun, 1962). Although many stable rare earth oxides are known to exist, the properties of only a few have been investigated. In this chapter the oxide of

praseodymium has been selected for the study of its dielectric and optical properties.

Praseodymium is known to form several oxides having compositions represented by PrO_x where x varied from 1.5 to 2.0, the two extreme compounds being Pr_2O_3 and PrO_2 (Hyde et al, 1966; Eyring, 1967). The existence of intermediate but non stoichiometric compounds such as Pr_6O_{11} and Pr_5O_9 have also been reported. Tensiometric measurements in conjunction with the X-ray diffraction patterns of these oxides indicate that there are two oxide phases, the lower one having a hexagonal structure whereas the higher oxide is a cubic one. For intermediate compositions lying between $PrO_{1.55}$ and $PrO_{1.75}$ both the phases can exist. This was confirmed from the thermoelectric measurements on praseodymium oxide by Martin (1950). The oxide $PrO_{1.83}$ represented by Pr_6O_{11} is nonstoichiometric and dark brown in colour. According to McCullogh (1950), Pr_6O_{11} had a f.c.c. type of structure with $a_o = 5.468$ Å and could be oxidised to PrO_2 by oxygen at high pressures.

Grovald and Loriers (1962) showed that the dipole relaxation of PrO_x depended on the value of x. This variation of relaxation and activation energy with the composition was also correlated to the structure. Although the magnetic properties of the bulk praseodymium oxide were

studied by several workers (Rabideau et al, 1951; Yosida, 1952; MacChesney et al, 1964; Kern, 1964; etc.) practically no work has been carried out on the evaporated oxide films. Hass et al (1959), however, in their study of the rare earth oxide films reported the value of the refractive index of praseodymium oxide films to be between 1.85 to 1.95 in the visible region.

From the above scanty references that are available it can be seen that not much effort has yet been made to study the properties of praseodymium oxide films. In this chapter, perhaps for the first time, the dielectric properties of vacuum deposited praseodymium oxide films are reported. Simultaneously a systematic study has also been made on its optical properties.

(B) EXPERIMENTAL

Pure praseodymium oxide (supplied by the Bhaba Atomic Research Centre, Trombay) powder brownish black in colour was deposited in vacuo ($\approx 10^{-5}$ mm Hg) from an initially flashed molybdenum boat. Prior to the deposition, the powder was degassed at a low heat of the boat for about 45 minutes. The deposited films of praseodymium oxide were found to be highly transparent to visible light. Al/praseodymium oxide/Al capacitors were then prepared

from the deposits formed at room as well as at high substrate temperatures to study their a.c. behaviour. Transmittance of these films was measured in a Beckman DK2 spectrophotometer, as well as in a special spectrophotometer designed in this laboratory and described in Chapter II.

All a.c. properties were measured in the manner described for ZnS film capacitors in the earlier chapter. To obtain stable values of C and tan δ , these capacitors were annealed by repeated heating and cooling cycles in vacuo.

Praseodymium oxide films were also deposited on polycrystalline NaCl tablets at room as well as high substrate temperatures to study and identify their structure by electron diffraction techniques. X-ray powder patterns of the bulk material were investigated.

(C) RESULTS

(a) Structure

Praseodymium oxide films whether deposited at room or at higher substrate temperatures ($\simeq 450^{o}C$) on polycrystalline NaCl tablets did not yield any coherent diffraction patterns when examined in the electron diffraction camera, thus suggesting that the films were amorphous in nature.

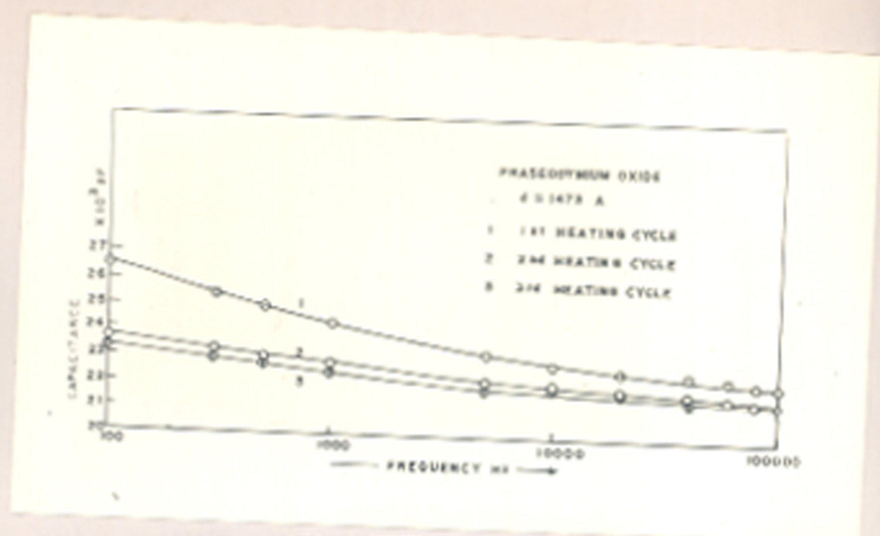

Fig IV.1

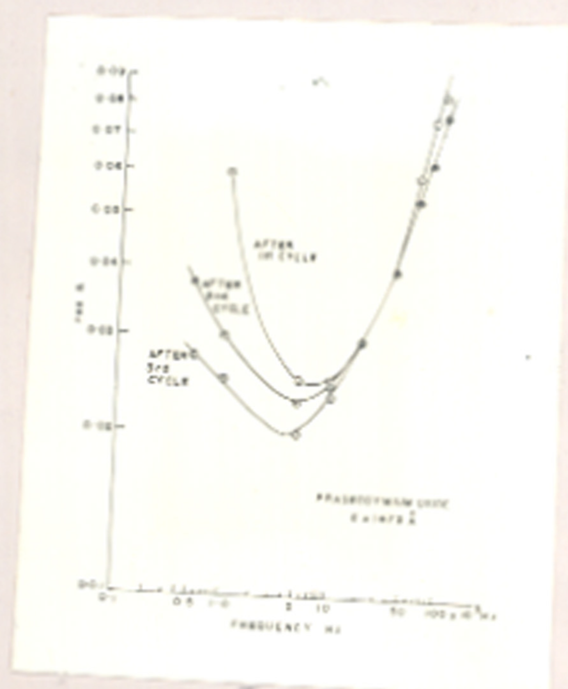

Fig IV.2

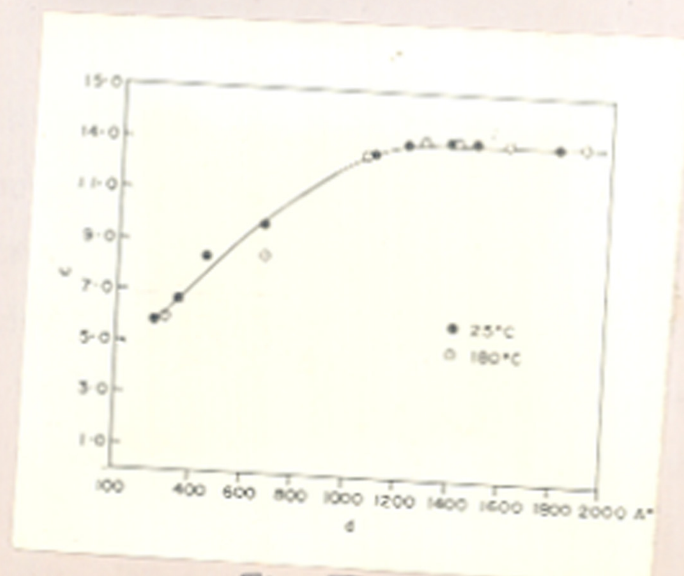

Fig IV.3

(b) Dielectric Properties

(i) Ageing and annealing effects

All capacitors when aged in air for a few days showed a decreasing tendency in the values of C and tan δ. However, on stabilising them in vacuo by several heating and cooling cycles, both capacitance and tan δ decreased considerably and attained constant values.

The variation of capacitance and tan δ with the frequency at each cycle of annealing is illustrated in Figs. IV.1 and 2 for a film thickness of 1473 Å. As can be observed, capacitance variation with frequency reduced with the annealing cycles and became nearly invariant during the third such cycle (cf. Fig. IV.1). Tan δ showed a sharp minimum that shifted to the lower frequency region with each cycle of annealing and its magnitude was also reduced (cf. Fig. IV.2).

(ii) Effect of film thickness

Table IV.1 shows the variation of capacitance with the dielectric film thickness. It was found that capacitance was proportional to 1/d for thickness greater than say about 1000 Å; but below this thickness range the proportionality law did not hold good. Dielectric constant (ϵ) as calculated from C showed an increasing

TABLE IV.1

Thickness (d) Å	Capacitance (C) pF	ϵ	tan δ
	Deposited at 28°C		
250	52,000	4.9	0.025
440	43,300	8.3	0.02
670	35,600	9.7	0.02
1075	31,800	13.0	0.02
1200	28,000	93.3	0.05
1473	23,000	13.3	0.025
1800	18,000	13.2	0.025
	Deposited at 180°C		
290	52,400	5.2	0.05
670	31,400	8.3	0.04
1220	27,600	13.3	0.04
1400	24,000	13.3	0.04
1600	21,000	13.3	0.07
1920	17,600	13.4	0.05

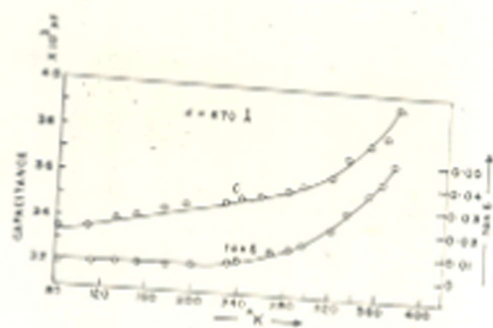

(a)

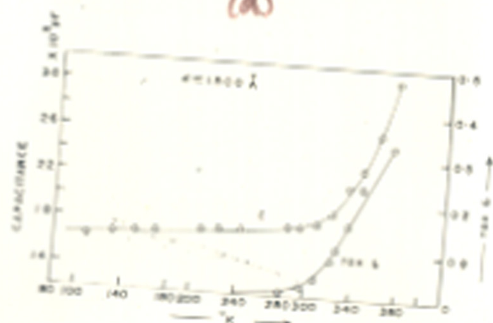

(b)

Fig IV. 4

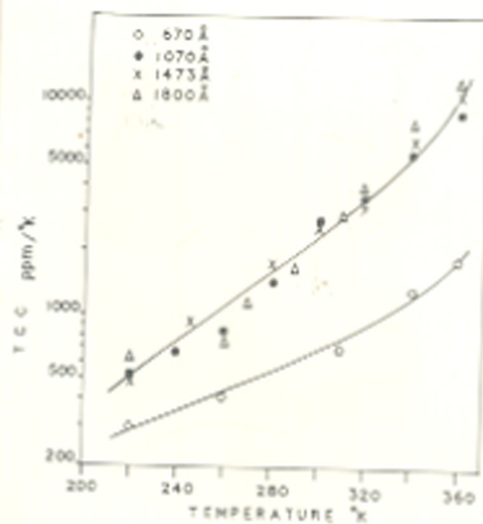

Fig IV. 5

trend with film thickness but attained a constant value for thicknesses larger than 1200 Å (Fig. IV.3). Tan δ ($\simeq$ 0.03) was however independent of film thickness. Praseodymium oxide films deposited at higher substrate temperatures (180°C), also showed a similar thickness dependence of dielectric constant. No significant changes in the values of ϵ and tan δ were observed for these films (Fig. IV.3).

(iii) Effect of temperature on C and tan δ

Capacitance and tan δ in general increased with the temperature. Figs. IV.a and b show the typical variations of C and tan δ with the temperature at 1 kHz. It is seen that C and tan δ both changed very little at low temperatures (< 280°K) but increased rapidly at higher temperatures. For a film thickness of about 1473 Å, C increased from 22,000 pF at 280°K to 39,000 pF at 372°K, and tan δ from 0.005 to 0.45 in the same temperature region. Similar behaviour was also observed for all films studied with the thickness ranging between 600 to 2000 Å.

Fig. IV.5 shows the TCC of four capacitors measured between 80°K and 360°K at 1 kHz. TCC was in general small (< 500 ppm/°K) at low temperatures but at higher temperatures it increased rapidly to values as

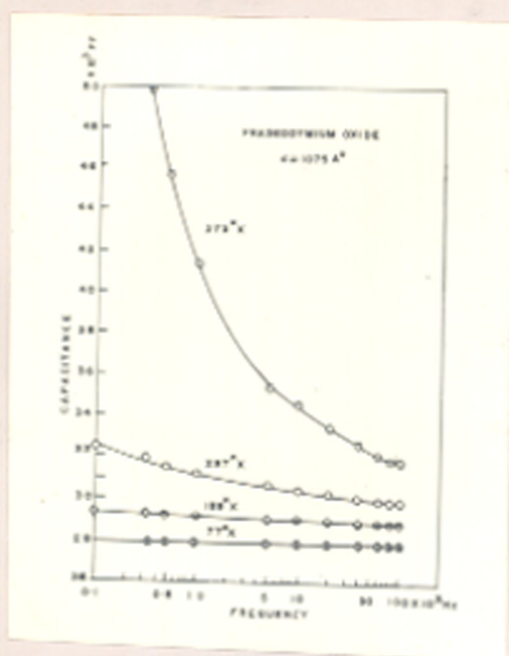

Fig IV.6a

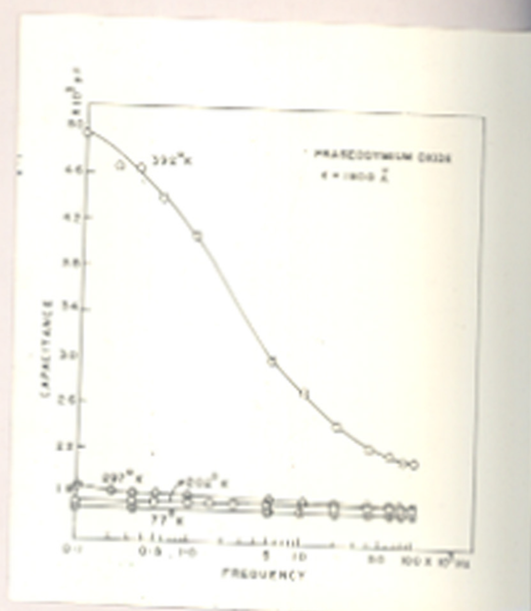

Fig IV.6b

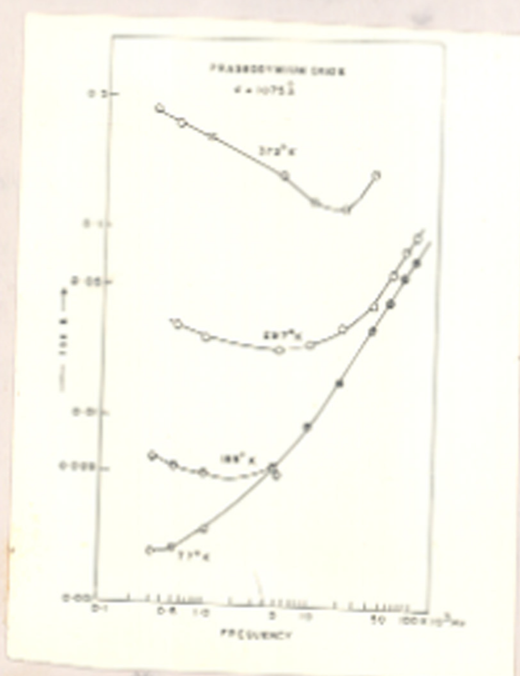

Fig IV.7a

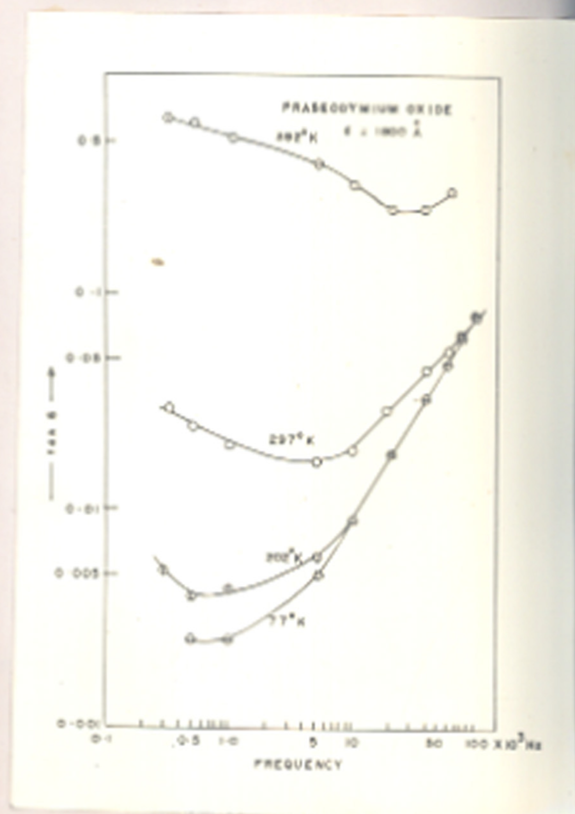

Fig IV.7b

high as 10,000 ppm/^{o}K at about 360°K. As can be seen from the graph, TCC was in general independent of the film thickness except for thinner films

(iv) Variation of capacitance with frequency

Capacitance decreased with the increasing frequency but became invariant at both low temperatures and high frequencies. A typical behaviour of capacitance with the frequency and temperature is illustrated in Figs. IV.6a and b for film thicknesses 1075 Å and 1800 Å respectively. At high temperatures, say above 392°K, capacitance fell rapidly from 50,000 pF at 100 Hz to 23,000 pF at 50 kHz for a film capacitor of d = 1800 Å. On the other hand, when the measurements were carried out below the room temperature, capacitance was found to be invariant with the frequency. It is interesting to note that at high frequencies, say greater than 60 kHz, capacitance became nearly invariant with frequencies even if the measurements were made at higher temperatures. Similar results were also obtained for films deposited at higher substrate temperatures.

(v) Variation of tan δ with frequency

The influence of frequency and temperature on loss factor is shown in Figs. IV.7a and b. Tan δ was found to

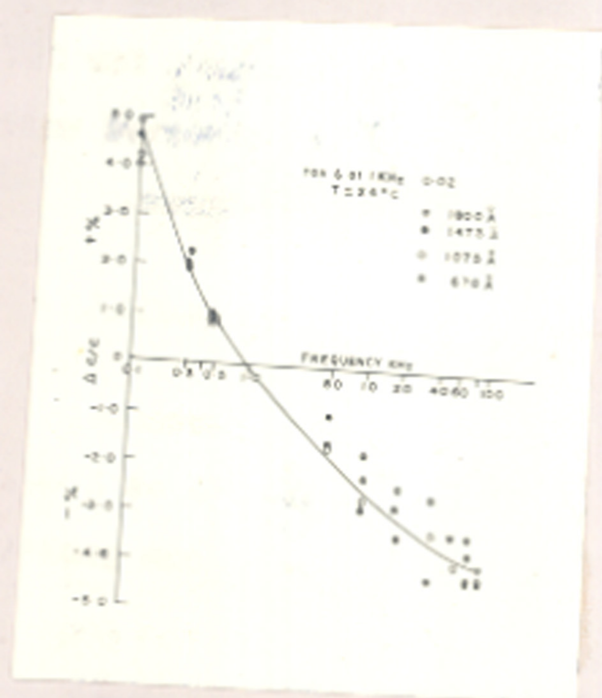

Fig IV. 8

decrease with the increasing frequency, passed through a minimum value ($\tan\delta_{min}$) and then again rose almost linearly with the applied frequency. The position of f_{min} (or ω_{min}) shifted to the higher frequency region with the increase of temperature. At higher temperatures, the shift of f_{min} or ω_{min} was very large and the values of $\tan\delta$ and $\tan\delta_{min}$ also increased with the temperature. Similar results were also obtained for films deposited at 180°C. Table IV.2 shows the observed values of ω_{min} and $\tan\delta_{min}$ at different temperatures.

(vi) <u>Percentage variation of capacity with frequency</u>

$\frac{\Delta C}{C}$ expressed as a percentage was measured with reference to the capacitance (C) at 1 kHz as an arbitrary standard. Below 1 kHz, $\frac{\Delta C}{C}\%$ was positive and had a maximum value at about 100 Hz; but above 1 kHz it became negative and nearly constant at very high frequencies. Fig. IV.8 shows the behaviour of $\frac{\Delta C}{C}\%$ in the frequency spectrum of 100 Hz to 100 kHz for capacitors of different thicknesses when measurements were carried out at room temperature. In general this variation was between +4.5% and -3.75% in the frequency region mentioned and independent of the film thickness.

TABLE IV.2

d(Å)	T °K	ω_{min} rad/sec	tan δ_{min}
	77	-	-
	189	9.4×10^{3}	0.0047
1075	297	2.8×10^{4}	0.023
	372	1.25×10^{5}	0.13
	77	3.1×10^{3}	$<$ 0.0025
	202	3.75×10^{3}	0.004
1800	297	3.1×10^{4}	0.017
	392	1.89×10^{5}	0.24

(vii) Breakdown voltage (V_B) and field strength (F_B)

Breakdown voltage of these capacitors was very high. V_B was 14 volts and 17.5 volts for film thicknesses of 250 Å and 589 Å respectively corresponding to dielectric field strengths (F_B) of the order of 5.4 and 2.9 meV. V_B for thicker films could not be measured because of the large applied voltage necessary for this purpose.

(c) Optical Properties

Praseodymium oxide films were generally transparent showing interference colours.

(i) Transmittance

Figure IV.9 shows the transmittance of vacuum deposited praseodymium oxide films when measured by a Beckman DK2 spectrophotometer in the visible region. These films were deposited at room temperature and annealed in vacuo at 150°C for two hours before the measurements were made. Transmittance was rather high in the red region ($\approx$97%) even for thicker films. At lower wavelengths, however, transmittance reduced considerably for thicker films. Similar results were also obtained for films deposited at 300°C and subsequently annealed in vacuo.

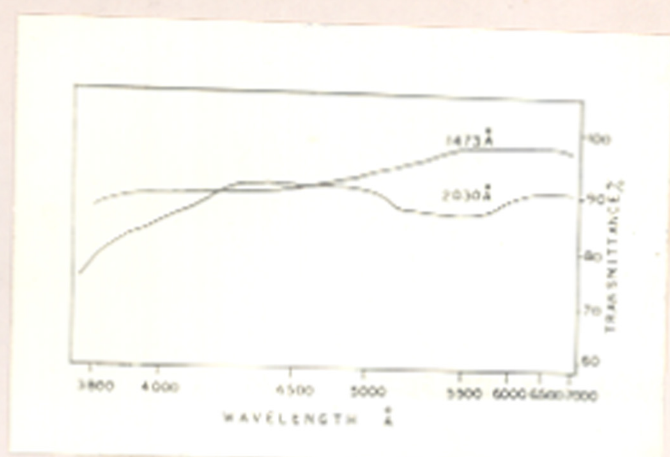

Fig IV.9

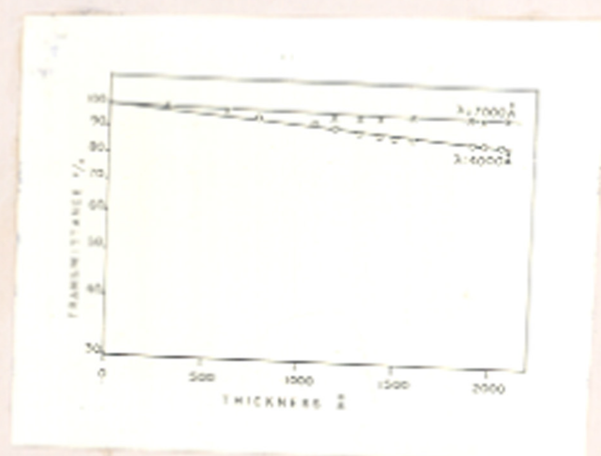

Fig IV.10

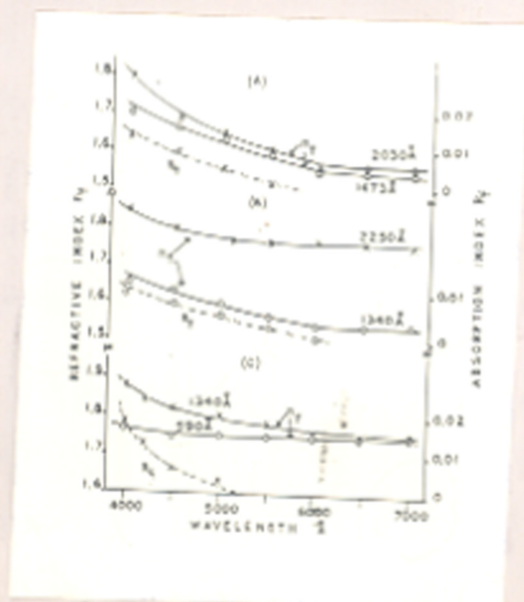

Fig IV.11

Praseodymium oxide films were also deposited at 300°C, annealed at about the same temperature and finally baked in air for nine hours at 300°C.

(ii) Optical constants, etc.

The absorption index was calculated from the Lambert's relation

$$I = I_o \exp\left(\frac{-4\pi k_f d}{\lambda}\right)$$

where I/I_o is the transmittance (T%) through the film, d is the film thickness and λ is the wavelength of the incident radiation. k_f was calculated from the slope of the plots of log T% and film thickness (d) (Fig. IV.10).

This value of k_f was inserted in the complex equations (II.3) and (II.4) and the refractive index was computed. n_f increased very slowly with the increase of incident energy. Film thickness did not have any significant influence on the optical constants. Absorption index k_f was zero for larger wavelength but slightly increased to 0.01 for wavelengths below 5000 Å (Fig. IV.11).

A comparison of the optical constants of praseodymium oxide films prepared under the three different conditions mentioned above i.e. (A) deposited at room temperature and annealed at 150°C in vacuo; (B) deposited

at $300^{o}C$ and annealed at $260^{o}C$ and (C) deposited at $300^{o}C$ and annealed at $260^{o}C$ and finally baked in air for nine hours at $300^{o}C$, was made on films whose thicknesses were nearly of the same order (Fig. IV.11). Table (IV.3) shows the values of the optical constants for such films. Absorption coefficient (α) was of the order of 10^{3} cm^{-1} at 4000 Å and more or less independent of the condition of preparation of the film.

(D) DISCUSSION

All praseodymium oxide films were amorphous in nature even when deposited at $400^{o}C$.

The a.c. behaviour of Al/praseodymium oxide/Al capacitors was identical with the ZnS film capacitors. Capacitance was found to be inversely proportional to film thickness for thicker films only, say greater than 1000 Å. In this region ϵ was independent of film thickness and had a value of 13.2. In the case of thinner films, however, ϵ increased with the film thickness. Here the capacitance no longer followed the proportionality law with 1/d. This deviation from the relation between capacitance and dielectric thickness may be attributed to the presence of defects such as voids, etc. in the dielectric films as explained in Chapter III.

TABLE IV.3

Wavelength (Å): Type	Thickness (d) Å		7000	6500	6000	5500	5000	4500	4000
A	1473	n_f:	1.54	1.54	1.54	1.60	1.64	1.66	1.70
		k_f:	0	0	0	0	0.0055	0.009	0.013
	2030	n_f:	1.56	1.56	1.56	1.60	1.64	1.66	1.80
		k_f:	0	0	0	0	0.0055	0.009	0.013
B	1340	n_f:	1.54	1.54	1.54	1.57	1.60	1.66	1.68
		k_f:	0	0	0	0.004	0.006	0.008	0.009
	2250	n_f:	1.76	1.76	1.76	1.76	1.76	1.80	1.84
		k_f:	0	0	0	0	0.006	-	0.010
C	590	n_f:	1.75	1.75	1.75	1.75	1.75	1.76	1.76
		k_f:	0	0	0	0	0	0	0
	1340	n_f:	1.75	1.75	1.76	1.78	1.80	1.82	1.88
		k_f:	0	0	0	0	0.004	0.006	0.018

Tan δ measurements with the frequency at each cycle of annealing provided some interesting information regarding the conductivity of the dielectric layers. As can be seen from Fig. IV.2 f_{min} and hence ω_{min} shifts to the lower frequency with each cycle of annealing. Capacitance, on the other hand, decreases and becomes nearly invariant with the frequency after a few annealing cycles. Looking back at equation (III.10) it is seen that the value of ω_{min} is solely determined by the sandwiched dielectric resistance R and capacitance C, as the variation of the lead resistance is negligible. If now ω_{min} were to shift to the lower frequency region, this could be brought about by increasing the value of the denominator in equation (III.10) which is possible only if the resistance R were to increase, because capacitance (C) reduced on annealing. In fact, as mentioned earlier, annealing helps to reduce the amount of defects present in the deposited film. In doing so, the carrier concentration would reduce and thereby increasing the resistivity of the dielectric.

The behaviour of capacitance and tan δ with the frequency at different temperatures are predicted by equations (III.10) and (III.13) obtained as a consequence of our proposed model for film capacitors. Here also capacitance became invariant with the frequency at low

temperatures. As the temperature increased the resistivity of the dielectric reduced and hence ω_{min} shifted to the higher frequency region.

Both capacitance and tan δ increased with temperature. This behaviour is also predicted by equations (III.11) and (III.11a) of the theoretical model.

As a consequence of the theoretical model, several electrical parameters of the dielectric material could be calculated. In the following paragraphs the method for computing lead resistance, resistivity of the dielectric and activation energy of praseodymium oxide films have been described.

Electrode and lead resistance 'r' is practically invariant with the temperature and the frequency in the region studied here. From the tan δ versus frequency curves 'r' can be calculated taking the help of equation (III.11b). Table IV.4 shows the values of 'r' as obtained at different frequencies and temperature for a 1800 Å thick film capacitor. It is seen that 'r' is nearly constant and has a value of about 6.3 ohms. If this value of r is substituted in the equation of ω_{min}, then the dielectric resistance R can be calculated as shown in Table IV.5

TABLE IV.4

d = 1800 Å

Temperature °K	Frequencies ($f_1 \sim f_2$) x 10^3 Hz	r ohms
77	40 ~ 50	6.5
	60 ~ 80	6.5
	80 ~ 100	6.5
	40 ~ 50	6.5
202	60 ~ 80	6.5
	80 ~ 100	6.5
	50 ~ 60	6.0
297	60 ~ 80	6.0
	80 ~ 100	6.0
392	50 ~ 60	6.4

Average r = 6.3 ohms

TABLE IV.5

Thickness (d) Å	Temperature (T) °K	ω_{min} rad/sec	Capacitance (C) pF	R ohms
	202	3.75×10^3	17,400	4.1×10^7
1800	297	3.15×10^4	17,800	5.2×10^5
	392	1.88×10^5	22,000	9.6×10^3
	189	9.4×10^3	29,100	2.28×10^6
1075	297	2.84×10^4	31,000	2.2×10^5
	372	1.26×10^5	33,500	9.5×10^3

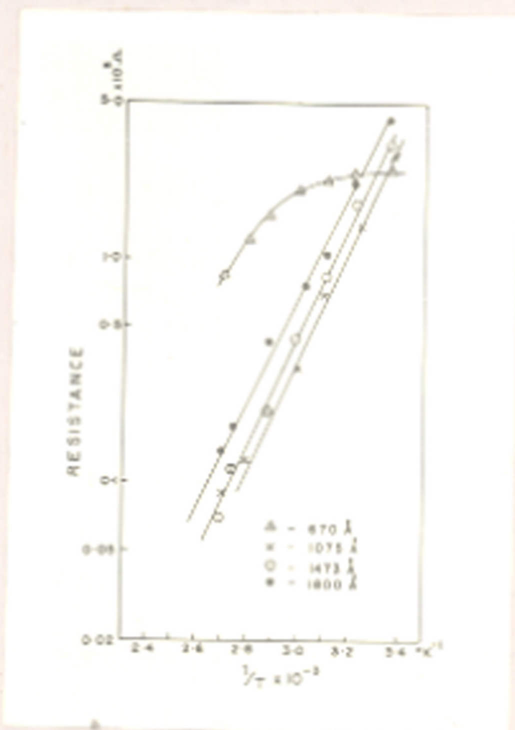

Fig IV. 12

The theoretical model also predicts the value of $\tan\delta$ at any frequency as $\tan\delta = \frac{1}{\omega RC} + \omega rC$ where ω, R, r and C have their usual meaning. Now at a low frequency say 1 kHz, the second term in $\tan\delta$ is very small as compared to $\frac{1}{\omega RC}$ and hence could be neglected. This can be verified by substituting the proper values of r and C in the above equation. From these measurable quantities, the value of the dielectric resistance R and resistivity ρ can be computed directly. In Table IV.6 the values of R so computed at different temperatures are shown for four different film thicknesses. It may be pointed out here that the values of R are nearly of the same order as those computed from ω_{min} (cf. Table IV.5). Resistance decreased with the increase of temperature. Fig. IV.12 shows the plots of resistance versus 1/T for these samples. If we now assume R to follow the relation $R = R_o \exp(\Delta E/kT)$ where ΔE is the activation energy, then from the slope of the above graphs ΔE can be computed. Since the slopes have the same value, the activation energy is nearly constant with a value of 1.8 eV between 297^oK and 380^oK for all film thicknesses.

The resistivity of praseodymium oxide films at room temperature was found to be about 7×10^9 ohm cm and independent of the film thickness.

TABLE IV.6

Calculation of R from $\frac{1}{\omega RC}$

d	T °K	$\frac{1}{T} \times 10^{-3}$	tan δ	C pF	R x 10^5 ohm
	297	3.37	0.018	35600	2.6
	310	3.23	0.018	35800	2.58
	322	3.11	0.02	36400	2.3
670 Å	335	2.99	0.022	37000	2.05
	347	2.88	0.028	37500	1.54
	360	2.78	0.035	38200	1.22
	372	2.69	0.05	39600	0.85
	297	3.37	0.02	31800	2.65
	310	3.23	0.035	33000	1.4
	322	3.11	0.07	34000	0.7
1075 Å	335	2.99	0.14	35800	0.33
	347	2.88	0.22	36900	0.195
	360	2.78	0.29	39600	0.128
	365	2.74	0.33	44400	0.113
	372	2.69	0.355	51000	0.092

TABLE IV.6 (CONTD.)

d	T °K	$\frac{1}{T} \times 10^{-3}$	tan δ	CpF	R x 10^5 ohm
	297	3.37	0.022	23000	3.26
	310	3.23	0.04	23800	1.75
	322	3.11	0.08	24600	0.845
1473 Å	335	2.99	0.14	27000	0.44
	347	2.88	0.27	30000	0.206
	365	2.74	0.37	32800	0.119
	372	2.69	0.5	49500	0.067
	297	3.37	0.023	18000	4.1
	310	3.23	0.04	18400	2.26
	322	3.11	0.08	19300	1.07
1800 Å	328		0.11	19500	0.77
	397	2.88	0.25	23000	0.435
	365	2.74	0.33	28200	0.177
	372	2.69	0.33	34000	0.15

From the above discussions it is seen that almost all the a.c. properties of praseodymium oxide capacitors could be very well explained by the theoretical model proposed in Chapter III. Further some of the electrical parameters could also be calculated in the light of the above theory, thus making it a powerful tool for the investigation of the dielectric and semiconducting properties of insulators.

Optical studies show that praseodymium oxide films are in general very transparent in the visible region. However for thicker films a slight absorption takes place at lower wavelengths. As can be observed from Fig. IV.11 refractive index 'n_f' was small ranging between 1.56 to 1.8 and depending on the deposition conditions of the films. It is now well known that many oxides when thermally evaporated in vacuo form lower oxide films on condensation (Goswami and Trehan, 1957; Goswami, 1965; Gadgil and Goswami, 1970). Thus it is also possible that such a decomposition might also take place in the case of praseodymium oxide films. With this in view, n_f and k_f were calculated for films deposited at room temperature, at higher substrate temperature, and also for films further baked in air at 300°C for 9 hours. These results are shown in Table IV.3.

It is interesting to see that n_f and k_f for a film

deposited at room temperature and vacuum annealed at 150°C (d = 1473 Å; type A) were almost the same for a film of nearly the same thickness (d = 1340 Å) but deposited at 300°C and annealed in vacuo (type B). However for a film of nearly identical thickness when deposited at 300°C and baked in air for 9 hours at the same temperature (typeC), the values of n_f and k_f became slightly higher than those obtained for the previous films. This small change in n_f and k_f could be due either to a slight difference in the state of oxidation in those two types of films, or to an increase in the grain growth which was still too small to be detected by the electron diffraction method. The increase of n_f with film thickness however suggests the latter possibility. The values of n_f obtained for praseodymium oxide films here were slightly less than the values of 1.85 to 1.95 obtained for Pr_6O_{11} by Hass et al (1959) in the visible region.

The optical dielectric constant for a film 1473 Å thick was found to be ≈ 3.0. This value was much less than the ϵ (13.2) obtained at low frequencies, thus indicating the presence of ionic polarisation.

The fact that praseodymium oxide films are very transparent in the visible region also indicate that the absorption edge will be somewhere near the u.v. region.

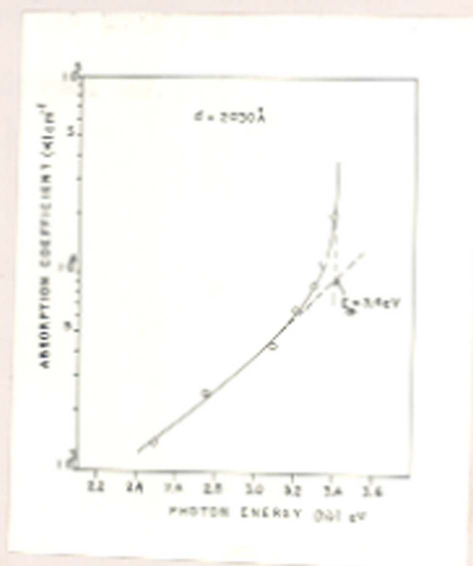

Fig IV.13

This is in conformity with the high resistivity (10^9 ohm cm) observed for praseodymium oxide films and a possible large forbidden energy gap. In fact a plot of α with incident photon energy (Fig. IV.13) shows the optical band gap to have a value of 3.4 eV. This seems to agree reasonably well with the value of $\Delta E = 3.6$ eV calculated from the dielectric results if one assumes an intrinsic conduction to take place so that the exponential term $\Delta E/kT$ would be replaced by $\Delta E/2kT$.

CHAPTER V

STUDIES ON ANTIMONY TRIOXIDE FILMS

(A) INTRODUCTION

Antimony forms two well known oxides namely Sb_2O_3 and Sb_2O_5. The existence of a suboxide (SbO) has recently been reported by Shimaushi (1960) but it could not be confirmed by other workers. The trioxide (Sb_2O_3) also known as a sesquioxide is of common occurence and exists in two different forms. This dimorphism was demonstrated experimentally by Tutton (1926). One form known as valentinite is stable above 570°C and has an orthorhombic structure with a_o = 4.92 Å, b_o = 12.46 Å, c_o = 5.42 Å (Buerger, 1936, 1937-38). The other form known as senarmontite is stable below 570°C and has a cubic structure (Bozorth, 1923; Almin and Westgren, 1941-42) with a_o = 11.13 Å. Bound and Richards (1939) oxidised antimony films on collodion in vacuo and found that no detectable oxidation took place upto 250°C and above this the patterns were due to a cubic structure with a_o = 11.1 Å. Acharya (1948) found that the oxidation of the cleavage face (111) of antimony single crystals yielded only a cubic form of Sb_2O_3 with a_o = 11.12 Å. Very recently Gadgil (1968) showed that the oxidation of antimony films in low vacuo ($\approx$ 2 mm of Hg) at high temperatures yielded

only cubic forms of Sb_2O_3 but no suboxide. He also found that thick films of antimony which were highly oriented yielded perfectly 1-d oriented Sb_2O_3 films on oxidation in air.

Arkel et al (1953) in their study of the electrical conductivity of molten oxides found the specific conductivity varied with the temperature. Korzh and Gulayeva (1969) measured the resistivity of antimony oxide at different temperatures and found a decrease of the resistivity from 10^{10} - 10^{11} ohm cm at room temperature to 10^3 ohm cm at 800°C. Activation energy was 1.6 eV between 170 to 470°C, 3.6 eV between 470 to 600°C and 2.8 eV between 600 to 850°C.

Sb_2O_3 films were found to be quite transparent even in the u.v. region. Because of its comparatively high refractive index (2.1), Barr and Jenkins (1956) were able to prepare all dielectric interference filters of Sb_2O_3 and cryolite films for their use in the ultraviolet region. With an even layer dielectric they obtained transmittance as high as 93.6% at 3725 Å. Sawaki (1958) prepared achromatic antireflection coatings by combining a Sb_2O_3 film with a MgF_2 film. The absorption of Sb_2O_3 films was studied by Doyle (1958). He found that these films absorbed strongly in the u.v. region with the absorption coefficient as high

as 10^5 cm^{-1} and that the threshold photon energy was 4.2 eV. Doyle and Clarke (1961) also studied the optical absorption of Sb_2O_3 films in the Schumann region. The optical properties of reactively sputtered and amorphous Sb_2O_3 films were studied by Lieberman and Medrud (1969). The optical constants of amorphous and crystalline (cubic and orthorhombic) bulk Sb_2O_3 have been compared by Wood et al (1972). The refractive indices of amorphous, cubic and orthorhombic forms of Sb_2O_3 were 1.65, 1.98 and 2.1 respectively in the visible region and the optical band gaps were found to be 3.25 to 3.3 eV for orthorhombic crystals, 4.0 eV for cubic crystals and 3.8 eV for the amorphous material. These gaps however corresponded to the indirect transitions.

Antimony oxide doped with Mn showed a green emission with a maximum at 5200 Å (Jamin and Bernard, 1953). According to Allaslu and Kil'k (1966) the exceptionally high sensitivity of the emission to temperature for luminiphosphors of Sb_2O_4:Mn could be utilized for determining surface temperatures.

The above survey shows that very little work has been done so far on the optical properties of vacuum deposited Sb_2O_3 films. Further, it seems that the dielectric properties of Sb_2O_3 films, which generally have a cubic

structure, have not been studied at all. Because of its high energy band gap (≈ 4 eV) and resistivity, it is likely that Sb_2O_3 films could be used as a good insulator or dielectric material in active and passive devices. With this in view, a systematic study was made on the dielectric and optical properties of Sb_2O_3 films.

(B) EXPERIMENTAL

Sb_2O_3 films were prepared by the evaporation of bulk Sb_2O_3 powder in vacuo ($\approx 10^{-5}$ mm Hg) from a silica boat heated by a tungsten filament. Pure Sb_2O_3 powder (supplied by Sujezcheme Export, Moscow, USSR) was placed in a silica boat and degassed in vacuo in the manner described previously. The temperature of the boat was then raised to enable the uniform deposition of Sb_2O_3 films. Films so formed on glass substrates were transparent and showed interference colours.

If, on the other hand, Sb_2O_3 was deposited directly from a molybdenum boat then blackish and opaque films were formed on the substrates and these films became transparent showing interference colours when baked in air. Because of the discrepancy in the physical appearance of the two types of films formed from silica and molybdenum boats, investigations reported here were confined only to those formed by the evaporation from the former.

Depositions were also made on polycrystalline NaCl tablets as mentioned before for their structural determinations.

All capacitors (Al/Sb_2O_3/Al) were subjected to heating and cooling cycles in vacuo prior to their dielectric measurements. Transmission in the visible region for these films were measured on a Unicam SP500 spectrophotometer.

(C) RESULTS

(a) Structure

A typical electron diffraction transmission pattern obtained for a film deposited on a polycrystalline NaCl tablet is shown in Fig. V.1. The deposits were crystalline and had a f.c.c. structure with a_o = 11.13 Å. The corresponding d values of the rings are shown in Table V.1.

It was also found that the blackish antimony oxide films deposited from a molybdenum boat on polycrystalline NaCl when oxidised in air, yielded electron diffraction patterns corresponding to those in Fig. V.1. This suggests that films deposited from silica boats or obtained by the oxidation in air of deposits from molybdenum boats

TABLE V.1

I/I_o	d (Å)	hkl
vs	3.21	222
m	2.80	400
m	2.52	331
vf	2.31	422
vf	2.12	511
ms	1.97	440
ms	1.69	622

average a_o = 11.13 Å

vs - very strong
ms - medium strong
m - medium
vf - very faint

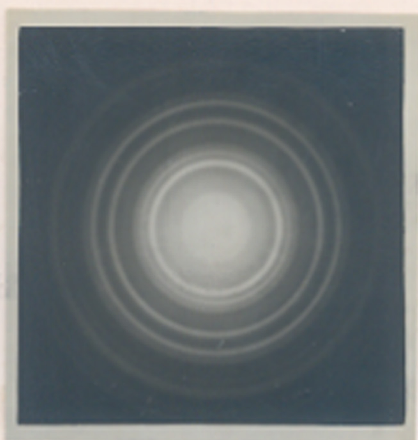

Fig V.1

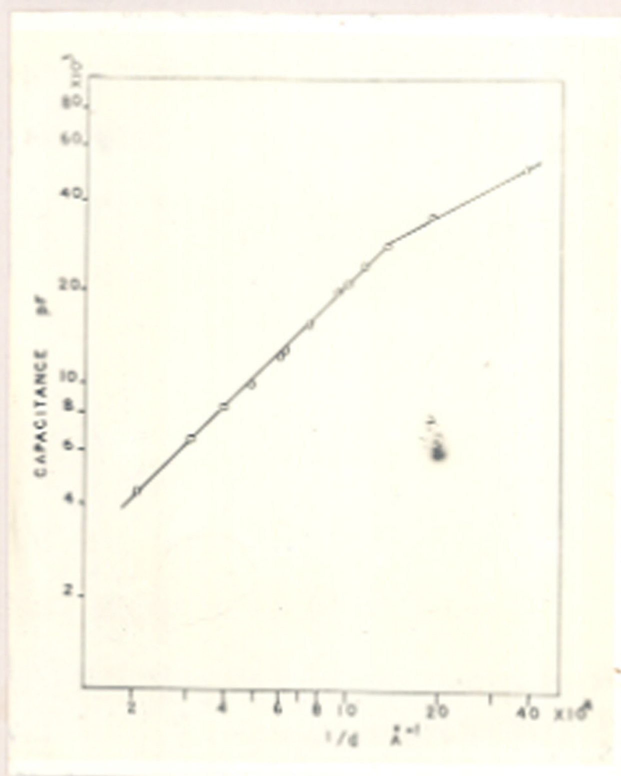

Fig V.2

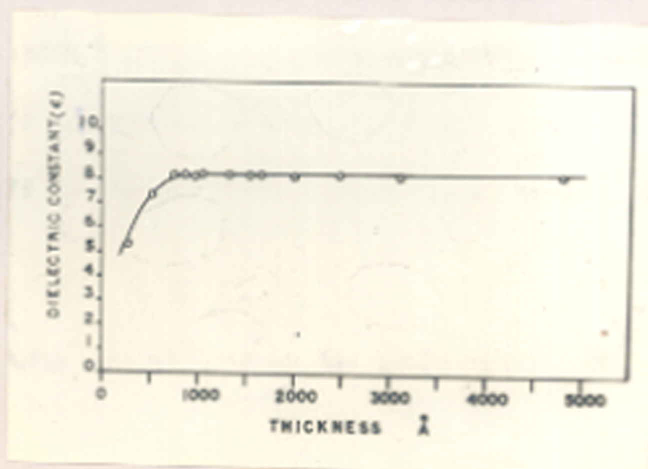

Fig V.3

consisted of Sb_2O_3 only.

(b) Dielectric Properties

(i) Ageing and annealing effect

Al/Sb_2O_3/Al film capacitors showed very little ageing in air. When these capacitors were subjected to heating and cooling cycles in vacuo, capacitance reduced only slightly and attained stability very early unlike the previous cases. Tan δ was very low and no observable change in its value on annealing was noticed.

(ii) Effect of film thickness

The effect of film thickness on capacitance and dielectric constant (ϵ) is shown in Figs. V.2 and 3 and in Table V.2. From these it is seen that the capacitance was inversely proportional to thickness (d) for film thickness greater than say 800 Å. ϵ however increased with d from 5.0 to 250 Å to 8.2 at 800 Å, and then became constant for thicker films as observed earlier for ZnS and praseodymium oxide films. Loss factor (tan δ) which was very low and less than 0.003 was independent of the film thickness. All these measurements were made at 1 kHz.

(iii) T.C.C.

The variation of capacitance and tan δ with

TABLE V.2

Thickness (d) Å	Capacitance (C) pF	ϵ	tan δ
260	51,000	5.3	0.003
520	35,200	7.35	0.005
740	28,300	8.2	$<$0.003
860	24,000	8.2	"
980	21,250	8.2	"
1050	20,000	8.3	"
1300	15,800	8.2	"
1580	12,820	8.2	"
1650	12,300	8.2	"
2050	9,980	8.1	"
2500	8,330	8.3	"
3200	6,520	8.3	"
4800	4,400	8.3	"

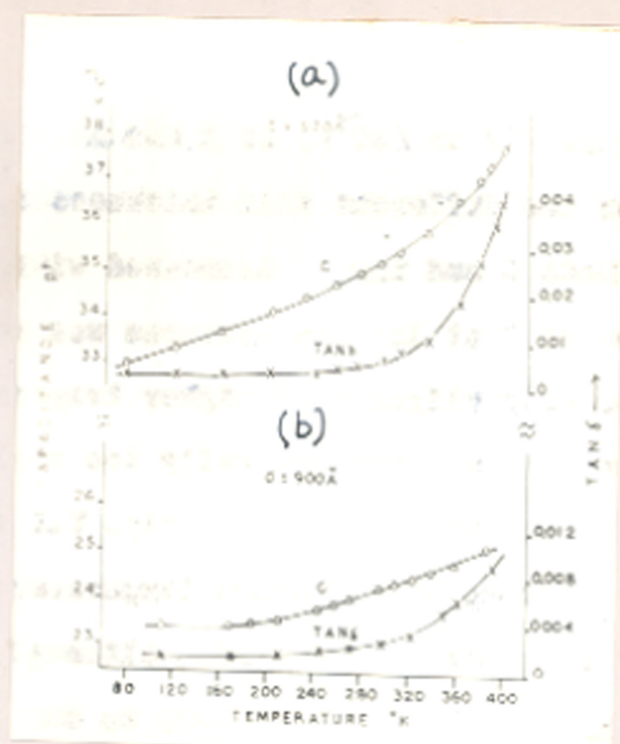

Fig V.4

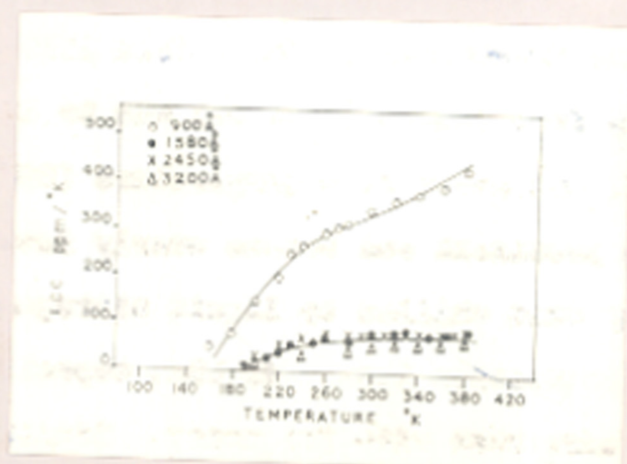

Fig V.5

temperature (77 to 380°K) at 1 kHz is shown in Figs. V.4a and b for two different film thicknesses, viz. 520 Å and 900 Å. Both C and tan δ increased with temperature. The variation of C at low temperatures was negligible, but increased only slightly at higher temperatures. The variation of tan δ was generally too small to be measured accurately for thicker films. Fig. V.5 shows the TCC of these capacitors at different temperatures. It is seen that TCC is positive and small, although the thinner films seem to have higher values (200 to 600 ppm/°K) as compared to the thicker ones. (< 100 ppm/°K).

(iv) Effect of frequency on capacitance

The variation of capacitance with frequency at different temperatures of measurement is shown in Figs. V.6a and b. Capacitance was found to decrease with increasing frequencies. For a film 1580 Å thick, C decreased from 12,820 pF at 0.1 kHz to 12,600 pF at 100 kHz at 350°K. At about room temperature (297°K) this variation was less prominent and became nearly invariant with frequency when chilled to liquid nitrogen temperature. At higher frequencies i.e. > 40 kHz, capacitance did not change very much with frequency. Similar results were also obtained for films of different thicknesses (Fig. V.6b).

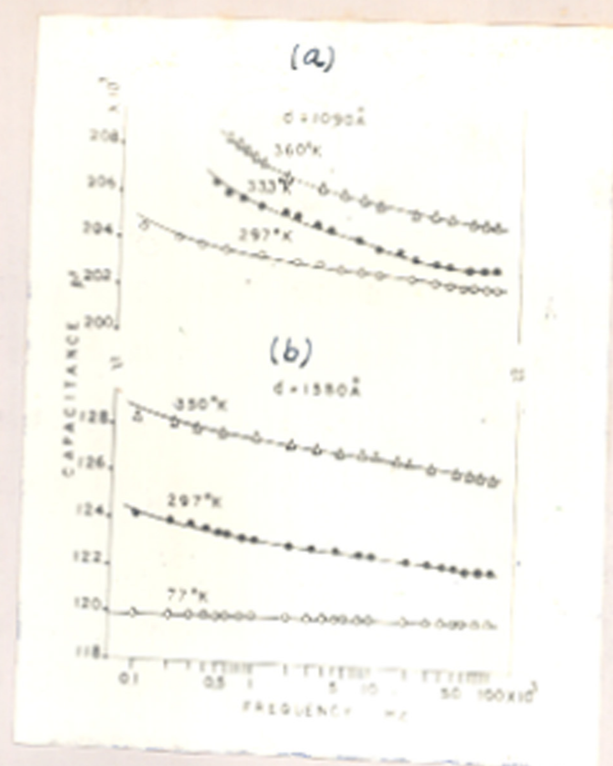

Fig V.6

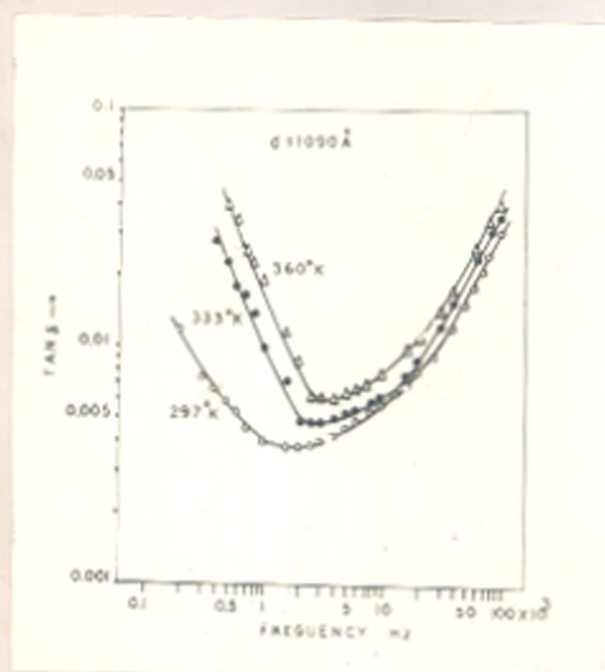

Fig. V.7a

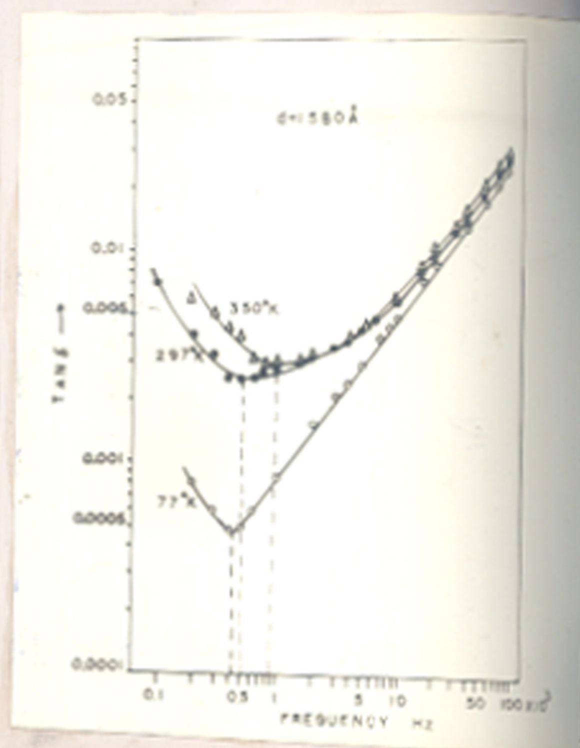

Fig V.7b

(v) Variation of tan δ with frequency

Frequency had a pronounced influence on tan δ of Sb_2O_3 film capacitors. Fig. V.7a and b show the typical variation of tan for two film thicknesses. Tan δ in general decreased with the rise of frequency, then passed through a minimum value at a frequency f_{min} and then again rose rapidly at higher frequencies. f_{min} and hence ω_{min} showed a shift to the higher frequency side of the frequency spectrum with the rise of temperature. The value of tan δ_{min} also increased with the temperature. Table (V.3) shows the values of ω_{min} and tan δ_{min} for films 1090 Å and 1580 Å thick. At very high frequencies tan δ was almost linearly proportional to the applied frequency and its values showed very small differences with the temperatures of measurement.

(vi) Percentage variation of capacitance:

The percentage variation of $\frac{\Delta C}{C}$ with the applied frequency is shown in Fig. V.8 for two different thicknesses. Below 1 kHz this variation was positive but became negative for frequencies greater than 1 kHz. $\Delta C/C\%$ was very small say about ±0.5% and more or less independent of thickness when measurements were made at room temperature.

TABLE V.3

Thickness (d) Å	Temperature (T) °K	Capacitance (C) pF	ω_{min} rad/sec	$\tan\delta_{min}$
	297	20,350	1.06×10^4	0.0038
1090	333	20,480	1.68×10^4	0.0048
	360	20,650	2.2×10^4	0.006
	77	12,000	2.8×10^3	0.00048
1580	297	12,400	3.15×10^3	0.0025
	350	12,800	6.3×10^3	0.0030

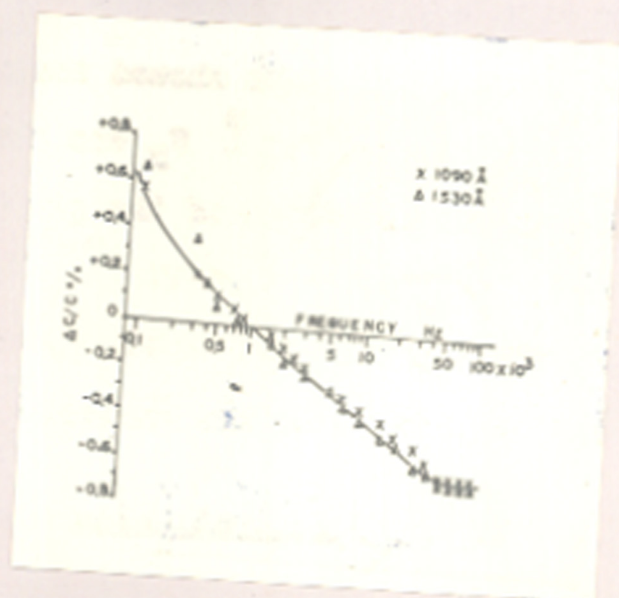

Fig V.8

(vii) **Breakdown voltage (V_B) and dielectric field strength (F_B)**

V_B increased with the film thickness from 2 volts for a thickness of 260 Å to 9.0 volts for a thickness 1300 Å (Table V.4 and Fig. V.9). Dielectric field strength (F_B), on the other hand, reduced with the film thickness. When F_B was plotted against the film thickness in the log-log scale, the graph showed two distinct slopes (Fig. V.10). Below 750 Å, F_B was nearly independent of film thickness and the slope of the graph was about zero. But for films thicker than 750 Å, the slope had a value of -0.5 showing that F_B obeyed a power law viz. $F_B \propto d^{-\frac{1}{2}}$, which happens to be the Forlani-Minnaja relation.

(c) Optical Properties

(i) Transmission

Transmittance of Sb_2O_3 films in the visible region was measured by a Unicam SP 500 spectrophotometer for film thicknesses greater than 4000 Å. Fig. V.11 shows the typical transmittance curves in the visible region. It is interesting to see that the curves were associated with extrema. For a film 4680 Å thick the transmittance maxima had values of about 98% in the red region, but reduced to about 96% when measurements were made in the

TABLE V.4

Thickness (d) Å	Breakdown voltage (V_B) volts	Dielectric field strength (F_B) volts/cm
260	2.5	9.6×10^5
520	5.0	9.6×10^5
740	6.8	9.4×10^5
850	7.2	8.5×10^5
1050	8.0	7.5×10^5
1300	9.0	6.9×10^5

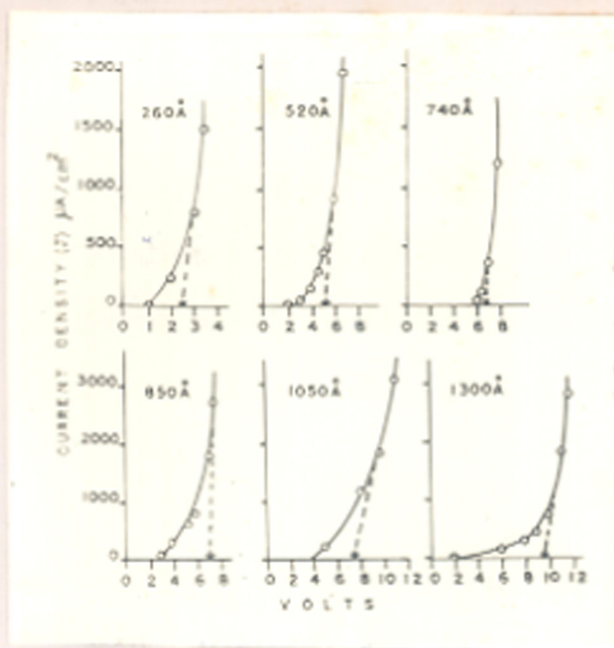

Fig V.9

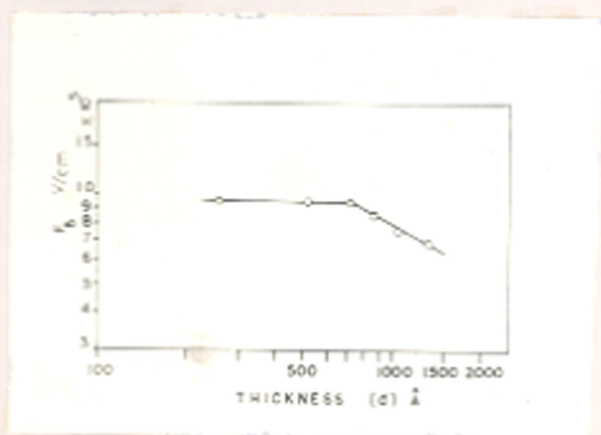

Fig V.10

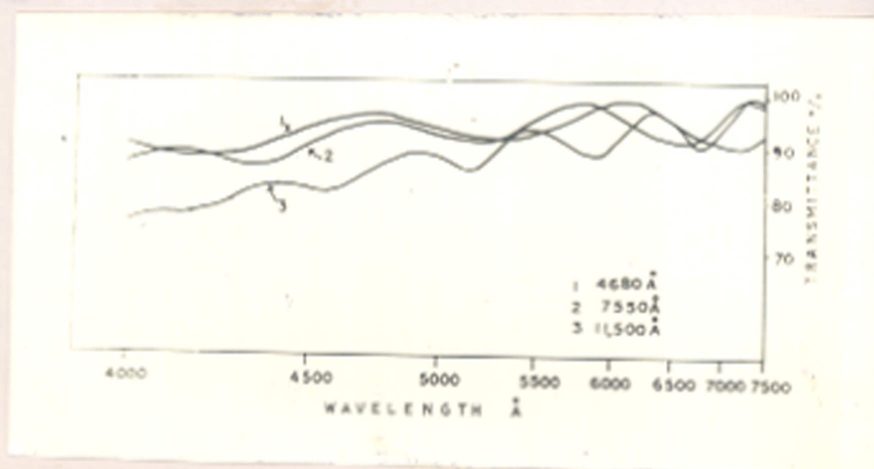

Fig V.11

violet region of the visible spectrum. For thicker film transmittance, though large, reduced greatly with the wavelength thus indicating the presence of absorption in the lower wavelength.

(ii) Optical constants

Refractive index was calculated by the help of equations (II.13) and (II.14). Table V.5 shows the values of n_f computed from the extrema at different wavelengths for films 4680 Å, 7550 Å, 10100 Å and 11500 Å thick. Fig. V.12 shows that refractive index was nearly independent of the film thickness and had very little dispersion between λ 7000 Å and λ 4500 Å. Below λ 4500 Å, n_f increased slightly.

Absorption index was computed from the complex relation of T_o given by equation (II.3). The values of n_f and wavelength as obtained from the transmission data above were inserted in equation (II.3) and k_f was then computed by the iterative method.

In case of films thinner than 5000 Å, k_f was nearly zero in the visible region but increased to 0.0064 for a film 10,100 Å thick in the same region (Fig. V.12).

(iii) Optical dielectric constant

Dielectric constant at optical frequencies was found

TABLE V.5

Thickness (d) Å	Maxima				Minima			
	λ Å	m	n_f	k_f	λ Å	m	n_f	k_f
	6100	3	1.95	0	7200	2	1.94	0
4680	4650	4	1.97	0	5250	3	1.96	0
					4100	4	1.98	0
	7400	4	1.95	0	6500	4	1.94	0
	5900	5	1.95	0	5400	5	1.96	0
7550	4950	6	1.95	0	4550	6	1.97	0.004
	4250	7	1.97	0.005				
	6400	6	1.90	0	7000	5	1.91	0
	5500	7	1.91	0	5950	6	1.91	0
10,100	4850	8	1.91	0.003	5150	7	1.915	0.001
	4300	9	1.92	-	4350	8	1.915	0.0064
	7350	6	1.915	-	6800	6	1.915	-
	6300	7	1.915	-	5900	7	1.915	-
11,500	5500	8	1.915	-	4950	8	1.91	-
	4900	9	1.915	-	4600	9	1.90	-
	4450	10	1.93	-				

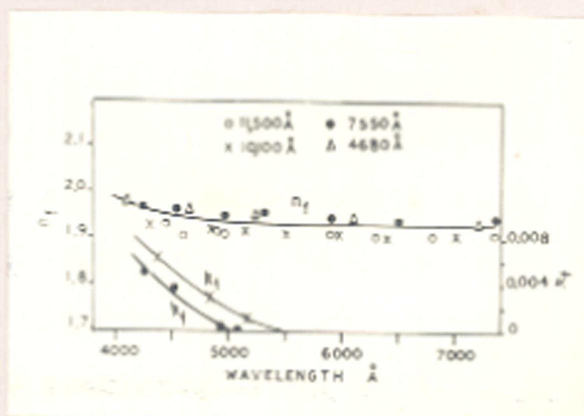

Fig V.12

to be independent of the film thickness and frequency. It was about 3.17, which was very much less than the value obtained in the audio range (8.2) thus indicating the presence of ionic polarisation in Sb_2O_3 films.

(D) DISCUSSION

Vacuum deposited films of Sb_2O_3 formed at room temperature were found to be crystalline and hence it could be inferred that the dielectric films of Sb_2O_3 were also crystalline in nature.

The thin film capacitor model proposed by us (discussed in Chapter III) has once again been found to be adequate in explaining all the a.c. behaviours of Sb_2O_3 film. The invariance of capacitance with frequency at high frequencies and at low temperatures follows from equation (III.13) of the theory proposed in Chapter III. However this variation of capacitance at the room temperature was very small and nearly independent of the film thickness. Loss factor which showed a minimum value at a frequency (f_{min}') that shifted to the higher frequencies with the increase of temperature is in accordance with equation (III.10). At high frequencies, the rise in tan δ governed by equation (III.11b) requires the lead resistance 'r' to be independent of frequency and temperature. Table V.6

TABLE V.6

Thickness (d) Å	Temperature (T) °K	Frequencies $f_1 \sim f_2$ (kHz)	r ohms
		40 ~ 50	2.0
	297	60 ~ 80	2.3
		80 ~ 100	2.0
		40 ~ 50	2.0
1090	333	60 ~ 80	2.1
		80 ~ 100	2.3
		40 ~ 50	2.3
	360	60 ~ 80	2.1
		80 ~ 100	2.3
	Average r = 2.2 ohms		
		40 ~ 50	2.25
	77	60 ~ 80	2.0
		80 ~ 100	2.0
		40 ~ 50	2.3
1580	297	60 ~ 80	2.2
		80 ~ 100	2.2
		40 ~ 60	2.5
	350	60 ~ 80	2.7
		80 ~ 100	2.2
	Average r = 2.2 ohms		

shows the values of r obtained for two different films capacitors from tan δ versus frequency measurements at different temperatures (cf. Figs. V.7a and b). The values of r so obtained agree reasonably well within the experimental errors. Similar values of r have also been observed for capacitors of different dielectric thicknesses.

Both tan δ and tan δ_{min} increased with the temperature, this being due to the increase of conductivity of the dielectric at higher temperatures (equation III.11a). TCC was therefore positive in nature as predicted by equation (III.13). The extremely low values of tan δ were probably due to the large dielectric resistance between the electrodes as $\tan \delta = \frac{1}{\omega RC}$. R as calculated from the above relation from ω_{min} (equation III.10) for a film 1090 Å thick are 0.3×10^7 and 1×10^7 ohms respectively at room temperature. Within the experimental error these two values are nearly of the same order. Resistivity (ρ) of Sb_2O_3 films which was about $10^{11} - 10^{12}$ ohm cm agrees well with the value of 10^{11} ohm cm reported by Korzh and Gulayeva (1969) for the bulk material. The high value of resistivity results chiefly from a very large forbidden energy gap of the dielectric, and has been verified from our optical results to be discussed later.

The dependence of ϵ on film thickness could be

attributed to defects chiefly voids present in the films. ϵ increased with the film thickness from 5.3 to 8.2 and then remained practically constant for all thicknesses greater than 800 Å.

Dielectric field strength (F_B) followed a power law with the film thickness. For thicker films ($>$ 800 Å), $F_B \propto d^{-\frac{1}{2}}$ was in accordance with the Forlani-Minnaja relation. Unfortunately this law was not obeyed in case of thinner films. It is, however, interesting to note that in this region ($<$ 800 Å), ϵ was dependent on film thickness.

Optical investigations of Sb_2O_3 films on glass substrates showed that these films were very transparent ($>$ 75%) in the visible region even for films as thick as 11,000 Å. However the transmittance decreased with the increase of film thickness indicating the presence of absorption in thicker films. Refractive index of these films was independent of thickness and varied from 1.91 to 1.98 between the wavelength regions 7000 Å and 4300 Å. This value agreed well with the reported value of 1.97 obtained for the cubic crystal of Sb_2O_3 by Wood et al. (1972). Their results also showed that n_f had only a little dispersion in the visible region.

Absorption index was practically zero for thinner

films, but increased slightly with the decreasing wavelength for thicker films. k_f obtained for a film 10,100 Å thick at 4350 Å was about 0.0064. This shows that as the excitation frequency passes into the ultraviolet region the transmittance will decrease due to the increasing absorption. From the value of k_f as obtained above it seems that the absorption edge must be in the u.v. region. This can also be accounted for from the very large value of resistivity (10^{11} ohm cm) observed for Sb_2O_3 films from dielectric measurements. In fact Doyle (1958) reported the optical band gap energy of Sb_2O_3 films to be about 4.2 eV.

From the above study it seems feasible to use Sb_2O_3 films as a good dielectric element for capacitors because of its low value of tan δ (< 0.003), low TCC (< 100 ppm/^oK), high breakdown field strength ($\geq 5 \times 10^5$ V/cm) and practically a near frequency invariant capacitance. ϵ was however low (8.2). These films may also be used as protective insulators because of its large value of resistivity. The optical properties, such as high refractive index with practically negligible absorption in the visible region could also be utilised in suitable optical devices such as reflectors and interference filters operating in the violet and near ultraviolet regions.

CHAPTER VI

STUDIES ON THERMALLY EVAPORATED NIOBIUM OXIDE FILMS

(A) INTRODUCTION

The need for insulators of high permittivity and low losses in microelectronic circuits has been realised recently with the advent of tantalum technology. Pentoxides of tantalum have been so useful in microelectronics that oxides of several other metals belonging to the same group as tantalum have also been investigated in recent years. Of these the oxides, particularly the pentoxide, of niobium has been extensively studied. Nb_2O_5 films have been prepared either by the anodic oxidation (Young, 1961) or by the reactive sputtering in oxygen atmosphere (Goldstein and Leonhard, 1967). The oxidation of niobium films has been studied in details by several workers. Kofstad and Esperik (1965) found that when niobium was oxidised at oxygen pressure from 2×10^{-4} to 0.5 Torr between 1200° to $1700^{\circ}C$ oxides such as NbO, NbO_2 and Nb_2O_5 were formed successively with the increasing temperature. The oxidation law was also studied for each stage. Klechovskaya et al. (1965) studied the structures of the thin films of cubic niobium oxide obtained by the oxidation of Nb films in air. The unit cell constant had a value of 7.80 Å. Shrachko et al. (1966) in their study of the oxidation of niobium by

the secondary ion-emission method found the existence of Nb_2O_3 between 1200°C and 2000°C. The kinetics of the oxidation of niobium was also studied by Sheasby (1968).

Electron diffraction and X-ray studies of Nb_2O_5 films formed by the oxidation of niobium at a pressure of 150 mm of Hg showed that the oxide consisted of a mixture of α and β phases at 700°C. As the temperature increased, the amount of α phase decreased whereas the proportionality of β-Nb_2O_5 increased (Korobkov et al, 1964). These results were later confirmed by Arbuzov and Chupriva (1965) who obtained α-Nb_2O_5 (orthorhombic) upto 850°C. Above this temperature β-Nb_2O_5 (also orthorhombic) was obtained but its lattice constants were nearly twice as large as the normal one. The lattice constants of Nb_2O_5 were calculated by Graehn (1966, 1970). The crystal structure of the high temperature form of Nb_2O_5, on the other hand, was found to be monoclinic belonging to the space group P_2 (Korobkov, 1964).

Janninck and Whitmore (1966) observed a phase change at 1070°K for NbO_2 accompanied by a transition from an insulating to a metallic behaviour. Kofstad (1968) observed 'n' type of semiconducting behaviour in the non stoichiometric α-Nb_2O_5 and this was attributed to the defect structure of Nb_2O_5 due to the deficiency in oxygen.

Dielectric constants of Nb_2O_5 films prepared by the anodic oxidation or by reactive sputtering were found to be high and of the order of 40. Dissipation factor in both the cases was about 0.018 (Young, 1961; Goldstein and Leonhard, 1967). Anodically grown Nb_2O_5 films were found to be amorphous in nature (Chopra, 1965). Emmeneegger and Robinson (1968) compared the dielectric constants and loss factor of the different modifications of Nb_2O_5 crystals. The values of dielectric constant were high and varied from 30 to 120 depending on the crystal structure. High values of permittivity, of the order of 100, were also observed in thick films of Nb_2O_5 prepared by chemical deposition (Brunner et al, 1968). But Nb_2O_5 films formed by the pyrolysis of niobium alcoholate in oxygen atmosphere, on the other hand, yielded low values of permittivity (about 11 $\pm$ 2 at 1 kHz).

Extensive studies have been made on the electrical properties of sandwiched Nb_2O_5 layers. Space-charge-limited-current (SCLC) flow has been observed in these films. The thickness dependence of the J-V characteristics due to SCLC flow in Nb-Nb_2O_5-In structures (Hickmott, 1966) and Nb-Nb_2O_5-Au structures (Chopra, 1965) have been studied. Current-controlled-negative-resistance (CCNR) was also observed by Chopra (1965) in anodically and thermally oxidised films of Nb sandwiched between metal electrodes.

Blumme (1968) from theoretical considerations of the J-V characteristics predicted, that, super concucting thin film tunnelling junctions composed of $Nb-Nb_2O_5-V$ could be operated at temperatures between 4.4^oK and 5.1^oK.

Chopra (1965) observed electroluminescence effect in $Nb-Nb_2O_5-Au$ sandwich layers. The electroluminescence energy was of the order of 1.2 to 1.3 eV and had a maximum photo voltage of 0.4 volts. The long wavelength absorption edge of anodic niobium pentoxide (amorphous) was found to be 3500 Å (Graven et al, 1960). This was later reinvestigated by Conlon and Doyle (1961) who found the value to be 3300 Å for thermally oxidised (Nb_2O_5) films. The difference in the values was attributed to the crystalline nature of the latter oxide films. Nb_2O_5 films show negligible absorption in the visible spectrum. Refractive index varied from 2.2 to 2.4 in the wavelength region 7000 Å and 4000 Å (Burgiel et al, 1968). These agreed well with the recent results of Duffy et al.(1969) for Nb_2O_5 films obtained by the pyrolysis of niobium alcholate.

From the above survey it can be seen that besides Nb_2O_5 no other oxide of niobium has drawn any attention so far. Further it appears that no attempt has been made to study the properties of thermally evaporated films of Nb_2O_5. It may be mentioned here that the thermal evaporation

of many oxides in vacuo often resulted in their dissociation to the lower oxides (Goswami and Trehan, 1957; Goswami, 1965; Gadgil and Goswami, 1971). Thus the possibility of obtaining lower oxides of niobium by the thermal evaporation of Nb_2O_5 cannot be ruled out completely, and hence a systematic study has therefore been made on the structural, dielectric and optical properties of vacuum deposited films obtained from the bulk Nb_2O_5 powder.

(B) EXPERIMENTAL

Pure Nb_2O_5 powder white in colour (supplied by Bhabha Atomic Research Centre, Bombay) was deposited in vacuo (about 10^{-6} mm of Hg) from a molybdenum boat. To avoid spitting during deposition the powder was degassed in vacuo at a low heat for about 45 minutes. It was found that on heating at this temperature, the white powder melted to a blackish mass and it was this mass which eventually evaporated when the temperature of the boat was raised to white heat. The deposits thus obtained on glass were greyish for thinner films but almost opaque and dark brown in colour for very thick films.

These films were also deposited on polycrystalline NaCl tablets and on the (100) faces of NaCl crystal at room as well as high substrate temperatures. X-ray studies

were also made on the original Nb_2O_5 powder as well as on the black mass formed in vacuo during the melting of the powder.

Transmittance and reflectance of these films were measured in the visible region by the special spectrophotometer designed here.

(C) RESULTS

(a) Structure

Electron diffraction studies of the oxide films formed at room temperature whether on single crystal NaCl or polycrystalline tablets or on glass substrates did not yield any clear diffraction patterns except the broad halos thus suggesting that these films were amorphous in nature or had fine grained structures. At higher substrate temperatures, say above 350°C, these films became crystalline and sharp diffraction patterns were obtained. Thus the deposits formed on a (100) face of NaCl yielded spot patterns (Fig. VI.1). The dispositions of different reflections and measurements of their d values suggest that deposits developed 2-d $\{100\}$ and $\{211\}$ orientations of a cubic phase (apparently $a_o \approx 5.38$ Å), together with $\{111\}$ twinning of deposits. The appearance of a few additional spots can be explained with the simultaneous formation of

TABLE VI.1

I/I_o	d Å	hkl	h'k'l'
vf	4.43		111
s	3.78	110	200
f(d)	3.14	111	211
s	2.70	200	220
m	1.90	220	400
m	1.71	310	420
vf	1.55	222	422
vf	1.36	400	440
vf	1.27	330	600

s - strong
f - faint
d - diffuse
m - medium
v - very

$a \simeq 5.38$ Å; $a' \simeq 7.65$ Å

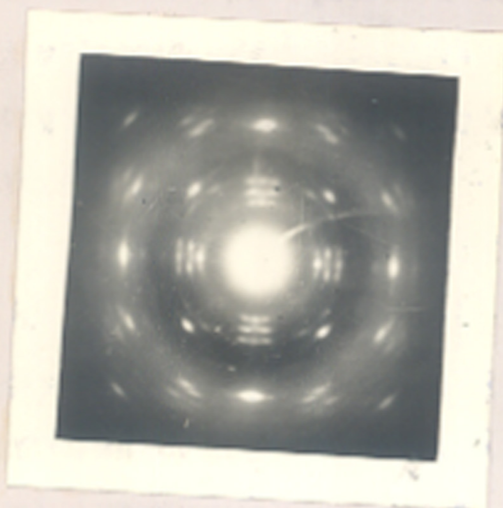

Fig VI.1

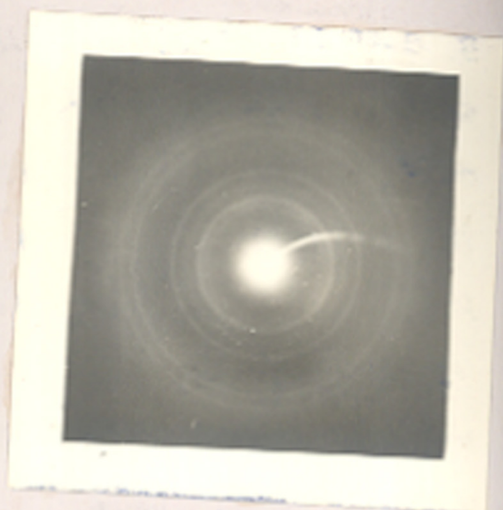

Fig VI.2

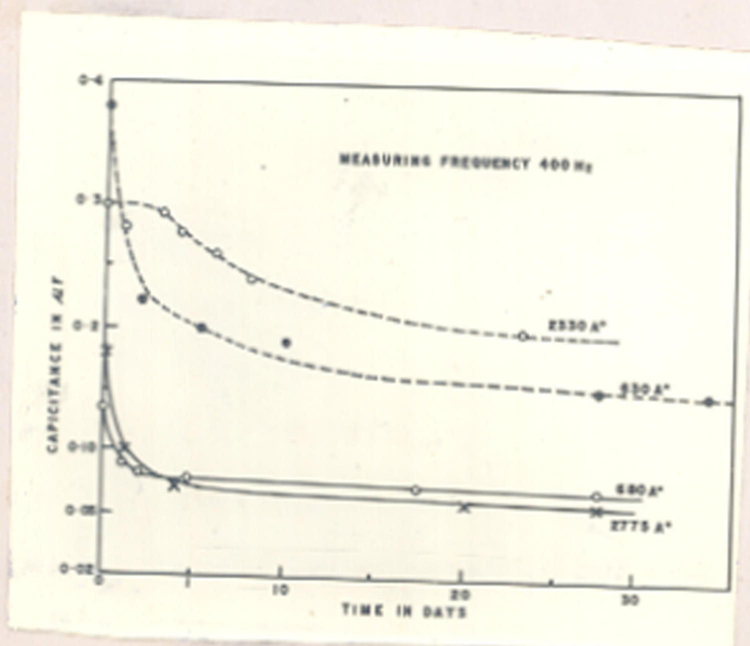

Fig VI.3

the 2-d $\{110\}$ orientation of a tetragonal phase (a ≈ 5.38 Å; c ≈ 4.42 Å). Patterns (Fig. VI.2) from the deposits formed on polycrystalline NaCl tablets also conform mostly to the cubic phase (Table VI.1). It may be mentioned here that these two structures (possibly subcells) might have arisen from a larger cell ($a' = a\sqrt{2}$ or $c\sqrt{3} = 7.65$ Å) by a slight rearrangement of atoms. In fact, Klechkovskaya et al (1965) obtained such a phase ($a_o = 7.80$ Å) having a variable composition $Nb_{1.64}O$ to $Nb_{1.68}O$ from the sputtered films of niobium. Thus the evaporated oxide films had a different composition and phase structure from those of Nb_2O_5, which was found by us by X-ray study to be orthorhombic (ASTM Card No.5-9352) and the black mass (high temperature form) monoclinic (ASTM Card No.5-0379).

(b) Dielectric Properties

(i) Ageing effect

These film capacitors attained stability only after a long time of ageing. Capacitance initially fell rapidly and then rather slowly with the time of ageing. Fig. VI.3 shows the change in capacitance of four films deposited at two substrate temperatures during ageing at room temperature for about a month. Unfortunately none of these attained complete stability even after such a long time.

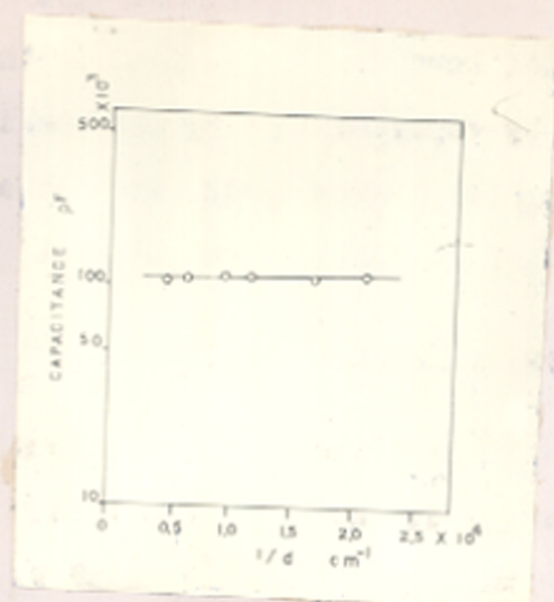

Fig VI.4

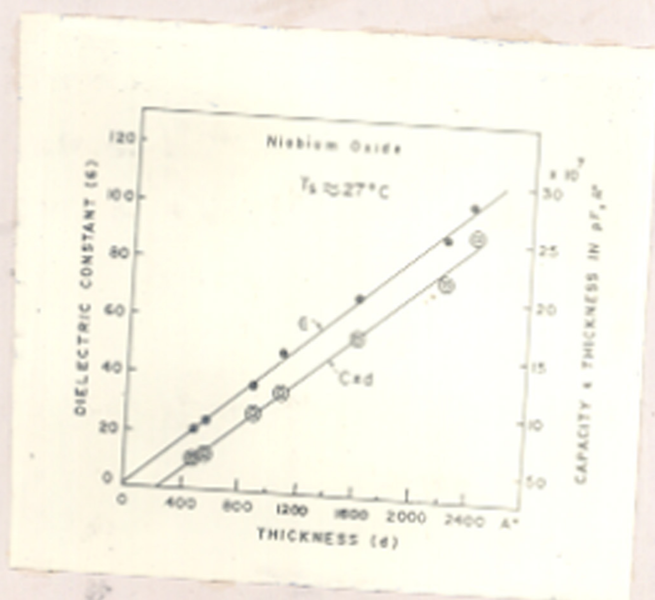

Fig VI.5

This could, however, be hastened if the capacitors were annealed by repeated heating and cooling cycles in vacuo. All subsequent measurements were therefore carried out only on fully stabilised capacitors.

(ii) Effect of film thickness

The variation of capacitance (C) with the reciprocal of film thickness (d) is shown in Fig. VI.4. Capacitance was large and varied between 180000 pF to 109000 pF with the increase of the film thickness (470 Å to 2300 Å). The product of capacitance and thickness (C x d) was found to increase with the thickness indicating the linear dependence of ϵ on d. This is clearly shown in Fig. VI.5 where both C x d and ϵ were plotted against d. ϵ increased linearly with the thickness and attained a value as high as 100 for a film 2300 Å thick. It may be mentioned here that so long as the film thickness was constant ϵ was also constant. Similar results were also observed in the case of films deposited at 100°C and the values of ϵ did not change appreciably from those deposits formed at room temperature. Tan δ in both cases was low and of the order of 0.03.

(iii) Effect of temperature

The effect of temperature on capacitance and tan δ

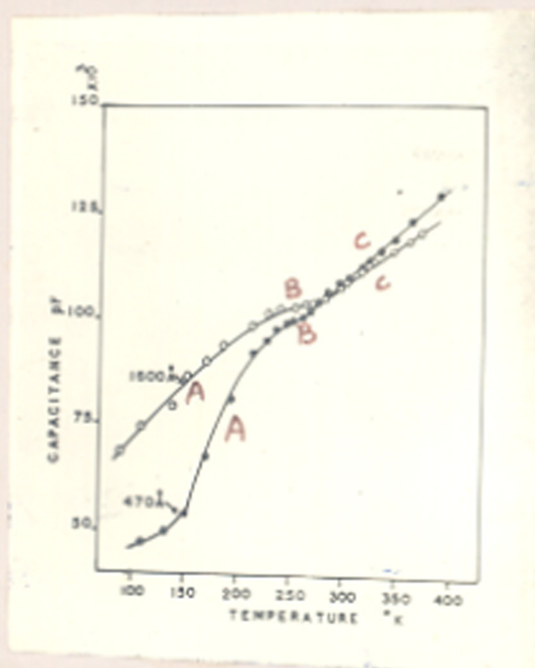

Fig VI. 6

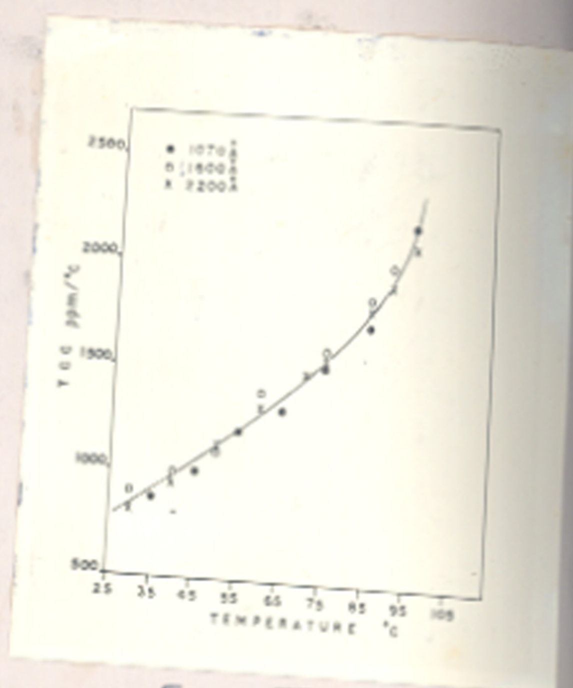

Fig. VI. 7

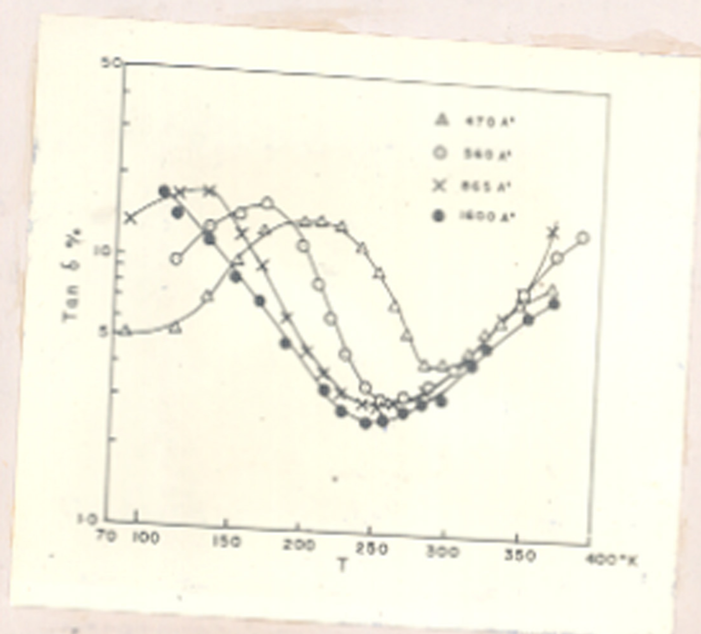

Fig VI. 8

was unlike those observed for ZnS, praseodymium oxide and Sb_2O_3 films capacitors studied earlier. Fig. VI.6 shows the variation of capacitance with the temperature for two different film thicknesses when measured at 1 kHz. Although the capacitance increased with temperature its behaviour was rather peculiar. In the C versus temperature plot, there were three distinct regions. In the region A (120°K to 230°K) capacitance rose very sharply. For a film 470 Å thick capacitance increased from 55,000 pF to 95,000 pF. In the region B (230°K to 270°K) the change in capacitance was very small but beyond 270°K capacitance once again increased rapidly. It may be pointed out here that below 120°K the variation of capacitance was slightly smaller than that observed in the region A. However, in case of thicker films (d = 1600 Å) this region seemed to be absent.

TCC measured for all capacitors above room temperature, varied between 600 ppm/°K and 2000 ppm/°K in the temperature range 290°K to 372°K. In general, TCC was independent of the film thickness for thicknesses greater than 1000 Å (Fig. VI.7).

A very unusual behaviour of tan δ with temperature at 1 kHz was observed (Fig. VI.8). Tan δ showed an oscillatory behaviour with the temperature. In general

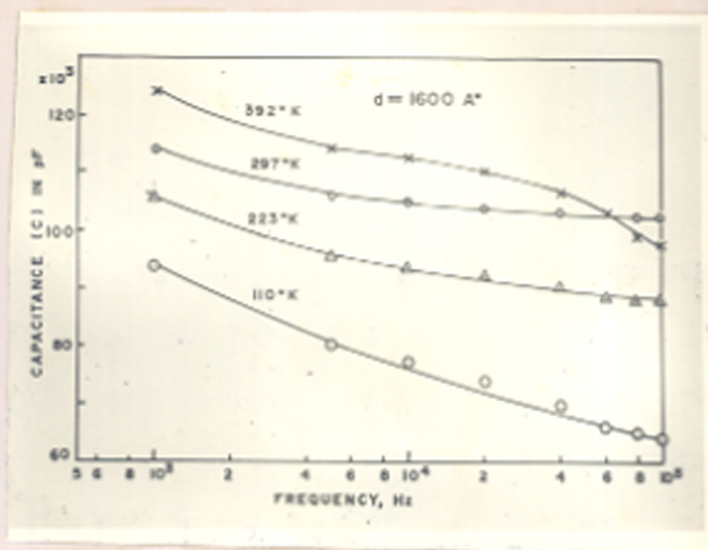

Fig VI.9a

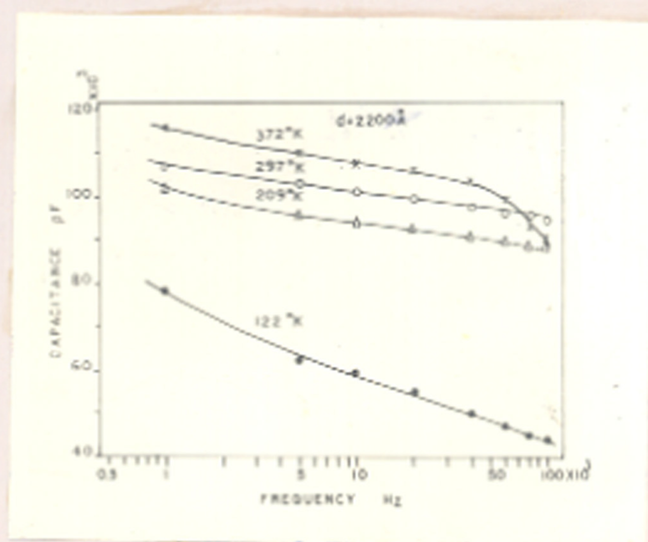

Fig VI.9b

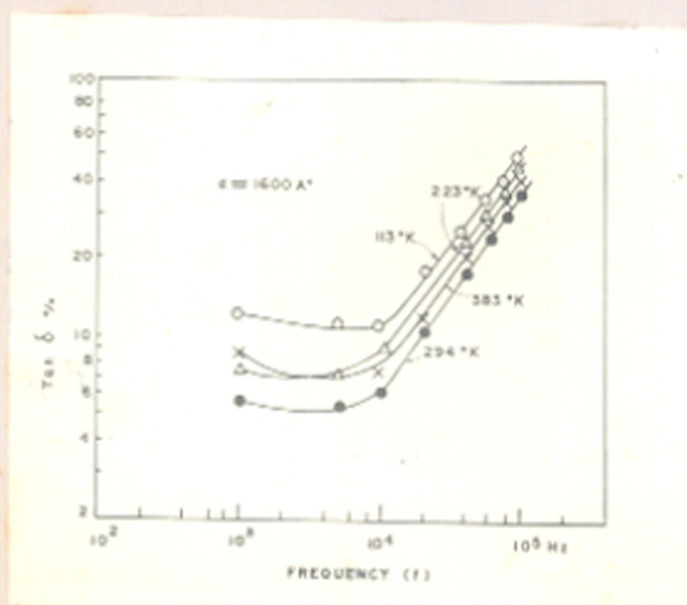

Fig VI.10a

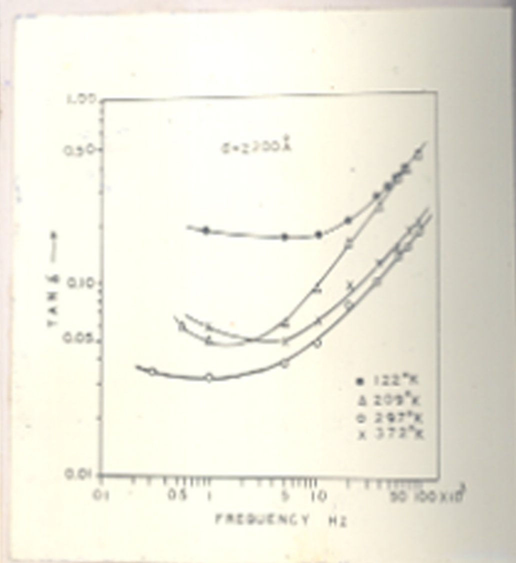

Fig VI.10b

tan δ passed through a maximum value at very low temperatures, then fell to a minimum between 250°K and 290°K and once again increased with the higher temperatures. As can be observed from Fig. VI.8 the position of the maximum value of tan δ seemed to shift with the increasing film thickness to the lower temperature region.

(iv) Effect of frequency

Figs. VI.9a and b show the variation of capacitance with frequency when measured at different temperatures. In general capacitance reduced with the applied frequency. At higher temperatures this variation was large but decreased when the measurements were made at room temperature. Below this temperature, however, the variation in capacitance again increased and became very large at very low temperatures.

As before frequency had a pronounced influence on tan δ. Fig. VI.10a and b show the variation of tan δ with frequency at different temperatures. It is interesting to see that similar to film capacitors of ZnS, praseodymium and Sb_2O_3, tan δ showed a minimum value in the frequency spectrum (10^3 to 10^5 Hz) studied. Moreover the position of f_{min} (or ω_{min}), where tan δ_{min} occurred, shifted with the temperature but this shift was not as regular as

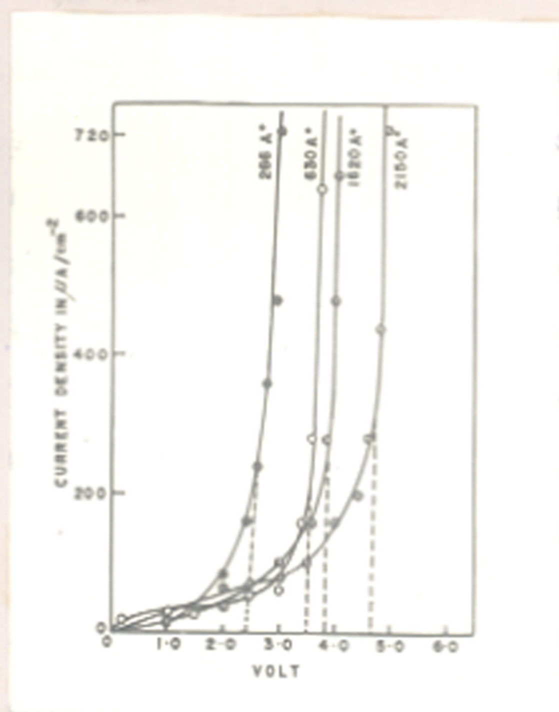

Fig VI.11

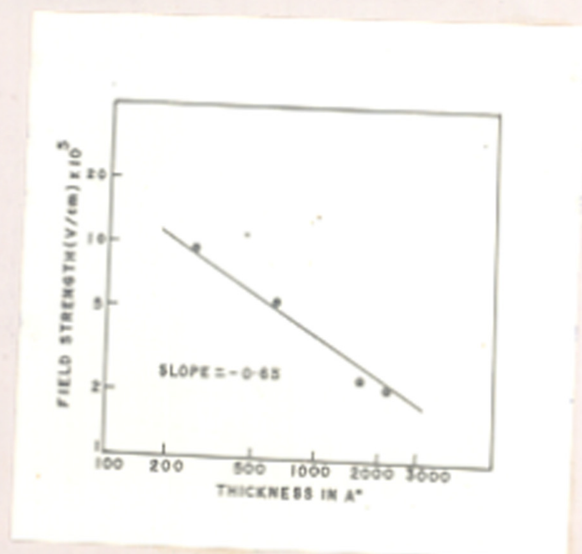

Fig VI.12

was in the case of other film capacitors (e.g. ZnS, etc.). Above room temperature, ω_{min} (or f_{min}) and hence tan $_{min}$ shifted to the higher frequency region as observed earlier for other capacitor materials. But below room temperature, ω_{min} and tan δ_{min} instead of shifting to the lower frequency region shifted again to the higher frequency side. This was true for all thicknesses of niobium oxide films studied by us.

(v) Breakdown voltage

Fig. VI.11 shows the J-V characteristic curves near the breakdown voltage (V_B). A sudden rise in the current with a small change in the voltage was taken as the onset of the voltage breakdown of these film capacitors. Although V_B increased with the film thickness (d), the dielectric field strength (F_B) reduced with d (Table VI.2). A plot of F_B against d in the log-log scale is shown in Fig. VI.12. As can be seen from the graph F_B follows a power law i.e. $F_B \propto d^{-0.65}$ the value of the power index being deduced from the slope of the graph. This value was slightly larger than the value of about −0.5 predicted from the Forlani-Minnaja relation.

TABLE VI.2

Thickness (d) Å	Breakdown voltage (V_B) volts	Dielectric field strength (F_B) V/cm
266	2.4	9.0×10^5
630	3.5	5.55×10^5
1260	3.8	2.34×10^5
2150	4.6	2.14×10^5

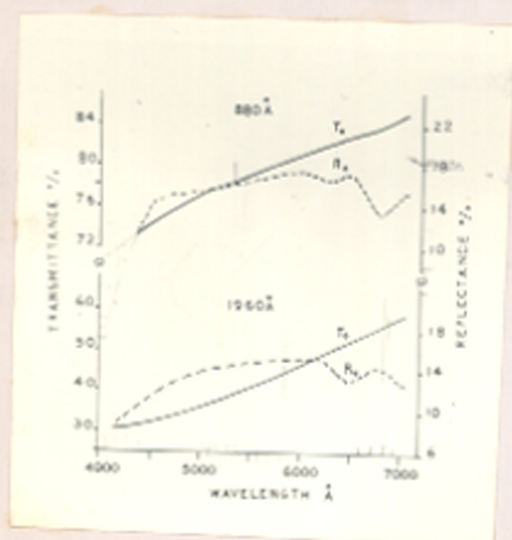

Fig VI.13

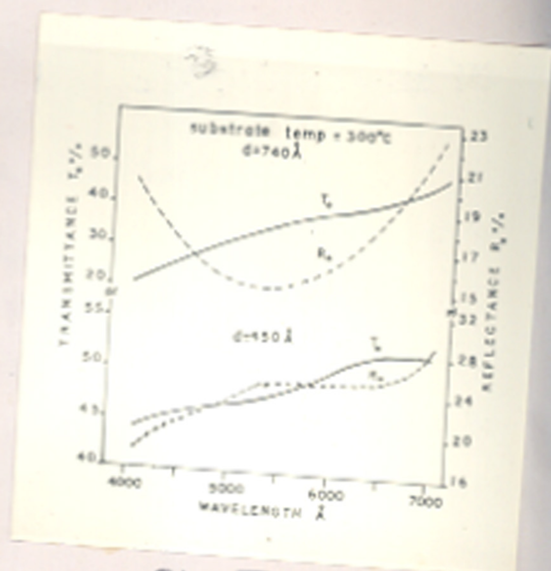

Fig VI.14

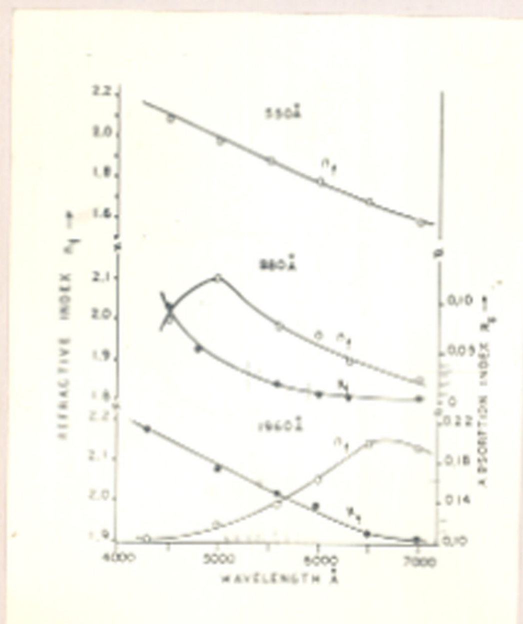

Fig VI.15

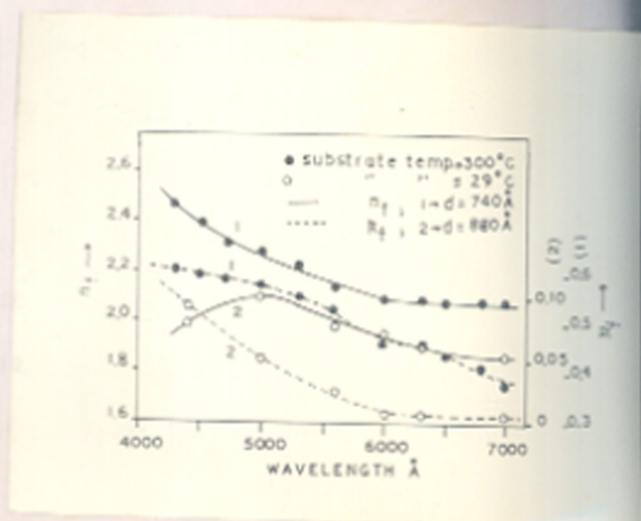

Fig VI.16

(c) Optical Properties

(i) Transmittance and reflectance

Transmittance and reflectance at near normal angles of incidence in the visible region for niobium oxide films is shown in Fig. VI.13 for two different film thicknesses. In case of the thinner film, transmittance was large and of the order of 85% in the red region but reduced to 74% when measurements were made at a wavelength of 4400 Å. Reflectance was almost constant in this region with a value of about 16%. For thicker films transmittance reduced very much and this reduction also continued in the violet region of the spectrum. Reflectance, however, did not decrease very much from the values observed for the thinner films. Absorption percentage defined as 100 - T% - R% was large in the case of thicker films.

When niobium oxide films were deposited on glass at high substrate temperatures, say about 350°C, transmittance and reflectance spectra of these films changed significantly. In general such films showed a large absorption throughout the visible region. Fig. VI.14 shows the transmittance and reflectance curves in the visible region for these films.

(ii) Optical constants

Refractive index and absorption index of niobium oxide films were calculated from the complex equations (II.3) and (II.4). Fig. (VI.15) shows the dispersion curves of n_f and k_f in the visible region for three different film thicknesses. For the thicker film n_f showed a maximum value which shifted to the longer wavelength region with increasing film thickness. k_f, on the other hand, increased with the increasing incident radiant energy (lower wavelength) and was dependent on the film thickness.

Films deposited at 350°C showed higher values of n_f and k_f. For a film of about 790 Å thickness, n_f increased from 2.1 to 2.47 in the wavelength region 7000 Å and 4300 Å respectively and k_f increased from 0.37 to 0.55 (Fig. VI.15). Absorption coefficient was high and of the order of 5×10^5 cm^{-1}.

The effect of substrate temperature on the optical constants of niobium oxide films is shown in Fig. VI.16 for two films of nearly the same film thickness but prepared under different deposition conditions.

(D) DISCUSSION

It is well known that vacuum deposited films are

often amorphous when deposited at room temperatures, but became crystalline when deposited at higher substrate temperatures. The same appears to be true for the niobium oxide films also. Electron diffraction studies revealed that the deposited films formed at high temperatures appeared to have a composition varying between $NbO_{1.64}$ to $NbO_{1.68}$, no doubt, due to the vacuum dissociation of Nb_2O_5 powder during deposition. Such dissociations of the higher oxide in vacuo by thermal treatment are not uncommon. In fact Goswami and his coworkers (1957, 1965, 1971) have shown that many oxides such as Co_3O_4, Mn_3O_4, CuO, Bi_2O_3, etc. during thermal evaporation in vacuo resulted in the formation of the lower oxides such as CoO, MnO, Cu_2O, BiO, etc. Similar observations have also been made on cupric chalcogenides to cuprous forms.

Since the oxide of niobium thus formed is a lower oxide, not reported earlier, its dielectric and optical properties are also likely to differ considerably from those reported for the well known Nb_2O_5 film. In the following paragraphs the a.c. behaviour and the optical properties of these films are discussed.

A.C. characteristics of thin film dielectrics as investigated by several workers can broadly be explained from two types of models namely (i) single capacity element

with appropriate dielectric resistances in parallel and a low series resistance due to leads, etc. as proposed by Goswami and Goswami (1973) in the case of ZnS, Sb_2O_3, etc. films (explained in Chapter III Discussion) and (ii) three capacity elements arising from two additional barrier layers at the electrode dielectric interface with appropriate parallel resistances, etc. proposed by Simmons et al (1970) as in the case of MoO_3 films. The basic features that distinguish these two models are as follows.

(a) In the model (i) capacitance is inversely proportional to film thickness (except for very thin films) when measurements are made at room temperatures. For the model (ii) Simmons et al predict that capacitance is independent of film thickness and that ϵ should linearly increase with the film thickness when measured at or above room temperatures. Only at very low temperatures C is inversely proportional to d.

(b) The model (i) predicts the increase of tan δ with temperature at all frequencies. On the other hand tan δ will show a maximum value which shifts to the higher temperature region with the increase of measuring frequency in model (ii).

(c) Goswami and Goswami predict in the model (i) the existence of a minimum value of tan δ (tan δ_{min}) at a

frequency ω_{min}, in the frequency spectrum, that shifts to the higher frequency region with the increase of temperature. Simmons et al's model, however, predicts a value ω_{max} where a maximum value of tan δ (tan δ_{max}) will occur, and this will shift to the higher frequencies with the increase of temperature.

(d) According to the model (i) capacitance will increase with the temperature in a manner governed by the rise in tan δ. But in the case of model (ii) although capacitance increases with temperature saturation in the values of C is observed both at high as well as at very low temperatures. In the intermediate temperature range a sharp rise in the value of capacitance should take place.

As can be seen from the results, a.c. behaviour of niobium oxide films seem to agree at first sight only in parts with either of the above two models. Thickness dependence of two dielectric constants throughout the film thickness range studied seems to be in accordance with the barrier layer model (ii), but the variation of loss factor with frequency and also the presence of tan δ_{min} appear to agree with the model (i). However the pronounced temperature effect on tan δ at 1·0 kHz viz. peak at lower temperature region and a minimum at an intermediate stage is not directly evident from either of the models at their

present state of development. Further considerations suggest that the peak observed at low temperatures may be a relaxation phenomenon.

Breckenridge (1950) during his investigation on the variation of tan δ with temperature at 1 kHz on doped single crystals of alkali halides and AgCl, observed a loss peak at the lower temperature range and suggested this to be due to relaxation caused by the presence of Frenkel defects or impurities present in the crystal as a result of doping. This relaxation effect was due to the jumping of positive ions to vacant lattice sites under the influence of the applied field. Similar dielectric relaxations showing peaks in tan δ at different frequencies, especially at low temperatures, have been observed by Harrop and Wanklyn (1964) for ZrO_2 films treated with hydrofluoric acid. The incorporation of fluorine ions on the surface of nonstoichiometric oxide layers favoured the formation of dipoles by the interstitial and substitutional fluorine ion pairs. Further, from the energy considerations also they showed that the relaxation mechanism was due to the dipole orientation rather than anion vacancy conduction as observed in alkali halides by Breckenridge.

It is interesting to note that both the mechanisms envisaged the presence of extensive defects on the surface

layers to cause the relaxation effect at low temperatures. Since niobium oxide films had a variable composition ($NbO_{1.64}$ to $NbO_{1.68}$) having inherent defect structures to accommodate the oxygen variation, such films would have, no doubt, a high concentration of defects in them. It is therefore likely that such a high defect concentration will also favour the relaxation effect at low temperatures as observed by us.

From the above it is now possible to explain the different features of Fig. VI.8 in terms of the relaxation effect occuring at the lower temperature region and the normal loss behaviour at a higher temperature range for a dielectric film having a single capacitor element in the circuit as proposed in the model (i) of ours. The peak in loss factor was therefore due to the relaxation process whereas the minimum value of tan δ was a consequence of equation (III.10) of the above model. The nature of the graph between the peak and minimum value of tan δ was no doubt due to the superimposition of the latter effect on the former. The shifting of tan δ_{min} position and hence the frequency (minimum) also to the higher frequency range (cf. Figs. VI.10a and VI.10b) both below and above 250°K can now be explained from the model proposed by us before. In such a case the minimum value of angular frequency ω_{min}

($= 2\pi f_{min}$) is given by equation (III.10) as

$$\omega_{min} = 1 \Big/ \sqrt{rRC^2} \quad .. \quad \text{(VI.1)}$$

where R is the dielectric resistance, r is the lead resistance which is of the order of a few ohms ($r \ll R$), and C is the inherent capacitance unaffected by temperature and frequency. The shifting of ω_{min} to the higher frequency region both at low as well as at high temperatures means a corresponding decrease in the value of the denominator in equation (VI.1), and this can be achieved only if R above was to decrease since both r and C are not significantly affected by frequency and temperature of measurements.

Dielectric conductivity (σ_D) which represents the sum of all loss mechanisms in the material is given by the relation (Anderson, 1964)

$$\sigma_D = \omega \epsilon_0 \epsilon'' \quad .. \quad \text{(VI.2)}$$

where ω is the angular frequency, ϵ_0 is the permittivity in vacuo and ϵ'' is the imaginary part of the complex dielectric constant. Loss factor is then given as

$$\tan\delta = \epsilon'' / \epsilon' \quad .. \quad \text{(VI.3)}$$

where ϵ' is the real part of the complex dielectric constant given by

$$\epsilon^{*} = \epsilon' - j\epsilon'' \quad .. \quad (VI.4)$$

Dielectric conductivity given by equation (VI.2) now takes the form

$$\sigma_D = \omega \epsilon_0 \epsilon' \tan\delta \quad .. \quad (VI.5)$$

thus showing that σ_D is proportional to tan δ. Since loss factor increased both with the rise and decrease of temperature around 250°K (cf Fig. VI.8), conductivity should also increase and hence there must be a corresponding decrease in the dielectric resistance R. Consequently ω_{min} position determined by the equation (VI.1) would shift to the higher frequency region both above and below 250°K as observed here.

The variation of capacitance with frequency and temperature especially at the lower temperature region can also be explained from the above model. It has already been shown that the measured capacitance (C_s) is given at any temperature and frequency by the equation (III.13) viz.

$$C_2 = C + 1/\omega^2 R^2 C \quad .. \quad (VI.6)$$

Since the dielectric resistance R decreased with the increase in loss factor (loc. cit) due to the relaxation effect at low temperature and dielectric conductivity at higher temperatures, the second term of equation (VI.6) cannot be neglected especially at low frequencies. Hence measured capacitance will depend on frequency as well as temperature thus showing large variation in 6_s.

It is interesting to point out here that the variation of capacitance with temperature for niobium oxide films (Fig. VI.6) below 260°K is very similar to those dielectrics where a dipolar orientation takes place giving rise to a relaxation mechanism at lower temperatures and obeying the Debye equations (Dekker, 1967).

The breakdown field (F_B) follows a power law $F_B \propto d^{-0.65}$. It is interesting to note that although this value is slightly more than the theoretical value of -0.5 reported by Forlani and Minnaja, the above power law seems to be applicable even for amorphous or fine grained films.

The above discussions show that all the a.c. properties of vacuum deposited niobium oxide films can now be qualitatively explained on the basis of the model proposed by Goswami and Goswami assuming however a relaxation mechanism at low temperatures. Although at present

it is not very clear as to which of the two mechanisms cited earlier is responsible for this process, the variation of capacitance with temperature at fixed frequency (Fig. VI.6) suggests the process may possibly be due to the dipole orientation.

Optical studies showed in general that these films though transparent were fairly absorbing in the visible region unlike Nb_2O_5 films where k_f is negligible. Film thickness also had a profound influence on the optical constants. Absorption index increased with the decreasing wavelength, but its values were higher for thicker films. The fact that k_f increased in the lower wavelength region indicated that the fundamental absorption edge of these films was below 4000 Å. This can also be seen from the high value of resistivity of niobium oxide films ($\approx 10^8$ ohm cm). These films were therefore partially transparent in the visible spectrum.

Refractive index increased as the wavelength of the incident radiation decreased. But for thicker films n_f attained a maximum value somewhere in the visible region and then fell with the lowering of the wavelength. This peak in n_f shifted to the higher wavelength side with the increase of film thickness. Zemel et al.(1965) during their study on epitaxial films of PbS, PbSe and PbTe

observed such peaks in refractive index in the energy range 0.10 to 0.60 eV (infra red) and showed that these peaks shifted to the lower energy side at lower temperatures. The authors attributed this shift in the peak due to the temperature dependence of the energy gap.

Sardomirskii (1963) showed from quantum mechanical treatments that when the thickness of a film became comparable with the effective wavelength of the charge carriers, the forbidden band width would decrease with the increasing film thickness. This prediction has been verified experimentally by measuring the shift in the absorption edge with film thickness for CdS and InSb films (Stasenko, 1968; Filatov and Karpovich, 1969). Tanenbaum and Briggs (1963) and Hrostowski et al. (1954) showed that the optical energy gap for both 'n'- and 'p'-type InSb and InAs crystals were dependent on carrier concentration, the purer materials (less carrier concentration) having lower values. This has been explained by Burstein (1954) as due to the small effective electron mass and the increasing degeneracy of the states in the conduction band as the carrier concentration in the material increases. In a series of publications from this laboratory, Goswami and his coworkers (1964, 1966, 1968) have shown from electrical measurements of several semiconducting films, that the activation energy decreased with the increase of

film thickness due to the reduction of the carrier concentration.

These considerations therefore suggest that the shift in the peaks of refractive index with film thickness to the longer wavelengths or lower energies is probably due to the decrease in the activation energy or band gap with increasing film thickness. Similar shifts in the optical band gap with thickness have also been observed by Goswami and coworkers in this laboratory.

Niobium oxide films deposited at high substrate temperatures showed higher values of optical constants than for those films deposited at room temperature (cf Fig. VI.16). This may be due to the crystalline nature of the films when deposited at higher substrate temperatures.

CHAPTER VII

STUDIES ON VACUUM DEPOSITED INDIUM OXIDE FILMS

(A) INTRODUCTION

Transparent oxide films of high resistivity are of immense value in optical and electronic devices. In recent years a large amount of investigations have been made for the search of these types of materials. Unfortunately, only a few materials are available that can fulfil the above requirements. Further the difficulties in preparation of stoichiometric oxide films have also posed severe restrictions on the choice of the materials. Although considerable success has been achieved with SiO, SiO_2, Ta_2O_5 and some rare earth oxides, there are a vast number of other untapped metal oxides whose properties may compare favourably or even better than the established oxide films. With this in view, a study has been made on indium oxide films as a potential material.

Thiel and Luckmann have reported as early as in 1928 that In_2O_3 dissociated to In_2O in gaseous state when the sesquioxide of indium was heated in vacuo. Various workers utilizing improved mass spectrophotometric techniques have been able to identify the composition of the gaseous state when yellow In_2O_3 was melted in vacuum.

Khrorostukhina (1962) found the dissociated products to be mostly InO and O_2. Burns (1966) and his coworkers (1963) made a detailed study on the dissociated products of spectroscopically pure In_2O_3 and found that the products consisted chiefly of In^+, O_2^+ and In_2O^+ and some traces of InO. At higher temperatures In_2O was predominant. It is interesting to note that no gaseous In_2O_3 was observed by these authors.

Marezio (1966) observed that In_2O_3 had a cubic structure ($a_o = 10.117 \pm 0.001$ Å). Very interesting results have been obtained for flux grown In_2O_3 crystals. Tippins and Chase (1966, 1967) prepared In_2O_3 crystals from a PbO-B_2O_3 flux. These crystals on electron microscopic examinations showed inclusions and striations, and because of the oxygen deficiency they were nonstoichometric and almost black in colour. However, the addition of MgO to the melt produced crystals that had no inclusions or striations and these had optical properties characteristic of stoichiometric In_2O_3 which were pale yellow in colour. The authors concluded that MgO acted as a good compensator for the oxygen deficiency.

Rupprecht (1954) studied the electrical and photoconducting properties of In_2O_3 films prepared by the oxidation of indium films in an oxygen atmosphere and these

showed 'n' type of conduction. Single crystals of indium oxide (In_2O_3) prepared by Weiher (1962) showed conductivity and mobility values of 10 ohm^{-1} cm^{-1} and 160 cm^2 $(v\text{-}sec)^{-1}$ respectively at room temperature and had a energy band gap of 3.1 eV. Groth (1966) prepared thick films of In_2O_3 using the spray technique. By incorporating different impurities, films were obtained with conductivity between $1.5x10^2$ and $4.2x10^3$ ohm^{-1} cm^{-1} and carrier concentration 'n' between 10^{19} and $6x10^{20}$ cm^{-3}. These films showed little absorption in the visible region, but because of large 'n' they had high reflectivities in the infra red. The mechanism of electron scattering in In_2O_3 films was discussed by Groth (1966), Fistul and Vainshtein (1967) and Muller (1968). Ryabova and Savitskaya (1968) prepared oriented In_2O_3 films by the pyrolysis method. Electron diffraction analysis and electrical conductivity measurements showed that these In_2O_3 films changed from an amorphous state to well oriented crystallites accompanied by a change of resistivity from 10^{12} to 10^2 ohm cm.

Holland and Siddall (1953) studied the transmission of reactively sputtered indium oxide films in the visible region. However, they could not identify the structure and composition of such oxide films. Weiher and Ley (1966) from the fundamental absorption edge at room temperature observed a direct allowed transition with an energy gap of

3.75 eV for In_2O_3 crystals. This was also confirmed by Tippins and Chase (1966) and later by Vaïnshtein and Fistul (1971). Ellipsometric measurements have been made by Elridge (1972) to determine the complex refractive index of vacuum deposited indium and then follow the oxide growth upon introducing oxygen. In recent years sputtered films of In_2O_3 with some percentage of SnO_2 or CdO have been used as transparent electrodes (Fischer, 1954; Vossen, 1971; Mehta and Volgel, 1972).

From the above survey it seems that no systematic work has been done so far on the optical properties of In_2O_3 films. Further, very negligible work seems to have been carried out on the a.c. properties of these films. A systematic study has therefore been considered necessary on the structural, dielectric and optical properties of indium oxide films.

During the present study, it was observed by us that indium sesquioxide deposited directly from a molybdenum boat, yielded films blackish in colour and these were partially transparent in the visible region. However when the same films were baked in air at 320°C for about 2½ hours, they became transparent and showed interference colours. Preliminary investigations showed that these films differed considerably in their dielectric and optical

behaviours. In the following, therefore, studies have been made under the different conditions of preparations viz. (A) Films as deposited (blackish) and (B) blackish films were oxidised in air before any measurements were carried out.

PART A

(B) EXPERIMENTAL

Specpure In_2O_3 (99.99% purity, supplied by Fulka AG PURISS) yellowish in colour was evaporated in vacuo from an initially flashed molybdenum boat. Prior to deposition the material was degassed in vacuo for about 45 minutes. It was observed that, on degassing, the bulk powder became blackish in colour. The deposits obtained by evaporating the above were also blackish in appearance. Depositions were made not only on glass substrates but also on polycrystalline NaCl tablets,the latter for their structural analysis by electron diffraction techniques. Thin film capacitors comprising of Al/Indium Oxide/Al were prepared and their dielectric behaviour studied in the usual way. Transmittance and reflectance measurements at a near normal angle of incidence in the visible region were carried out in the special spectrophotometer designed here. Transmittance was also measured by a Beckman DK2 spectrophotometer.

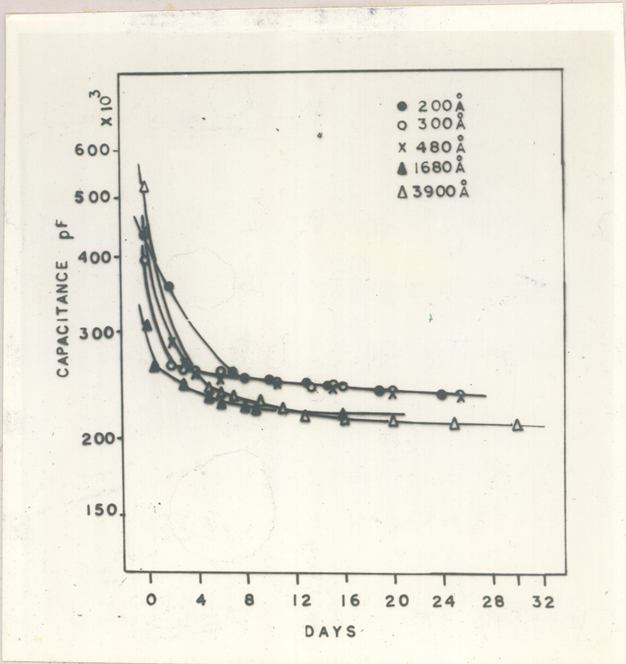

Fig VII.1

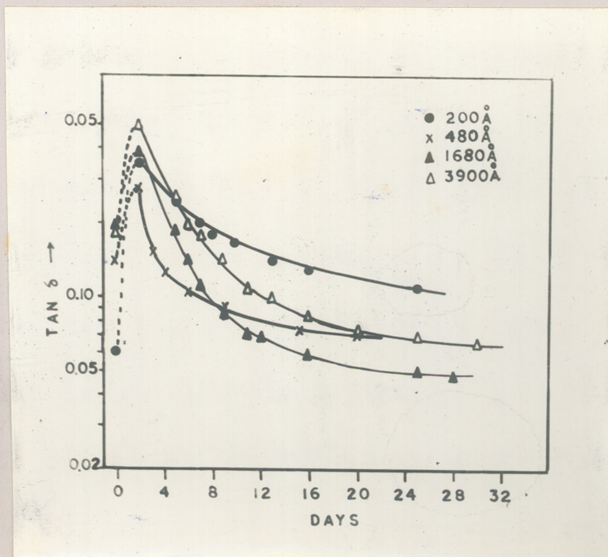

Fig VII.2

(C) RESULTS

Blackish films

(a) Structure

Black indium oxide films deposited on polycrystalline NaCl at room temperature did not yield any coherent diffraction patterns thus suggesting that the deposits were either amorphous or had a fine grained structure.

(b) Dielectric Properties

(i) Ageing and annealing effects

Figs. VII.1 and VII.2 show the ageing effect in capacitance and tan δ for five different film thickness. Capacitance (C) initially fell very rapidly and after about a few days of ageing in air the variation of C became more gradual tending to attain a constant value. Dissipation factor (tan δ), on the other hand, showed a sudden rise in the value of tan δ after one day's ageing in air. This, however, with time decreased in the same manner as capacitance. Even after ageing for about a month, neither C nor tan δ attained a stable value unless these film capacitors were annealed by repeated heating and cooling cycles in vacuo between 27°C and 110°C.

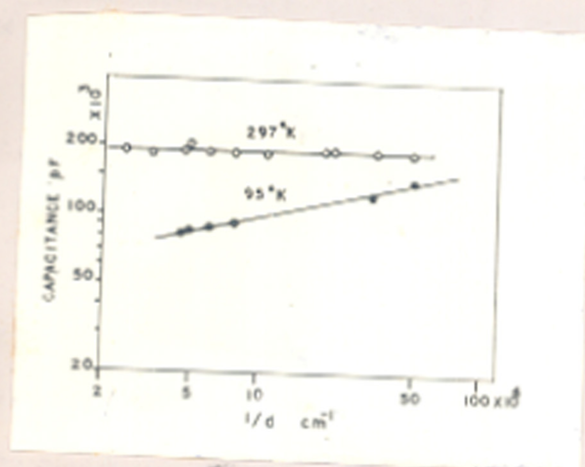

Fig VII. 3

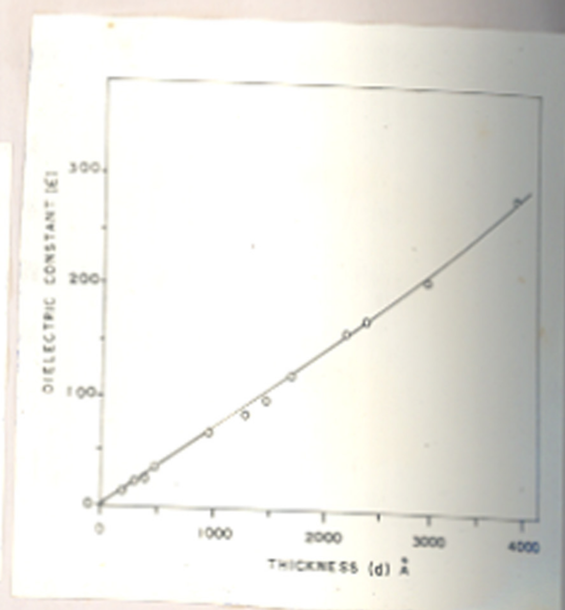

Fig VII. 4

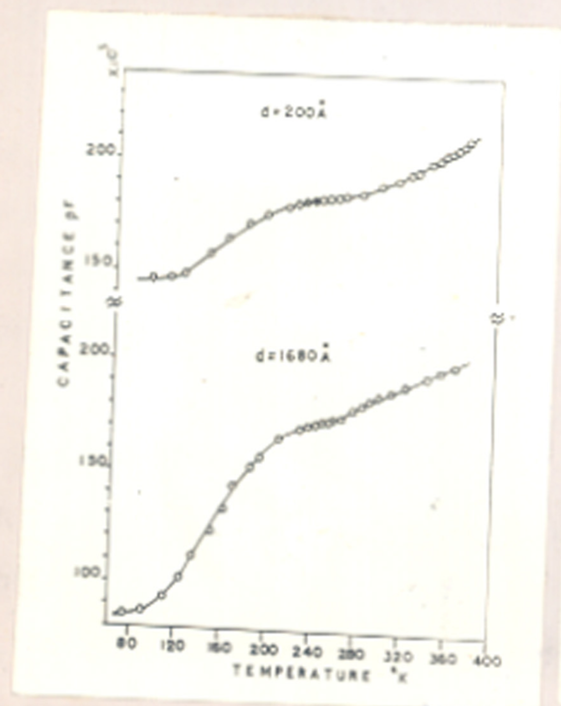

Fig VII. 5

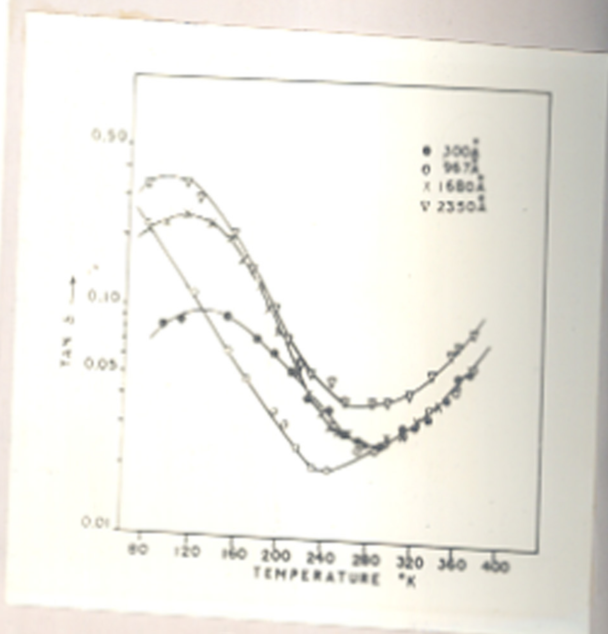

Fig VII. 6

(ii) Effect of film thickness

Fig. VII.3 shows the variation of capacitance with the reciprocal of film thickness (log-log scale) when measurements were carried out at room temperature. It is interesting to see that capacitance was independent of the film thickness (Table VII.1). However, when the samples were chilled to very low temperatures, say about 96°K, capacitance was found to decrease with the increasing film thickness, but the proportionality relation between these two parameters viz. $C \propto \frac{1}{d}$ still did not hold good as can be seen from Fig. VII.3 and Table VII.1. The dielectric constant (ϵ) computed at room temperature was found to be linearly proportional to the film thickness and attained values as high as 280 for a thickness of 4000 Å (Fig. VII.4).

(iii) Effect of temperature on C and tan δ

The effect of temperature on C and tan δ is similar to those observed for niobium oxide film capacitors. Figs. VII.5 and VII.6 show the typical variation of C and tan δ at 1 kHz. In general capacitance increased with temperature. As can be seen from Fig. VII.5 there appear to be distinct regions in the capacitance-temperature curves. Between the temperature range 120 to 250°K capacitance increased

TABLE VII.1

Thickness (d) Å	At room temperature Capacitance (C) pF	ϵ	$\tan\delta$	At 80°K Capacitance pF
200	192,000	15.2	0.032	146,000
300	200,000	24.0	0.022	124.000
480	200,000	37.0	0.03	-
967	180,000	69.0	0.027	-
1280	-			93,000
1476	171,000	98.0	0.03	-
1680	185,000	122.0	0.025	86,500
2050	214,000	-	0.03	-
2150	192,000	162.0	0.04	-
2350	188,000	178.0	0.04	80,000
2950	182,000	208.0	0.04	34,000
3900	191,000	290.0	0.04	-

with the temperature at a rapid rate, but between 260 to 280°K the rise in C was small. However, beyond the room temperature capacitance again increased. This trend was observed for all thicknesses studied.

TCC measured for all capacitors above the room temperature varied between 600 to 1600 ppm/°K in the temperature range 280 and 360°K. In general TCC was independent of the film thickness.

The variation of tan δ with temperature at 1 kHz showed some very interesting features. As the temperature was reduced the value of tan δ decreased, passed through a minimum value and then increased rapidly with the further lowering of the temperature. Near about liquid nitrogen temperature (80°K) tan δ curves showed a maximum value. This maximum showed some dependence on the film thickness. The above features were similar to those observed for niobium oxide films.

(iv) Effect of frequency on C and tan δ

Figs. VII.7a and b show the variation of capacitance with frequency when measured at different temperatures for films 1280 Å and 2350 Å thick. In general capacitance decreased with the increase of frequency. Like niobium oxide films, at higher temperatures, C tends to be a constant

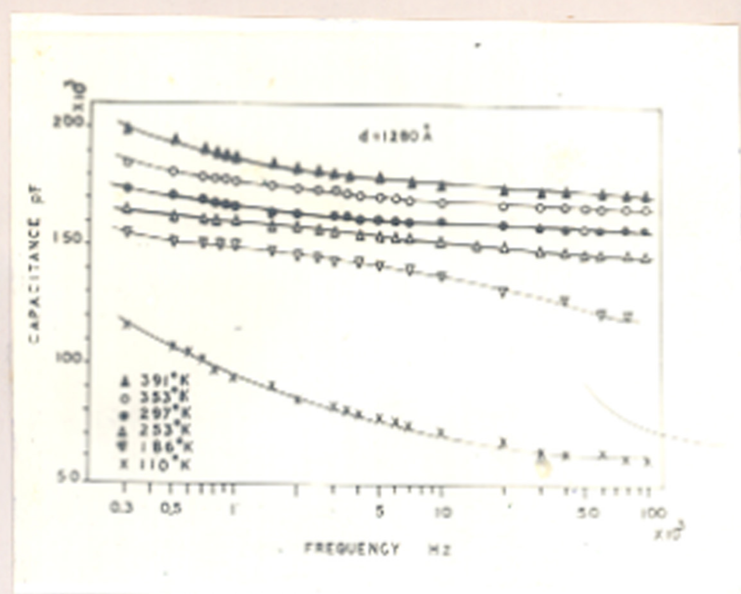

Fig VII. 7a

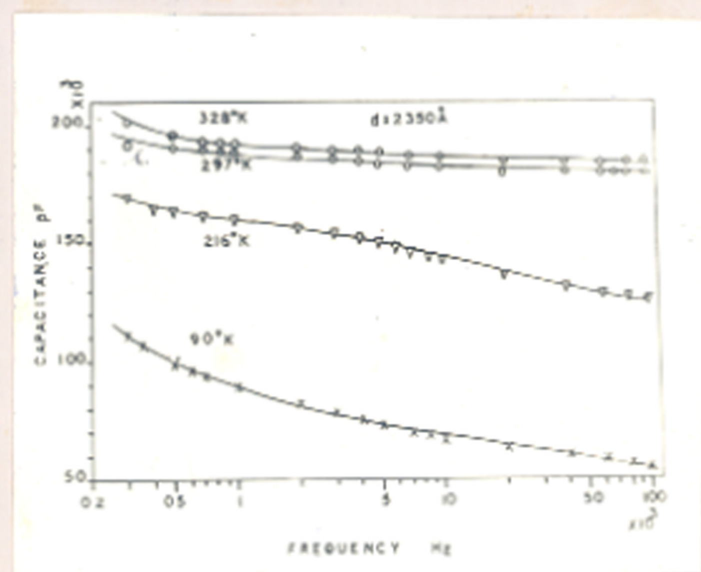

Fig VII. 7b

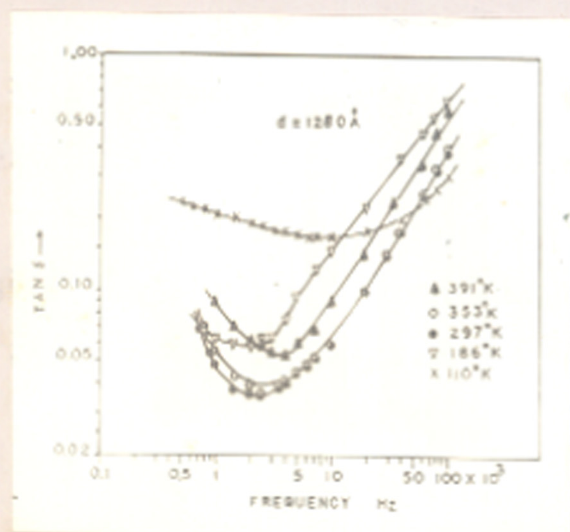

Fig VII. 8a

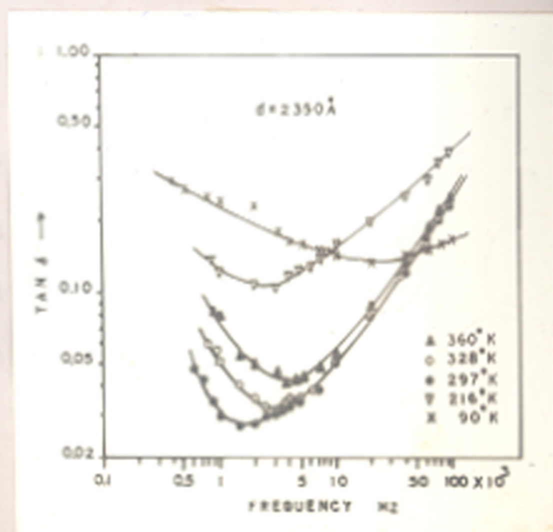

Fig VII. 8b

beyond say 20 kHz; but at lower temperatures, say $110^{o}K$, C did not attain saturation even beyond 70 kHz. The variation of C with applied frequency thus became larger at lower temperatures.

Frequency again had a profound influence on tan δ. Figs. VII.8a and b show the variation of tan δ with the frequency at different temperatures. Like other film capacitors studied earlier, tan δ showed a pronounced minimum value in the frequency spectrum (0.5 to 10^3 kHz) investigated. The shift of f_{min} or ω_{min} (where tan δ_{min} occurred) with the temperature was very similar to that of niobium oxide films capacitors. Above the room temperature f_{min} shifted to the larger frequency side as in the case of other film capacitors (ZnS, Sb_2O_3 and praseodymium oxide). But below $270^{o}K$ also, f_{min} and ω_{min} shifted to the higher frequency region. This was true for all film thicknesses.

(v) Breakdown voltage and percentage variation of capacitance

Fig. VII.9 shows the J-V characteristics for a few films. It is interesting to see that the breakdown voltage (V_B) had a value of about 3.0 volts and was independent of the film thickness. This is indeed a very peculiar case and apparently not reported before. The dielectric field strength (F_B) therefore decreased

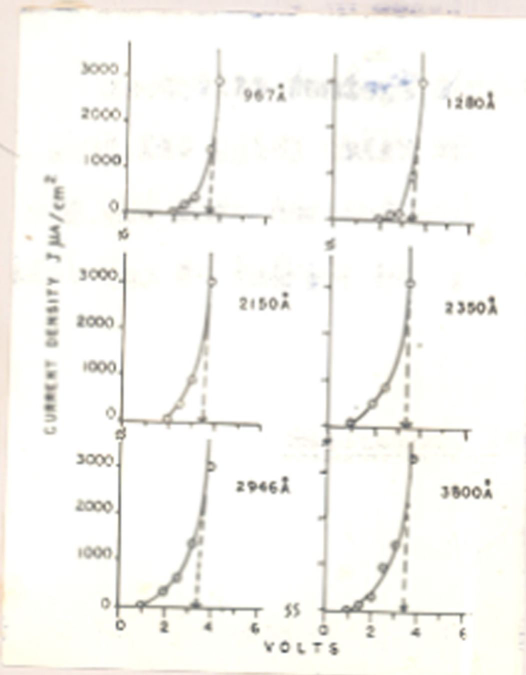

Fig VII.9

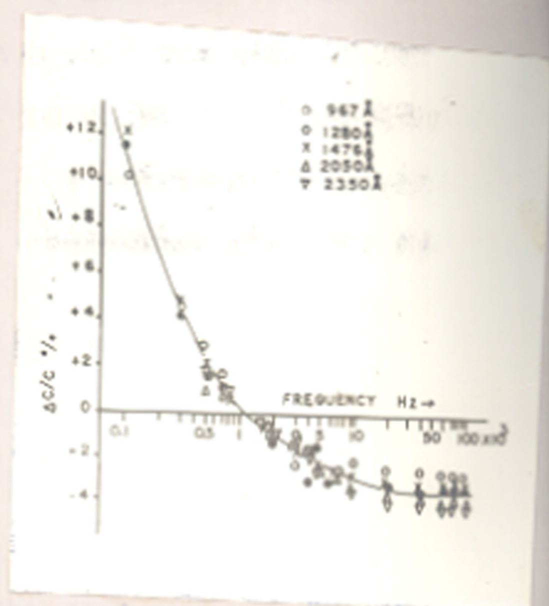

Fig VII.10

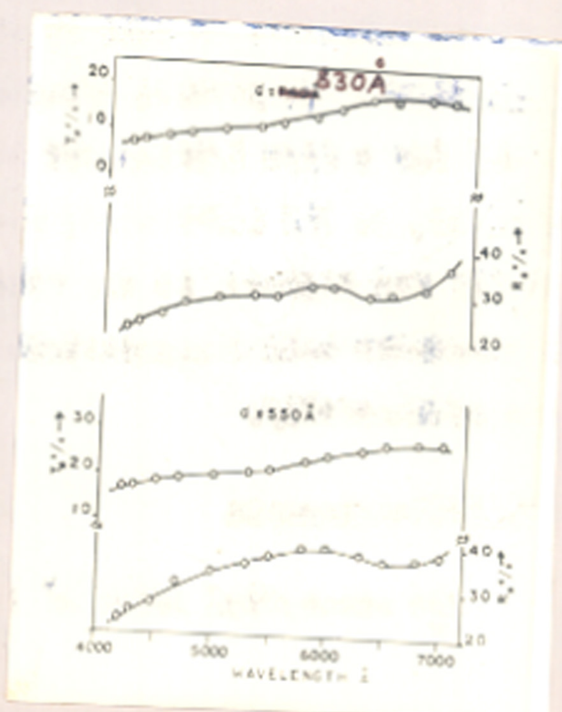

Fig VII.11

monotonically with the increasing film thickness.

The percentage variation of capacitance $\frac{\Delta C}{C}\%$ at room temperature is plotted against different frequencies for five different films (Fig. VII.10). This variation was large below 1 kHz but was much smaller at higher frequencies ($>$1 kHz). In general it was independent of the film thickness.

(c) Optical Properties

(i) Transmission and reflection

Fig. VII.11 shows the transmittance and reflectance spectra in the visible region at near normal angle of incidence for two films. Transmittance was dependent both on the film thickness as well as on the wavelength of the incident light. In general transmittance was small and was about 10% for a film thicknessof 830 Å. Reflectance from these films, on the other hand, was large and about 30 to 35% in the red region. As the wavelength of the incident light decreased both transmittance and reflectance values reduced considerably.

(ii) Optical constants

The absorption index of these films was calculated

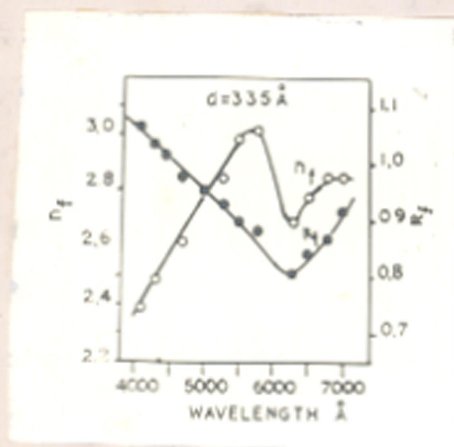

Fig VII.12a

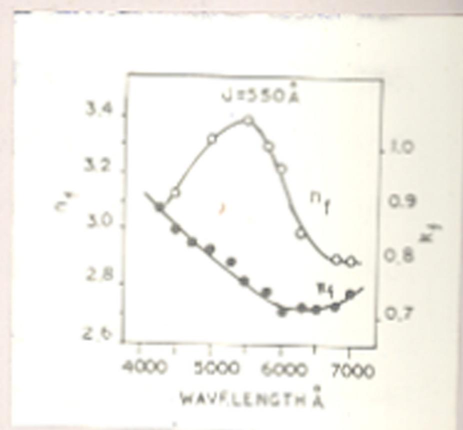

Fig VII.12b

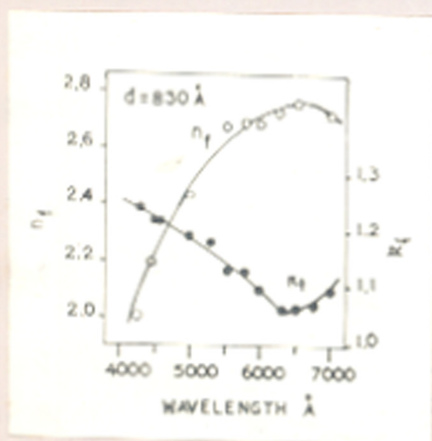

Fig VII.12c

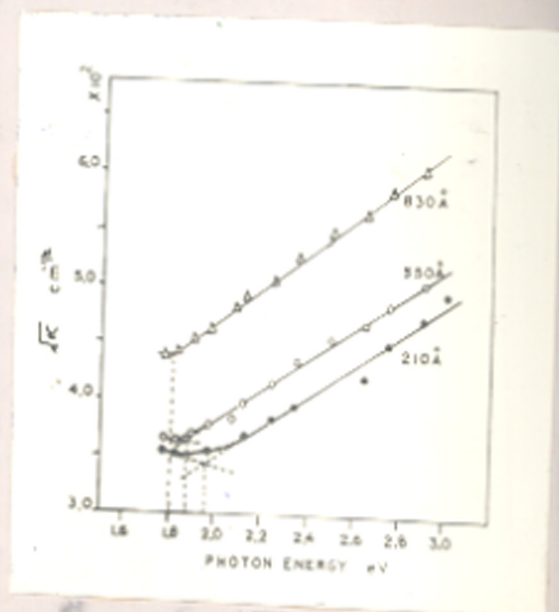

Fig VII.13

from the equation (II.8) of Chapter II; this value of k_f was then substituted in the complex equation (II.3) and the refractive index (n_f) was computed. Sometimes both n_f and k_f were computed from the complex equations (II.3) and (II.4) ~~xxxxx~~. The results obtained by the two methods agreed reasonably well. Figs. VII.12a,b and c show the dispersion curves of n_f and k_f in the visible region. Refractive index n_f showed a maximum value at about 5600 Å for a film thickness of 335 Å and 550 Å. For thicker films ($\approx$ 830 Å), however, the maximum shifted towards a higher wavelength (λ6500 Å) or to the lower energy region.

Absorption index for all films was rather high. As the wavelength was reduced, k_f initially decreased, passed through a minimum value and then increased as the wavelength changed from 7000 to 4200 Å. The minimum value of k_f was near the red region of the visible spectrum and shifted slightly to longer wavelengths with increasing film thicknesses (c.f. Figs. VII.12a, b and c).

(iii) <u>Absorption coefficient (α) and optical energy band gap (E_{op})</u>

Absorption coefficient was in general large and it increased with the film thickness (Table VII.2). Fig. VII.13 shows a plot of $\sqrt{\alpha}$ with the energy of the incident radiation for a few film thicknesses. The intersection of

TABLE VII.2

Thickness α/wavelength (λ) Å	880 Å	550 Å	210 Å
7000	1.97×10^5 cm^{-1}	1.33×10^5 cm^{-1}	1.26×10^5 cm^{-1}
6800	1.98×10^5 "	1.33×10^5 "	1.24×10^5 "
6500	2.06×10^5 "	1.38×10^5 "	-
6300	2.13×10^5 "	1.45×10^5 "	1.25×10^5 "
6000	2.32×10^5 "	1.48×10^5 "	1.23×10^5 "
5800	2.44×10^5 "	1.585×10^5 "	1.37×10^5 "
5500	2.57×10^5 "	1.75×10^5 "	1.48×10^5 "
5300	2.80×10^5 "	1.90×10^5 "	1.56×10^5 "
5000	3.04×10^5 "	2.08×10^5 "	1.54×10^5 "
4700	3.15×10^5 "	2.18×10^5 "	1.76×10^5 "
4500	3.46×10^5 "	2.36×10^5 "	2.05×10^5 "
4300	3.67×10^5 "	2.58×10^5 "	2.26×10^5 "
4100	-	-	2.60×10^5 "

the tangential lines drawn through the two portions of the curve therefore give an estimate of the optical band gap (E_{op}) of the material (c.f. Fig. VII.13). It is interesting to see that the values of E_{op} were not constant but varied with film thickness, the thinner films having slightly higher values.

(D) DISCUSSION

Films formed by the thermal evaporation of pure In_2O_3 were opaque and blackish in colour. Since In_2O_3 films are known to be very transparent in the visible region as reported by various workers (Tippins and Chase, 1966; 1967; Weiher and Ley, 1966), it can therefore be inferred that these blackish films are not due to the crystalline sesquioxide of indium. However such blackish films may result either from the dissociation of In_2O_3 say to In_2O and In as reported by Burns and co-workers (1963, 1966) or from the amorphous films having defects such as inclusions. The dissociation to lower oxides by the thermal evaporation of many oxides such as CuO, Bi_2O_3, etc. has been very well illustrated by Goswami and his co-workers (1957, 1971). In the previous chapter too it has been shown that Nb_2O_5 also dissociated to a lower oxide which had a oxygen deficient structure and therefore possibly causing the blackish colour in the deposited films.

Tippins and Chase (1966) have already reported that the oxygen deficiency in In_2O_3 resulted in the blackish appearance of In_2O_3 crystals and when compensated the crystals became transparent. In the present case, however, it was not possible to conclude unequivocally whether the deposits were a new form namely a suboxide of indium (In-O), or only an oxygen deficient phase of In_2O_3, since the deposits did not yield any coherent diffraction patterns. The phase structure and the nature of these blackish deposits are still open for further investigations.

A.C. behaviour of indium oxide films was very similar to those of vacuum deposited niobium oxide films.

Pronounced effects of ageing causing reduction of C and tan δ with time were due to the reduction of defect or imperfection concentrations in the evaporated films by the self annealing process. This would reduce the number of charge carriers (n) and thereby increasing the film resistance R. Tan δ being related to the reciprocal of R as $\frac{1}{\omega RC}$ must therefore reduce. This is obvious as can be seen from Fig. VII.2. It is interesting to see that initially tan δ increased to very high values after one day's ageing in air. This was possibly due to the adsorption of moisture by the freshly prepared samples when exposed to air. Moisture thus acts as a shunting resistance to the

dielectric film thereby decreasing the effective resistance between the electrodes and consequently increasing the value of tan δ .

Capacitance was found to be independent of the film thickness, a condition that follows if the barrier layers (Schottky barriers) were formed at the dielectric electrode interface (Simmons et al, 1970). The barrier layer model further predicts that if capacitance measurements are carried out at very low temperatures say at about $80^{o}K$, then the capacitance will be inversely proportional to the film thickness. In the case of indium oxide film capacitors, when measurements were made at $80^{o}K$, it was found that although C decreased with the increasing thickness the proportionality law viz. $C \propto \frac{1}{d}$, did not hold even for a film 3000 Å thick.

The a.c. behaviour of these films could therefore be understood from the physical picture elaborated in the case of niobium oxide capacitors dealt in the earlier chapter. The large rise in tan δ at 1 kHz with the lowering of temperature, and its tendency to a maximum value or near saturation at $80^{o}K$ is possibly due to a dielectric relaxation phenomenon as discussed for niobium oxide films. This relaxation can occur if there are impurities in the

film or the films have a defect structure (Breckenridge, 1948; Harrop and Wanklyn, 1964). In fact we have not ruled out the possibility of either of these features being absent. As discussed earlier, the blackish nature of the vacuum deposited films have been associated with the presence of impurities such as indium, or its lower oxides, or even an oxygen efficiency of the materials. Whatever might be the case, these will favour the relaxation effect at 1 kHz especially at low temperatures. The variation of capacitance and tan δ_{min} with frequency and temperature can then be explained on the same lines as explained for niobium oxide films capacitors.

The thickness independent behaviour of the breakdown voltage (V_B) is very peculiar. In this case F_B is inversely proportional to film thickness. According to Forlani and Minnaja (1969) if the injection of electrons into the insulator is governed by a Schottky mechanism rather than by a tunneling effect, then the breakdown voltage V_B would be independent of the film thickness and dependent on the temperature. In the present case therefore such a Schottky mechanism may be the cause for the thickness-independent behaviour of V_B even though the temperature effect could not be investigated by us.

Thermally evaporated indium oxide films were in

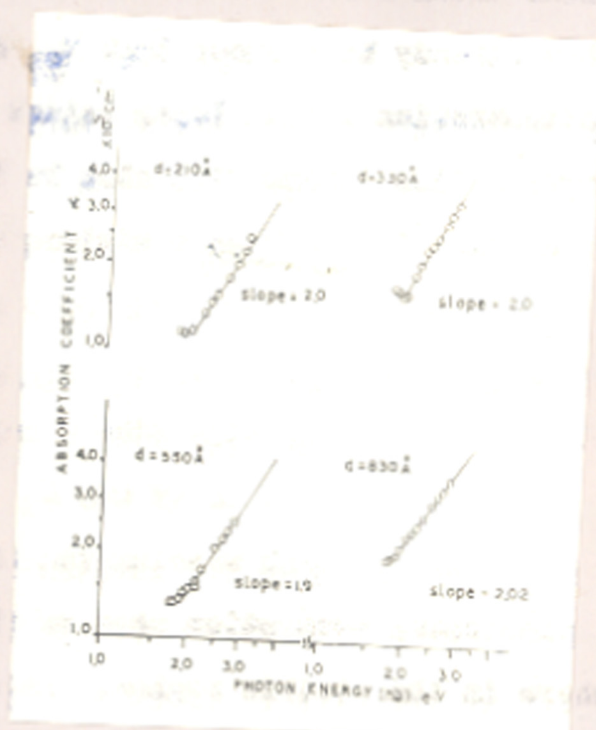

Fig VII.14

general absorbing in the visible region. Refractive index increased with the decreasing wavelength of the incident radiation and passed through a maximum value, after which it fell very rapidly in the violet region of the spectrum. The peak value of n_f shifted to the longer wavelength for thicker films which means the decrease of the energy band gap. It has already been shown that E_{op} depends on the carrier concentration giving lower values of band gap for lesser concentration, which will also be true for thicker films. Absorption index shows a minimum value in the visible region. This minimum position also shifts slightly with the increasing thickness to the longer wavelength region. k_f was in general high with a value of about 1.1 at 7000 Å for a film thickness of 830 Å. k_f increased both at low as well as high wavelengths thus suggesting that the fundamental absorption edge of these films must lie somewhere in the visible region. This is illustrated better in Fig. VII.13 where $\sqrt{\alpha}$ is plotted against the incident photon energy.

The optical energy band gap (E_{op}) obtained by extrapolation showed it to be sensitive to the film thickness and increasing for thinner films. The values of E_{op} obtained for film thicknesses 830 Å, 550 Å and 210 Å were 1.6, 1.7 and 1.95 eV respectively. Such changes in energy band gap with film thickness have already been

demonstrated by Stasenko (1968) and by Filatov and Karpovich (1969) for CdS and InSb films.

It is also possible to have some idea of the electron transition mechanism. A plot of α against $h\nu$ in log-log scale (Fig. VII.14) shows a definite power law. The average value of the power indices for four different films thicknesses was about 2.0 viz.

$$\alpha \propto (h\nu)^2$$

This corresponds to an indirect but allowed transition arising because of impurity levels in the forbidden energy gap.

As the fundamental absorption edge lies in the visible region, these films showed less transmittance and were heavily absorbing.

PART B

Oxidised Films

(B) EXPERIMENTAL

Blackish films obtained by the evaporation of In_2O_3 from molybdenum boats as described in PART A of this chapter were then oxidised in air at about 320°C for 2½ hours. By this treatment the blackish films became

completely transparent showing interference colours depending on the film thickness.

The film capacitors were prepared in the following manner. After the deposition of the aluminium base electrode, the blackish indium oxide was deposited on it as in PART A of this chapter. These films with the underlying electrode were then oxidised for 2½ hours at about 320°C in air when the dielectric layer became completely transparent. The counter electrode also of aluminium was then deposited in the usual way. It may be mentioned here that the oxidation of the blackish films in air did not cause any significant change in the base aluminium electrode at least from electrical contact point of view, since no measurable change in its (i.e. aluminium) resistance was observed during the oxidation process. Gulbransen and Wysong (1947) already reported that aluminium films remained unaffected even when baked in an oxygen ambient at 400°C for a very long time.

Indium oxide films formed on NaCl tablets were also oxidised in a similar way and then examined by the electron diffraction method for their structures.

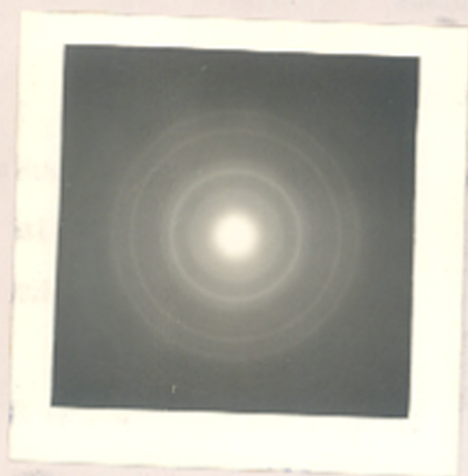

Fig VII.15

Fig VII.16

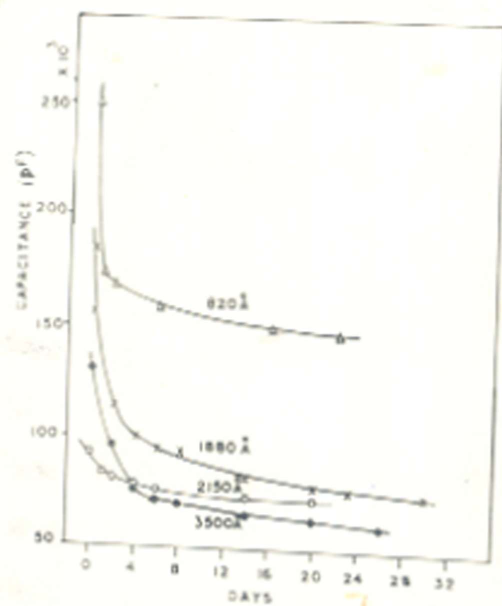

Fig VII.17

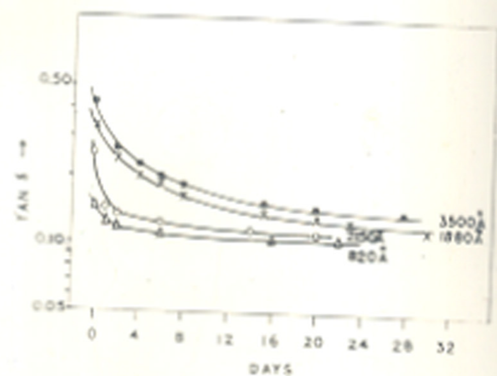

Fig VII.18

(C) RESULTS

(a) Structure

Fig. VII.15 shows a typical transmission pattern obtained from oxidised films formed on polycrystalline NaCl tablets. An analysis of this pattern showed that the films were due to In_2O_3 having a b.c.c. type of structure with $a_o = 10.12$ Å. Table VII.3 shows the d values and the indices for these films. Reflection patterns (Fig. VII.16) were also taken from films deposited on glass substrate and subsequently oxidised in air at 320°C for 2½ hours. Sharp reflections clearly showed that these films were crystalline even when formed on amorphous glass substrates.

(b) Dielectric Properties

(1) Ageing and annealing effects

All these capacitors showed a pronounced ageing effect as both capacitance and tan δ decreased with time. For the first few days capacitance decreased very rapidly but later on the decrement was rather small tending to a steady value with time. A similar trend was also observed for tan δ . These are clearly shown in Figs. VII.17 and 18. It may be pointed out here that in spite of such a

TABLE VII.3

I/I_o	d Å	hkl
s	2.92	222
f	2.58	400
vvf	2.2	332
vvf	2.0	431
ms	1.81	440
vvf	1.65	611
m	1.53	622

$a_o \approx 10.12$

s - strong f- faint
m - medium v- very

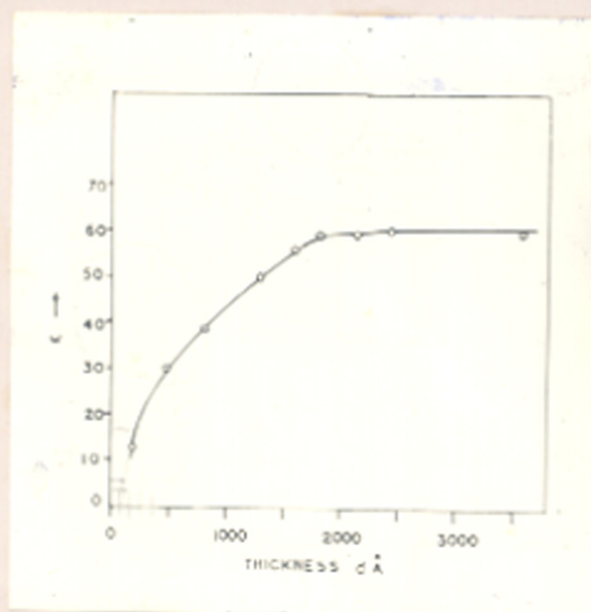

Fig VII.19

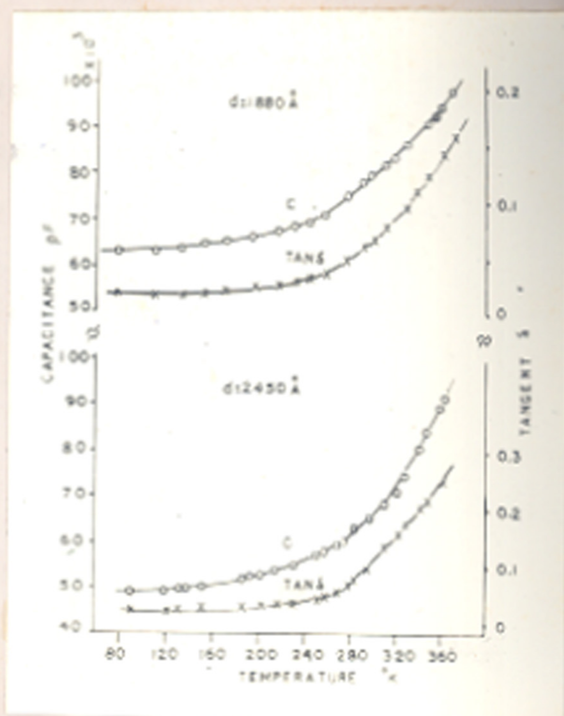

Fig VII.20

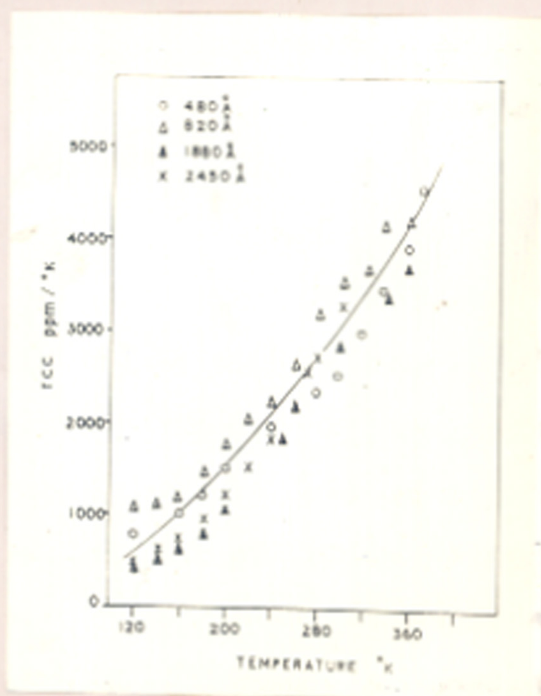

Fig VII.21

long time of ageing, stable values of C and tan δ were obtained only after annealing these capacitors by cyclic heating and cooling in vacuo as mentioned earlier.

(ii) Effect of film thickness

In general capacitance reduced with the increasing film thickness. However the proportionality law viz. $C \propto \frac{1}{d}$ was found to be valid only for thicker films say beyond 1800 Å. (Table VII.4). Fig. VII.19 shows the variation of dielectric constant (ϵ) with the film thickness. It is seen that ϵ increased with the film thickness from 13 at 200 Å to about 58 at 1600 Å. Beyond this thickness, dielectric constant was more or less constant with a value of about 60. Tan δ in all cases was low (0.05 to 0.07) and more or less independent of the film thickness.

(iii) Effect of temperature

The effects of temperature on C and tan δ of In_2O_3 film capacitors were similar to those of ZnS, Sb_2O_3 and praseodymium oxide film capacitors. Both capacitance and tan δ increased with the temperature. Fig. VII.20 shows the typical variation of C and tan δ with temperature. Capacitance increased rather slowly upto 240°K, but beyond this temperature the rise was rapid. Tan δ also varied in

TABLE VII.4

Thickness (d) Å	Capacitance (C) pF	ε
200	158,000	12.5
480	156,000	30.0
820	120,000	38.5
1400	34,200	53.0
1600	91,700	59.0
1880	80,200	60.0
2150	72,700	61.0
2450	65,300	62.0
3600	41,600	59.5

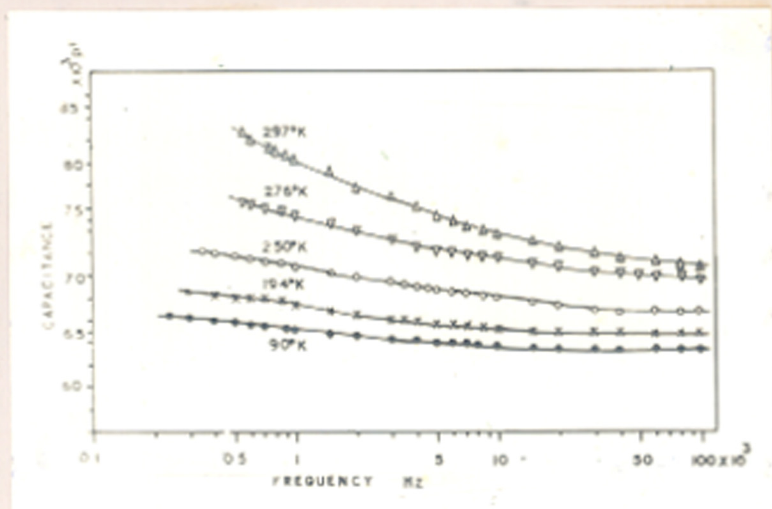

Fig VII.22

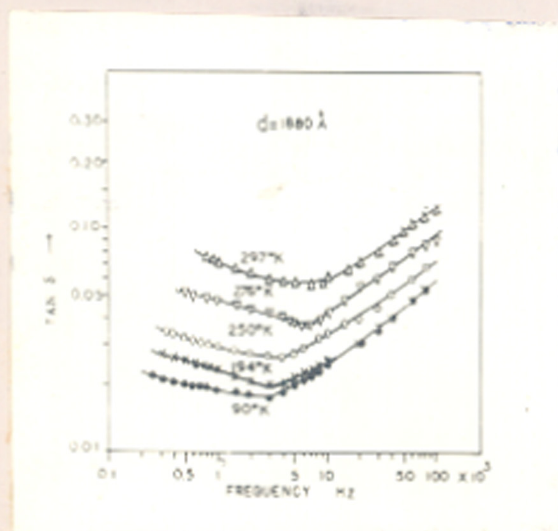

Fig VII.23

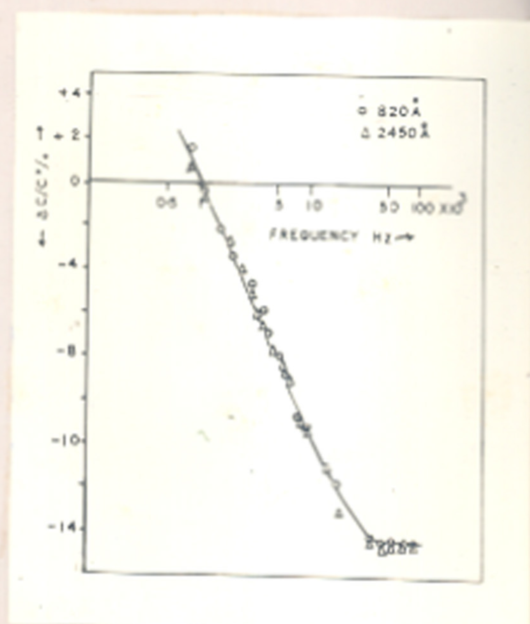

Fig VII.24

a similar manner. This trend was true for all film thicknesses.

TCC of these films was positive and increased with temperature. Below 200°K TCC was less than 1500 ppm/°K but increased to values as large as 4000 ppm/°K at 360°K. In general TCC was independent of the film thickness (Fig. VII.21).

(iv) Effect of frequency on capacitance and tan δ

Frequency as usual had a pronounced influence on both C and tan δ. The variation of capacitance with frequency at different temperatures of measurement is shown in Fig. VII.22 for a film 1880 Å thick. It can be seen from the above curves that capacitance decreased with the increasing frequency. This variation although large at higher temperatures and low frequencies, tends to a steady value at high frequencies say above 60 kHz. At low temperatures this variation in capacitance decreased, and ultimately near 90°K capacitance became almost invariant with the frequency. Similar results were also observed for film capacitors of different film thicknesses.

Fig. VII.23 shows the variation of tan δ with frequency at different temperatures. As usual, tan δ showed a minimum value (tan δ_{min}) at a frequency f_{min}

(or ω_{min}) which shifted to the higher frequency region with the increasing temperature. The value of tan δ_{min} also increased with the rise of the temperature. Table VII.5 shows the values of ω_{min} and tan δ_{min} at different temperatures for a film 1880 Å thick.

(v) Percentage variation of capacitance and breakdown voltage

The percentage variation of capacitance $\frac{\Delta C}{C}\%$ with the applied frequency at room temperature is shown in Fig. VII.24 for two capacitors of extreme thicknesses. This variation ranging from +1.5% at 0.8 kHz to -14% at 40 kHz was rather large rand independent of the film thickness. The dielectric field strength of these films was found to be rather poor. The application of even a small voltage, say less than 2 volts, resulted in the electrical breakdown of these capacitors. D.C. resistance measurements of the sandwiched dielectric layers showed that the resistance decreased continuously even when a potential of 1 volt (d.c.) was applied between the electrodes. This is in conformity with the observations of Korzo (1966) who reported a large rise in current followed by an avalanche multiplication process when the field between the sandwiched dielectric layer of In_2O_3 was greater than 10^5 volts/cm. Hence no proper measurements could be

TABLE VII.6

d = 1880 Å

T °K	ω_{min} rad/sec	tan δ_{min}
90	2.2×10^4	0.017
194	2.4×10^4	0.020
250	2.83×10^4	0.026
276	4.3×10^4	0.038
297	5.65×10^4	0.054

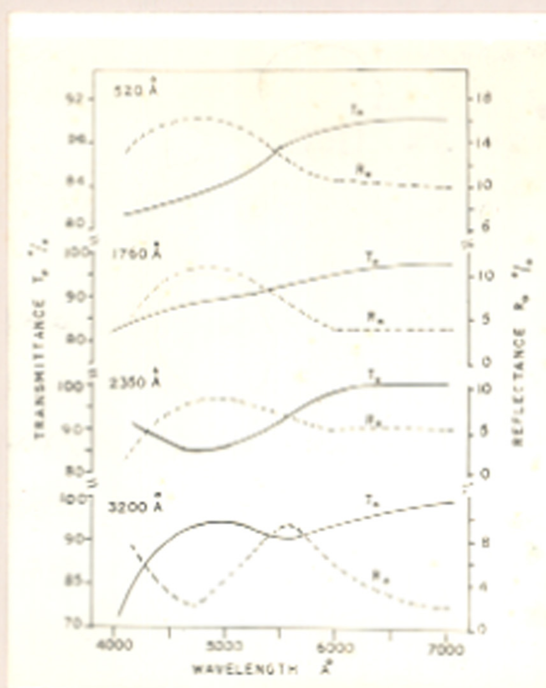

Fig VII.25

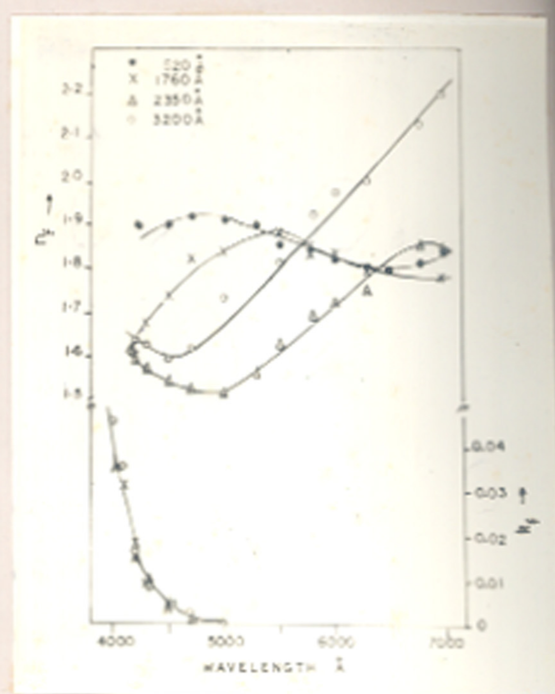

Fig VII.26

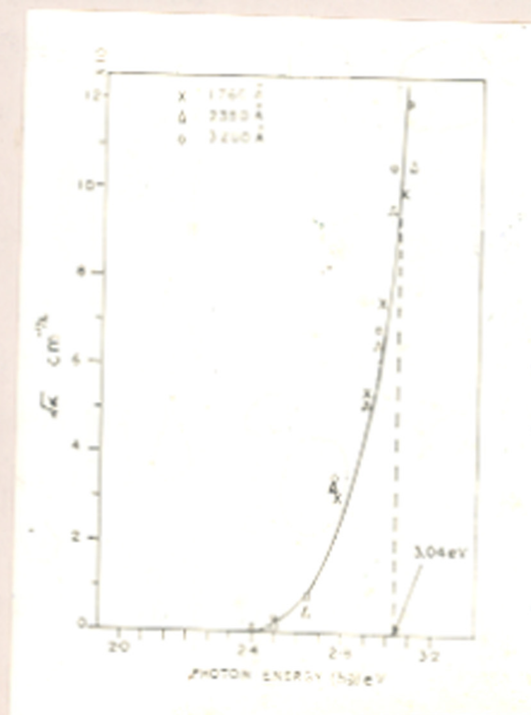

Fig VII.27

carried out to estimate the breakdown voltage (V_B) and consequently the field strength (F_B).

(c) Optical Properties

(i) Transmission and reflection

Oxidised (In_2O_3) films of indium were in general very transparent in the visible region. Fig. VII.25 shows the typical transmittance and reflectance spectra of several oxide films. Transmittance decreased in the violet region of the spectrum. Reflectance (R_o) at near normal angle of incidence was small and of the order of about 15%.

(ii) Optical constants

Refractive index and absorption index were computed from the complex equations (II.3) and (II.4) given in chapter II. Fig. VII.26 shows the dispersion curves of n_f and k_f in the visible region for a few films of different thicknesses. For the thinnest film, n_f increased with the lowering of wavelength, attained a maximum and then fell rather sharply as the incident radiation passed into the violet region. Similar trends were also observed for thicker films ($\approx$1760 Å and 2350 Å) though the peaks shifted towards the longer wavelength. It is interesting to see that a minimum was also observed at lower wavelengths.

However for a film 3200 Å the trend of the curve was similar to the film 2350 Å thick, except that the peak was apparently beyond the red region.

Absorption index though small showed some interesting features (Fig. VII.26). It is seen that it was more or less independent of the film thickness but varied with the wavelength. k_f increased rapidly at very low wavelengths but was negligible in the higher wavelength region viz. $>$ 5000 Å.

(iii) <u>Absorption coefficient and optical energy band gap</u>

Absorption coefficient 'α' of the oxidised films was also negligible above λ 5000 Å, but became appreciable as the wavelength decreased to the violet region of the spectrum. In this region α had values as high as 4.5×10^3 cm^{-1}. A plot of $\sqrt{\alpha}$ against the incident photon energy ($h\nu$) is shown in Fig. VII.27 for a few thicknesses. It is interesting to see that beyond 2.9 eV α increased very sharply suggesting the beginning of the absorption edge. The optical band gap for three such films determined from the steepest portion of the curve was about 3.05 eV, a value close to the one reported (3.1 eV) by Weiher (1962) for In_2O_3 single crystals.

(D) DISCUSSION

In_2O_3 films prepared by oxidising the blackish oxide films of indium in air were crystalline and had a b.c.c. type of structure with $a_o = 10.12$ Å. These films even when formed on glass substrates were crystalline thus suggesting that the substrates did not affect the crystallinity of the deposits at all.

A.C. behaviour of these film capacitors were very similar to ZnS, Sb_2O_3 and praseodymium oxide film capacitors. The dependence of ϵ on film thickness for very thin film deposits ($<$ 1400 Å) could be attributed chiefly to the defects present in these films. For thicker films ($>$ 1600 Å), ϵ was a constant with a value of about 60. The variation of capacitance and tan δ with temperature at 1 kHz and the positive nature of TCC can be explained in the same manner as for ZnS film capacitors (Chapter III). The effect of frequency on capacitance at different temperatures can also be explained from our earlier discussions with regard to the theoretical model proposed by Goswami and Goswami (1973). The occurence of tan δ_{min} and its shift to higher frequencies with the increasing temperature are direct consequences of the above model.

It seems therefore that the model proposed by Goswami and Goswami (1973) as explained in Chapter III also fits very well with the experimental observations of the a.c. behaviour of the above In_2O_3 films.

The electrode lead resistance (r) of these films as calculated from the equation (III.14) was about 1.6 ohms and was independent of frequency and temperature, a condition predicted by the theoretical model. From the value of ω_{min} resistance (R) and hence the resistivity (ρ) of the dielectric film was calculated. A similar calculation of resistance (R) can ~~also~~ were be made from the relation $\tan\delta = \frac{1}{\omega RC}$ at 1 kHz. Table VII.6 shows a comparison of R and also ρ by these two methods at different temperatures for a film thickness of 1880 Å. It is interesting to note that the values of resistance so computed agree reasonably well with each other.

In_2O_3 films (oxidised) were transparent in the visible region of the spectrum. However, transmission through these films reduced as the wavelength of the incident radiation decreased. The dispersion curves of refractive index showed a peak value which shifted to the longer wavelength for thicker films. This was no doubt due to the lowering of the impurity concentration and hence

TABLE VII.6

$d = 1880$ Å

Temperature (T) °K	R (from ω_{min})	R (from $\frac{1}{\omega RC}$) ohms	Average ρ ohm cm
90	3.5×10^{5}	1.8×10^{5}	2.87×10^{9}
194	2.7×10^{5}	1.12×10^{5}	1.78×10^{9}
250	1.75×10^{5}	8×10^{4}	1.28×10^{9}
276	6.6×10^{4}	4.4×10^{4}	7×10^{8}
297	3.8×10^{4}	2.9×10^{4}	4.05×10^{8}

the activation energy or band gap with the increase of film thickness.

Absorption index was negligible beyond λ 5000 Å but increased steeply as the wavelength was further reduced, thus indicating the presence of the absorption edge in the violet or ultraviolet region. In fact a plot of $\sqrt{\alpha}$ against the incident photon energy shows that the fundamental absorption edge for In_2O_3 films was at about 4000 Å, corresponding to an optical band gap of about 3.05 eV. This value agrees reasonably well with the value of 3.1 reported by Weiher (1962) for In_2O_3 crystals. Higher band gap energies such as 3.5 and 3.75 eV have however been reported for reactively sputtered amorphous In_2O_3 films (Rupprecht, 1954; Weiher and Ley, 1966). The high value of resistivity ($\approx 10^8$ ohm cm) for oxidised films is also in consonant with the large energy band gap.

The optical dielectric constant due to electronic polarisability (≈ 3.6) is very much less than the ϵ obtained by the a.c. measurements in the audio range. This clearly suggests that the contribution to polarisation at lower frequencies (audio range) was likely to be ionic since no peaks in tan δ versus temperature curves (due to dipole orientation or interfacial polarisation) were observed.

SUMMARY AND CONCLUSIONS

In the present investigations a detailed study has been made on the structural, dielectric and optical behaviour of different vacuum deposited films, with a view to a basic understanding not only of the interaction of the electromagnetic wave with matter, particularly the absorption of light, band structure, electron transition process from different energy states, dispersion effects, but also of the polarisation process at audio and optical frequencies, dielectric phenomena, relaxation mechanisms, etc. A simultaneous study of these vacuum deposits by other independent techniques has thrown some light on the basic mechanisms involved and an overall picture of the interaction of electromagnetic field with matter. These investigations, concerned particularly with the vacuum deposited films of ZnS, praseodymium oxide, Sb_2O_3, niobium oxide and oxides of indium, were carried out at different frequencies, temperatures, film thickness and substrate temperatures, to study their effect on tan δ, permittivity, capacitance and breakdown voltages. Optical properties such as, transmittance and reflectance at near normal angle of incidence at different wavelengths, refractive index, absorption coefficient, as well as energy band gap,

electron transition mechanisms, etc., have also been investigated in the visible region. Simultaneous studies by the electron diffraction technique offered a suitable means for identifying the nature and structures of the deposits.

These studies revealed that although the optical properties were sensitive to the substrate temperature and film thickness, the latter had little effects on the a.c. behaviour of the deposited films. Higher substrate temperatures however facilitated the grain growth process. The presence of defects such as voids, discontinuities, interstitials or impurities, etc., considerably affected the dielectric and optical constants of thin films and these defects could often be reduced by a suitable process of annealing.

A.C. behaviour of these film capacitors showed some very interesting features not reported before. In general capacitance decreased with the applied frequency. This variation was large at low frequencies and at higher temperatures. On the other hand, at very low temperatures and at high frequencies C became nearly invariant with the frequency. The frequency on the other hand had a pronounced influence on the loss factor (tan δ) of a film capacitor. Tan δ increased with the frequency, passed

through a minimum value (tan δ_{min}) at a frequency f_{min} and then increased almost linearly at higher frequencies. Further, it was found that f_{min} shifted to the higher frequency region when the temperature of measurement was raised. This is indeed a peculiar observation not reported earlier. Both C and tan δ increased with the temperature and TCC was positive in nature for all cases. All these variations including $\frac{\Delta C}{C}\%$ were found to be independent of the dielectric film thickness. Transparent films of ZnS, praseodymium oxide, Sb_2O_3 and In_2O_3 showed such behaviours. In all these cases, capacitance was <u>inversely proportional</u> to thickness for thicker films (> 800 Å) and dielectric constant was independent of the same at any particular frequency, except for very thin films.

Vacuum deposited films of niobium oxide and indium oxide (In-O) were blackish in colour and had dielectric properties slightly different from those above. In such capacitors, capacitance was <u>independent</u> of the film thickness so that dielectric constant was dependent on the same. Frequency also had a pronounced influence on C and tan δ . Here also tan δ showed a minimum value in the frequency spectrum studied, but f_{min} and tan δ_{min} shifted to higher frequencies both at high as

well as at low temperatures; capacitance therefore had a large variation with the frequency at these temperatures. Tan δ showed an unusual oscillatory behaviour with temperature. Although TCC was positive the increase of C with temperature was irregular. The formation of these films, as confirmed by the electron diffraction studies, involved the dissociation of the bulk material to its lower oxides (at least for niobium oxide) and sometimes even a suboxide (possibly for indium oxide). This process would give rise to a dielectric relaxation at very low temperatures, due to a vacancy conduction mechanism or a dipole orientation process as a result of the incorporation of impurities or defects, and thus showing an oscillatory behaviour in tan δ with temperature at 1 kHz.

The dielectric properties of the above solid films could then be classified into two groups (i) and (ii). The chief features that distinguish the two are that, in group (i) the films were transparent, showed capacitance inversely proportional to dielectric film thickness and tan δ increased with temperature. On the other hand, films in group (ii) were nonstoichiometric and blackish/brownish in appearance showing capacitance independent of film thickness. Tan δ showed a pronounced relaxation effect at low temperatures.

A new model for the capacitor has been proposed that satisfy both qualitatively and quantitatively all the features mentioned above. In this model the capacitor comprises of an inherent capacity C unaffected by frequency and temperature, in parallel with the dielectric resistance R (between the electrodes) varying exponentially with temperature, and in series with a small resistance 'r' arising due to lead resistances, etc. A direct outcome of this theory is that it provides a method to estimate the resistance of the sandwiched dielectric film which would otherwise be difficult eto measure. The theory also shows that a suitable combination of the parameters C, R and r would help as a guideline in preparing high quality thin film capacitors in microcircuits. In case of niobium oxide and black indium oxide (In-O) films, if one assumes a dielectric relaxation process in the proposed capacitor model, then the a.c. behaviour of these films capacitors could be explained qualitatively thus making the model a very powerful tool for the study of the dielectric properties of thin films.

Dielectric field strength (F_B) for crystalline films was found to obey the Forlani-Minnaja relation, $F_B \propto d^{-\beta}$(thickness), where β had a value of 0.5 for ZnS and Sb_2O_3 films and 0.65 for niobium oxide films. These

relations demonstrate that an avalanche process takes place due to the tunnelling of electrons from the electrode into the dielectric. In case of black indium oxide (In-O) which was amorphous in nature, a Schottky mechanism took place to initiate the avalanche process because the breakdown voltage (V_B) was independent of the dielectric thickness.

Optical constants viz. refractive index and absorption index, on the other hand, were strongly influenced by the deposition conditions and film thickness. Most of these films were transparent but absorbed heavily in the violet region of the visible spectrum. In the cases of ZnS and Sb_2O_3 films refractive index increased with the lowering of wavelength. This dispersion though small in the visible region was independent of the film thickness. k_f in this region was nearly zero. A similar type of dispersion was also observed for praseodymium oxide films, but here n_f increased with the film thickness due to the increase in the grain size. k_f which was negligible in the visible region increased sharply at 4000 Å indicating the presence of absorption.

Films of niobium oxide, black indium oxide (In-O) and In_2O_3 showed some interesting dispersion features. For these oxides, n_f showed a maximum value that shifted

to the longer wavelength or lower energy side with increasing film thickness. This was found to be true for all films in the thickness region 500 to 3000 Å. Such shifts in the peaks of n_r with the film thickness appears to be due to the lowering of the activation energy or the forbidden energy band gap because of the presence of defects in the depoited films. This has been verified in the case of black indium oxide (In-O) films from the plots of α (absorption coefficient) against the incident photon energy. Optical energy band gap (E_{op}) for these films were 1.6, 1.7 and 1.95 eV for film thicknesses 830, 550 and 210 Å respectively. An indirect but allowed transition mechanism took place between the different energy states.

E_{op} for praseodymium oxide and In_2O_3 films were 3.4 and 3.05 eV respectively. For ZnS and Sb_2O_3 films, E_{op} and the absorption edge were in the ultraviolet region and hence could not be measured.

A comprehensive data for the different dielectric and optical parameters of the materials are given in a Table at the end of this chapter.

Recent investigations on the electrical and other properties of thin films have shown that the film thickness

has a profound influence on their behaviours. This arises because of the numerous defects present in the evaporated films. Our present work however shows that this parameter does not play any significant role in the dielectric properties. Barring the dielectric constant, no other a.c. behaviour of these films mentioned earlier is dependent on film thickness. Even the theoretical model proposed for the capacitor does not take into account the effect of film thickness, yet explains explicitly all the a.c. behaviours of the dielectrics. These findings therefore lead us to suggest that, unlike the semiconducting and optical properties, the dielectric behaviour of thin films are in general an intrinsic property dependent on the atomic and molecular dispositions of the material. Simultaneous optical studies on these materials show that the dielectric constant or permittivity at 1 kHz arises chiefly due to ionic as well as electronic polarisation, although the contribution from the latter is rather small. In the case of niobium oxide and In-O films, however, the contribution to permittivity is mainly from polarisation due to the dipole orientation.

The above studies in general give a coherent picture of the dielectric and optical properties of thin films. Although the dielectric properties could be adequately

explained with the help of the capacitor model proposed by us, some of the optical properties, on the other hand, could only be qualitatively speculated due to the lack of a suitable rigorous theoretical treatment. The optical studies, however, clearly show the thickness dependence of the energy band gap, but this could not be corroborated in the present cases by a corresponding measurement of their electrical properties both for lack of time and also the nonavailability of suitable sensitive measuring bridges. But this trend, however, conforms to the observations on semiconducting films made here by Goswami and his coworkers i.e. thicker films having less carrier concentration have ΔE lower than thinner films with a larger carrier concentration. However a simultaneous study by electron microscopy and diffraction would, no doubt, throw more light on the above subjects and particularly on the role of microstructural features and defects, and their influence over the dielectric and optical properties. It is therefore necessary to carry out more research work on this aspect to bring out a closer relationship between these two physical behaviours.

MATERIAL	NATURE	ϵ (1 kHz)	$\tan \delta$ (1 kHz)	TCC ppm/°K	$\Delta C/C$% (0.3 to 100 kHz)	F_B V/cm	n_f (7000 Å -	k_f 4000 Å)	E_{op} eV
ZnS	Crystalline f.c.c.	8.2	0.005	200 to 600	+1.0% to -1.5%	1.5×10^6	2.21 to 2.40	0.0	-
Praseodymium oxide	Amorphous	13.2	0.025	500 to 10,000	+4.5% to -3.75%	3.0×10^6	1.56 to 1.80	0.00 to 0.013	3.4
Sb_2O_3	Crystalline f.c.c.	8.2	0.003	100	+0.5% to -0.5%	0.5×10^6	1.92 to 1.97	0.0 to 0.006	-
*Niobium Oxide	Fine grain structure at room temp.	12-100 (V)	0.030	600 to 2000 for T > 290°K	-	0.5×10^6	(V)	0.005 to 0.015	-
*Indium Oxide (blackish)	Amorphous	15-250 (V)	0.030	600 to 1600 for T > 290°K	+12% to -4%	-	(V)	0.700 to 1.100	1.6 to 1.9
In_2O_3 (transparent)	Crystalline b.c.c.	60.0	0.050 to 0.070	1000 to 4000	+1.5% at 0.8 kHz to -14%	10^5	(V)	0.000 to 0.040	3.05

*Relaxation effect

(V) - Varies with film thickness

ACKNOWLEDGEMENTS

I am extremely grateful to Dr. A. Goswami, Ph.D.(Lond), D.Sc.(Lond), for his interest, guidance and constant encouragement throughout the course of work.

I also wish to thank the National Council of Educational Research and Training for the award of the National Science Talent Search Scholarship and to the Director, National Chemical Laboratory, Poona 411008, for permission to submit the present investigations in the form of a thesis.

Finally, but not the least, I am grateful to all my colleagues in the Electron Diffraction and Thin Films Laboratory for their cheerful and hearty co-operation during this present work.

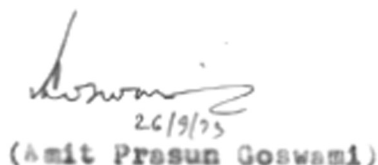

(Amit Prasun Goswami)

REFERENCES

1. Abelès, F. (1950) J. Phys. Rad., 11, 310.

2. Acharya, H.K. (1948) Ph.D. Thesis, London University.

3. Aggarwal, P.S. and Goswami, A. (1963) Ind. J. Pure & Appl. Phys., 1, 366.

4. Allsalu, M. Y. and Kil'k, I.R. (1966) Bull. Acad. Sci. USSR-Phys. Ser., 30, 1496.

5. Almin, K.E. and Westgren, A. (1941-1942) Arkiv. Kemi. Min. Geol., 15B, No.22.

6. Aminoff, G. (1923) Z. Krist., Festband. P.V. Growth, 58, 203.

7. Anderson, J.C. (1964) "Dielectrics," Chapman & Hall Ltd., London.

8. Arbuzov, M.P. and Chupriva, V.G. (1965) Soviet Phys. J., No.2, 87

9. Argall, F. and Janscher, A.K. (1968) Thin Solid Films, 2, 185.

10. Arkel, A.E. van., Flood, E.A. and Bright, N.F.H. (1953) Canad. J. Chem., 31, 1009.

11. Aven, M. (1962) Ext. Abstr. Meet Electrochem. Soc., 11, 46.

12. Aven, M. and Mead, C.A. (1965) Appl. Phys. Letters, 5, 160.

13. Axelrod, N.N. (1968) "Optical Properties of Dielectric Films," The Electrochem. Soc. Inc., N.Y.

14. Badachhape, S.B. and Goswami, A. (1964) Ind. J. Pure Appl. Phys., 2, 250.

15. Bardeen, J., Blatt, F.J. and Hall, L.H. (1954/56) Photoconductivity Conference; Wiley, N.Y.

16. Barr, W.L. and Jenkins, F.A. (1956) J. Opt. Soc. Am., 46, 141.

17. Behrndt, M.E. and Moreno, S.C. (1971) J. Vac. Sci. Tech., 8, 494.

18. Blumme, H.J.C. (1968) Proc. I.E.E., 56, 1395.

19. Bode, H.W. (1945) "Network Analysis and Feedback Amplifier Design, " Van Nostrand, London and New York.

20. Born, M. and Wolf, E. (1965) "Principles of Optics" Pergamon Press, Oxford.

21. Bound, M. and Richards, P.A. (1939) Proc. Phys. Soc., 51, 256.

22. Bozorth, R.M. (1923) J. Am. Chem. Soc., 45, 1621.

23. Bragg, W.L. (1920) Phil. Mag., 39, 647.

24. Bridgman, P.W. (1939) Am. J. Sci., 237, 7.

25. Breckenridge, R.G. (1950) J. Chem. Phys., 18, 913.

26. Brooks, H. (1955) "Advances in Electronics and Electron Physics", Vol. 7, Acad. Press, N.Y.

27. Brunner, H.R., Emmeneegger, F.P., Robinson, M.L.A. and Rotshi, H. (1968) J. Electrochem. Soc., 115, 1287.

28. Buckel, W. and Hilsch, R. (1954) Z. Phys., 138, 109.

29. Budenstein, P.P. and Hayes, P.J. (1967) J. Appl. Phys., 38, 2837.

30. Buerger, M.J. (1936) Amer. Min., 21, 206.

31. Buerger, M.J. and Hendricks, S.B. (1937-1938) Z. Krist., A98, 1.

32. Burkhardt, P.J. (1966) I.E.E.E. Trans. Electron Devices, ED13, 268.

33. Burgiel, J.C., Chen, Y.S., Vratny, F. and Smolinsky, G. (1968) in "Optical Properties of Dielectric Films," Ed. N.N. Axelrod, p.251.

34. Burstein, E. (1954) Phys. Rev., 93, 632.

35. Burns, R.P., DeMaria, G., Drowart, J. and Inghram, M.G. (1963) J. Chem. Phys., 38, 1035.

36. Burns, R.P. (1966) J. Chem. Phys., 44, 3307.

37. Burstein, E. (1954) Phys. Rev., 93, 632.

38. Campbell, D.S. (1970) in "Handbook of Thin Film Technology", Ed. Maissel, L.I. and Glang, R., McGraw-Hill Book Comp., New York.

39. Chase, A.B. and Tippins, H.H. (1967) J. Appl. Phys., 38, 2469.

40. Chopra, K.L. (1965) J. Appl. Phys., 36, 184.
ibid 655
(1969) "Thin Film Phenomena", McGraw-Hill Book. Comp., N.Y.

41. Cockbain, A.G. and Harrop, P.J. (1968) Brit. J. Appl. Phys. (J. Phys. D), 1, 1109.

42. Conlon, R.C. and Doyle, W.P. (1961) J. Chem. Phys., 35, 752.

43. Coogan, C.K. (1957) Proc. Phys. Soc., B70, 845.

44. Cooper, R. (1966) Brit. J. Appl. Phys., 17, 149.

45. Cox, J.T., Waylonis, J.E. and Hunter, W.R. (1959) J. Opt. Soc. Am., 49, 807.

46. Debye, P. (1912) Phys. Z., 13, 97.

47. Dekker, A.J. (1967) "Solid State Physics" Macmillan & Comp. Ltd., London.

48. Deokar, V.D. and Goswami, A. (1968) Z. Naturforchg., 23a, 348.

49. Dexter, R.N. (1956) Phys. Rev., 104, 637.

50. Dhere, N.G. and Goswami, A. (1969) Thin Solid Films, 3, 439.

51. Ditchburn, R.W. (1955) "Light", Interscience Publishers, Inc. N.Y.

52. Doyle, W.P. (1958) J. Phys. Chem. Solids., 4, 144.

53. Doyle, W.P. and Clarke, F.J.P. (1961) Brit. J. Appl. Phys., 12, 574.

54. Duffy, M.T., Wang, C.C., Waxman, A. and Zaininger, K.H. (1969) J. Electrochem. Soc., 116, 234.

55. Eldridge, J.M. (1972) Thin Solid Films, 12, 447.

56. Emmeneegger, F.P. and Robinson, M.L.A. (1968) J. Phys. Chem. Solids., 29, 1673.

57. Eyring, L. (1967) in "Advances in Chemistry Series", Ed. Gould, R.F., Vol. 71, p.6.

58. Faraday, M. (1837-1838) Phil. Trans.

59. Filatov, O.N. and Karpovich, I.A. (1969) Soviet Phy. - Solid State, 10, 2284.

60. Fischer, A. (1954) Z. Naturforchg., 9a, 508.

61. Fistul, V.I. and Vainshtein, V.M. (1967) Soviet Phys. - Solid State, 8, 2769.

62. Forlani, F. and Minnaja, N. (1964) Phys. Stat. Solidi, 4, 311; (1969) J. Vac. Sci. Tech., 6, 518.

63. Frohlich, H. (1948) "Theory of Dielectrics", Oxford Univ. Press, Fair Lawn, N.J.

64. Frohlich, H. and Paranjapé, B.V. (1956) Proc. Phys. Soc. (London), B69, 866.

65. Fuchshuber, R., Gullien, R and Roizen, S. (1960) C.R. Acad. Sci. (Paris), 251, 51.

66. Gadgil, L.H. (1968) Ph.D. Thesis, Poona University.

67. Gadgil, L.H. and Goswami, A. (1970) Ind. J. Chemistry, 8, 431.

68. Gagaliano, A., Kramer, B. and Kallman, H. (1967) J. Phys. Chem. Solids, 28, 737.

69. Gevers, M. (1946) Philips Res. Rep., 1, 279.

70. Gisolf, J.H. (1939) Physica, 6, 84.

71. Goldstein, R.M. and Leonhard, F.N. (1967) Proc. Electron. Components Conf., Washington, D.C., p.66.

72. Goswami, A. (1965) Ind. J. Chemistry, 3, 385.

73. Goswami, A. and Goswami, Amit P. (1973) Thin Solid Films, 16, 175.

74. Goswami, A. and Jog, R.H. (1964) Ind. J. Pure Appl. Phys., 2, 407.

75. Goswami, A. and Koli, S.S. (1966) Z. Naturforchg., 21a, 1462.

76. Goswami, A. and Rao, B.V. (1973) Ind. J. Pure Appl. Phys., (accepted).

77. Goswami, A. and Trehan, Y.N. (1957) Proc. Phys. Soc., 70B, 1005.

78. Graven, W.M., Salomen, R.E. and Adams (Jr.), G.B. (1960) J. Phys. Chem., 33, 954.

79. Groth, R. (1966) Phys. Stat. Solidi, 14, 69.

80. Grove (1852) quoted by Holland, L. in "Microelectronics", in Chapman and Hall Ltd.

81. Grovald, G. and Lorriers, J. (1962) C.R. Acad. Sci., 255, 2753.

82. Gruehn, R. (1966) J. Less Common Metals, 11, 119.

83. Gudden, B. and Pohl, R. (1921) Z. Physik, 5, 176.
(1922) ibid., 23, 417.

84. Gulbransen, E.A. and Wysong, W.S. (1947) J. Phys. Chem., 51, 1087.

85. Hacskaylo, M. (1964) J. Opt. Soc. Am., 54, 198.

86. Hacskaylo, M. and Feldman, C. (1962) J. Appl. Phys., 33, 3042.

87. Hadley, L.N. and Dennison, D.M. (1947) J. Opt. Soc. Am., 37, 451.

88. Hall, J.F. and Fergusson, W.F.C. (1955) J. Opt. Soc. Am., 45, 73.

89. Hammer, K. (1943) Z. Tech. Phys., 24, 169.

90. Harris, L., Beasly, J.K. and Loeb, A.L. (1951) J. Opt. Soc. Am., 41, 604.

91. Harrop, P.J. and Campbell, D.S. (1968) Thin Solid Films, 2, 273.

92. Harrop, P.J. and Campbell, D.S. (1970) in "Handbook of Thin Film Technology", Ed. Maissel, L.I. and Glang, R. McGraw-Hill Book Comp. Inc., New York.

93. Harrop, P.J. and Wanklyn, J.N. (1964) J. Electrochem. Soc., 111, 1133.

94. Hass, G., Ramsey, J.B. and Thun, R. (1959) J. Opt. Soc. Am., 49, 116.

95. Hass, G. and Salzberg, C.D. (1954) ibid., 44, 181.

96. Heavens, O.S. (1955) "Optical Properties of Thin Solid Films", Butterworths Scientific Publications, London.

97. Heavens, O.S. and Smith, S.D. (1957) J. Opt. Soc. Am., 47, 469.

98. Hickmott, T.W. (1966) J. Electrochem. Soc., 113, 1223.

99. Hippel, von (1967) in "Handbook of Physics" Ed. Condon, E.U. and Odinshaw, H. McGraw-Hill, N.Y.

100. Hochshild, P. (1908) News Jahrle. Min. Geol. Beilband, 26, 151.

101. Holland, L. (1956) "Vacuum Deposition of Thin Films", Chapman and Hall Ltd., London.

102. Holland, L. and Siddall, G. (1953) Vacuum, 3, 375.

103. Hoogenstratten, W. (1958) Philips Res. Repts., 13, 515.

104. Hrostwoski, H.J., Wheatley, G.H. and Flood, W.F. (1954) Phys. Rev., 95, 1683.

105. Huldt, L. and Staflin, T. (1959) Optics Acta, 6, 27.

106. Hyde, B.G., Bevan, D.J.M. and Eyring, L. (1966) Phil. Trans. Roy. Soc. (London), 259, 583.

107. Jamin, J. and Bernnard, R. (1953) C.R. Acad. Sci. (Paris), 237, 798.

108. Janninck, R.F. and Whitmore, D.H. (1966) J. Phys. Chem. Solids, 27, 1183.

109. Kazan, B. and Nicoll, F.H. (1957) J. Opt. Soc. Am., 42, 221.

110. Kelly, J.C. and Heavens, O.S. (1959) Opt. Acta., 6, 339.

111. Kern, S. (1964) J. Chem. Phys., 40, 208.

112. Khvorostukhina, N.A. (1962) Tr. Vost. Sibirsk. Filiala. Akad. Nauk. SSR, 78.

113. Kittel, C. (1966) "Introduction to Solid State Physics", Asia Publishing House, Bombay.

114. Klechkovskaya, V.V., Troitskaya, V.V. and Pinsker, Z.G. (1965) Soviet Phys. (Crystallography) 10, 28.

115. Klein, N. and Gafni, H. (1966) IEEE Trans. Electron Devices, ED13, 281.

116. Klein, N. and Levanon, N. (1967) J. Appl. Phys., 38, 3721.

117. Kofstad, P. (1968) J. Less Common Metals, 14, 153.

118. Kofstad, P. and Anderson, P.B. (1961) J. Phys. Chem. Solids, 21, 280.

119. Kofstad, P. and Esperik, S. (1965) J. Electrochem. Soc., 112, 153.

120. Koller, L.R. and Coghill, H.D. (1960) J. Electrochem. Soc., 107, 973.

121. Korobkov, I.I. Revyakin, B.N. and Khe-Min, C. (1964) STAR, 2, 607(A).

122. Korzh, P.D. and Gulayeva, G.P. (1969) Fiz. tekh. Poluprov., 3, 782.

123. Korzo, V.F. and Korobov, A.I. (1966) Fiz. Tverd. Tela, 8, 613.

124. Korozo, V.F. and Lyaschenko, G.A. (1968) ibid., 10, 3375.

125. Korzo, V.F. and Ryabova, L.A. (1967) Soviet Phys.-Solid State, 9, 745.

126. Kroger, F.A. (1956) Physica, 22, 637.

127. Kuwabara, G. and Ishiguro, K. (1952) J. Phys. Soc. (Japan), 7, 72.

128. Lakshmanan, T.K. and Mitchell, J.M. (1965) IEE TRANS. PMPI, S-272.

129. Lieberman, M.L. and Medrud, R.C. (1969) J. Electrochem. Soc., 116, 242.

130. Lomer, P.D. (1950) Nature, 166, 191.

131. MacChesney, J.B., Williams, H.J.W., Sherwood, R.C. and Potter, J.F. (1964) J. Chem. Phys., 41, 3177.

132. Macfarlane, J.C. and Weaver, C. (1966) Phil. Mag., 13, 671.

133. Maddocks, F.S. and Thun, R.E. (1962) J. Electrochem. Soc., 109, 99.

134. Maissel, L.I. and Glang, R. (1970) "Handbook of Thin Film Technology", McGraw-Hill Book Company, New York.

135. Malkin, G.M. and Terman, Yu.A. (1971) Soviet Phys. Semicond., 4, 1878.

136. Marezio, M. (1966) Acta. Cryst., 20, 723.

137. Martin, R.L. (1950) Nature, 165, 202.

138. Matthews, J.W. (1959) Phil. Mag., 4, 1017.

139. Mayer, H. (1950) "Physik dunner Schichten", Wissenschaftliche Verlagsgesellschaft m.b.H., Stuttgart.

140. Mayer, H. (1959) "Structure and Properties of Thin Films", p.225, Wiley, New York.

141. Mayer, H. (1961) Symposium on "Electrical and Magnetic Properties of Metallic Thin Layers", LouVin Belg.

142. McCullough, J.D. (1950) J. Am. Chem. Soc., 72, 1386.

143. McLean, D.A. (1961) J. Electrochem. Soc., 108, 48.

144. Mehta, R.R. and Volgel, S.F. (1972) J. Electrochem. Soc., 119, 752.

145. Merril, R.C. and West, R.A. (1963) Spring Meeting of the Electrochem. Soc., Pittsburg.

146. Merz, (1958) "Brussels Solid State Congress", Acad. Press, New York.

147. Mikhailov, G.P. and Borisova, T.I. (1964) Soviet Phys. Usp. English Transl., 7, 375.

148. Milovslavskii, V.K., Naboikina, E.N. and Kiyan, T.S. (1967) Soviet Phys. Semicond., 1, 527.

149. Moss, T.S. (1953) Proc. Phys. Soc. (Lond), B66, 141.

150. Moss, T.S. (1959) "Optical Properties of Semiconductors", Butterworths Scientific Publications, London.

151. Mott, N.F. and Jones, H. (1936) "Properties of Metals and Alloys", Oxford Univ. Press.

152. Muller, H.K. (1968) Phys. Stat. Solidi, 27, 723.

153. Nadkarni, G.S. and Simmons, J.G. (1970) J. Appl. Phys., 41, 545.

154. Narita, S. and Nagasaka, K. (1965) J. Phys. Soc. Japan, 20, 1728.

155. Neugebauer, C.A. and Webb, M.B. (1962) J. Appl. Phys., 33, 74.

156. Nicol, N.S. (1968) Proc. IEEE, 56, 109.

157. Nozieres, P. and Pines, D. (1958) Phys. Rev., 109, 741, 762, 1062.

158. Pashley, D.W., Stowell, M.J., Jacobs, M.H and Law, T.J. (1964) Phil. Mag., 10, 127.

159. Pashley, D.W. and Presland, A.E.B. (1954) J. Inst. Metals, 87, 419.

160. Phillips, V.A. (1960) Phil. Mag., 5, 571.

161. Phillip, R. and Tromptee, J. (1955) C.R. Acad. Sci. (Paris), 241, 627.

162. Piper, W. (1953) Phys. Rev., 92, 23.

163. Polster, H.D. and Woodruff, R.W. (1953) J. Opt. Soc. Am., 43, 326.

164. Rabidean, S.W. (1951) J. Chem. Phys., 19, 874.

165. Ramazanov, K.A. (1962) Soviet Phys. Solid State, 3, 1640.

166. Ramdhor, P. (1931) Neues Jahrt Mineral. Geol., Beil-Bd., A64, 681.

167. Reynolds, W.N. and Czyzak, S.J. (1950) Phys. Rev., 79, 543.

168. Reynolds, W.N. and Czyzak, S.J. (1954) ibid., 96, 1705.

169. Rood, J.L. (1951) J. Opt. Soc. Am., 41, 201.

170. Rosenfeld, L. (1951) "Theory of Electrons", North Holland Publishing Co., Amsterdam.

171. Rupprecht, G. (1954) Z. Phys., 139, 504.

172. Ryabova, L.A. and Savitskaya, Y.S. (1968) Thin Solid Films, 2, 141.

173. Sardomirskii, V.B. (1963) Soviet Phys. JETP, 16, 1630.

174. Sasaki, K., Kurita, S. and Omoto, Y. (1968) Jap. J. Appl. Phys., 7, 1039.

175. Sawaki, T. (1958) Sci. of Light (Tokyo), 7, 1.

176. Schulz, L.G. (1949) J. Chem. Phys., 17, 1153.

177. Sennett, R.S. and Scott, G.A. (1950) J. Opt. Soc. Am., 40, 203.

178. Shalimova, K.V., Morozova, N.K. and Karetnikov, I.A. (1971) Optics & Spectroscopy, 30, 573.

179. Sheasby, J.S. (1968) J. Electrochem. Soc., 115, 695.

180. Shimaushi, M. (1960) Sci. of Light (Japan) 9, 109.

181. Shrachko, V.I., Nadykto, B.T., Fogel, Y.M., Vasyntiskii, B.M. and Kartmazov, G.N. (1966) Soviet Phys.-Solid State, 7, 152.

182. Simmons, J.G., Nadkarni, G.S. and Lancaster, M.C. (1970) J. Appl. Phys., 41, 538.

183. Smyth, C.P. (1955) "Dielectric Behaviour and Structure", McGraw-Hill Book Comp. Inc., N.Y.

184. Soeya, T. and Kimura, Y. (1966) Jap. J. Appl. Phys. 5, 838.

185. Stasenko, A.G. (1968) Soviet Phys.-Solid State, 10, 186.

186. Stratton, J.A. (1941) "Electromagnetic Theory", McGraw-Hill Book Comp. Inc., New York.

187. Sutton, P.M. (1964) J. Am. Ceram. Soc., 47, 188.

188. Tamura, H. and Kimura, H. (1965) Jap. J. Appl. Phys., 4, 622.

189. Tanenbaum, M. and Briggs, H.B. (1953) Phys. Rev., 91, 1561.

190. Thiel, A. and Luckmann, H. (1928) Z. anog. Chem., 172, 353.

191. Tippins, H.H. and Chase, A.B. (1966) Bull. Am. Soc., 11, 765.

192. Tolansky, S. (1948) "Multiple Beam Interferometry", Oxford Univ. Press.

193. Tutton, A.E.H. (1926) "Crystalline Form and Chemical Constitution", London.

194. Uchida, W. (1968) Jap. J. Appl. Phys., 7, 378.

195. Ulrich, F. and Zachariasen, W. (1926) Z. Krist., 62, 260.

196. Vainshtein, V.M. and Fistul, V.I. (1971) Soviet Phys. Semicond., 4, 1278.

197. Vašíček, A. (1960) "Optics of Thin Films", North Holland Publishing Company, Amsterdam.

198. Vohl, P., Buchan, W.R. and Genthe, J.E. (1971) J. Electrochem. Soc., 118, 1842.

199. Vossen, J.L. (1971) RCA Review, 32, 289.

200. Vratny, F. (1969) "Thin Film Dielectrics", The Electrochem. Soc. Inc., New York.

201. Weaver, C. (1962) Advan. Phys., 11, 83.

202. Weiher, R.L. (1962) J. Appl. Phys., 33, 2834.

203. Weiher, R.L. and Ley, R.P. (1966) J. Appl. Phys., 37, 299.

204. Wood, C., Pelt, B. van. and Dwight, A. (1972) Phys. Stat. Solidi., 54, 701.

205. Wurzburg, J.W. (1908) Z. Krist., 44, 212.

206. Yosida, K. (1952) J. Chem. Phys., 20, 202.

207. Young, L. (1961) "Anodic Oxide Films" Academic Press. Inc., New York.

208. Zemel, J.N., Jensen, J.D. and Schoolar, R.B. (1965) Phys. Rev., 140, A.330.

209. Zener, C. (1934) Proc. Roy. Soc. (London), A145, 523.